SANDIA REPORT
SAND2007-0131
Unlimited Release
Printed January 2007

Taiwan Industrial Cooperation Program Technology Transfer for Low-Level Radioactive Waste Final Disposal – Phase I

Bill W. Arnold, Robert G. Knowlton, F. Joseph Schelling, Patrick D. Mattie,
John C. Cochran, and Hong-Nian Jow

Prepared by
Sandia National Laboratories
Albuquerque, New Mexico 87185 and Livermore, California 94550

Sandia is a multiprogram laboratory operated by Sandia Corporation,
a Lockheed Martin Company, for the United States Department of Energy's
National Nuclear Security Administration under Contract DE-AC04-94AL85000.

Approved for public release; further dissemination unlimited.

Issued by Sandia National Laboratories, operated for the United States Department of Energy by Sandia Corporation.

NOTICE: This report was prepared as an account of work sponsored by an agency of the United States Government. Neither the United States Government, nor any agency thereof, nor any of their employees, nor any of their contractors, subcontractors, or their employees, make any warranty, express or implied, or assume any legal liability or responsibility for the accuracy, completeness, or usefulness of any information, apparatus, product, or process disclosed, or represent that its use would not infringe privately owned rights. Reference herein to any specific commercial product, process, or service by trade name, trademark, manufacturer, or otherwise, does not necessarily constitute or imply its endorsement, recommendation, or favoring by the United States Government, any agency thereof, or any of their contractors or subcontractors. The views and opinions expressed herein do not necessarily state or reflect those of the United States Government, any agency thereof, or any of their contractors.

Printed in the United States of America. This report has been reproduced directly from the best available copy.

Available to DOE and DOE contractors from
U.S. Department of Energy
Office of Scientific and Technical Information
P.O. Box 62
Oak Ridge, TN 37831

Telephone: (865) 576-8401
Facsimile: (865) 576-5728
E-Mail: reports@adonis.osti.gov
Online ordering: http://www.osti.gov/bridge

Available to the public from
U.S. Department of Commerce
National Technical Information Service
5285 Port Royal Rd.
Springfield, VA 22161

Telephone: (800) 553-6847
Facsimile: (703) 605-6900
E-Mail: orders@ntis.fedworld.gov
Online order: http://www.ntis.gov/help/ordermethods.asp?loc=7-4-0#online

SAND2007-0131
Unlimited Release
Printed January 2007

Taiwan Industrial Cooperation Program Technology Transfer for Low-Level Radioactive Waste Final Disposal – Phase I

Bill W. Arnold, Robert G. Knowlton, F. Joseph Schelling, Patrick D. Mattie,
John C. Cochran, and Hong-Nian Jow

Sandia National Laboratories
P.O. Box 5800
Albuquerque, New Mexico 87185-MS0779

Abstract

Sandia National Laboratories and the Institute of Nuclear Energy Research, Taiwan have collaborated in a technology transfer program related to low-level radioactive waste (LLW) disposal in Taiwan. Phase I of this program included regulatory analysis of LLW final disposal, development of LLW disposal performance assessment capabilities, and preliminary performance assessments of two potential disposal sites. Performance objectives were based on regulations in Taiwan and comparisons to those in the United States. Probabilistic performance assessment models were constructed based on limited site data using software including GoldSim, BLT-MS, FEHM, and HELP. These software codes provided the probabilistic framework, container degradation, waste-form leaching, groundwater flow, radionuclide transport, and cover infiltration simulation capabilities in the performance assessment. Preliminary performance assessment analyses were conducted for a near-surface disposal system and a mined cavern disposal system at two representative sites in Taiwan. Results of example calculations indicate peak simulated concentrations to a receptor within a few hundred years of LLW disposal, primarily from highly soluble, non-sorbing radionuclides.

ACKNOWLEDGMENTS

The Sandia team that worked on Phase I of this ICP Technology Transfer Project for Taiwan Low-Level Radioactive Waste Disposal would like to thank Mr. Joe Ostuni of Lockheed Martin Maritime Systems and Sensors (LM MS2) - Syracuse for his funding support for the benefit of the AADS An-Yu 4 Industrial Cooperation Agreement (ICA), Mr. Robert Kelly at the Lockheed Martin Missiles and Fire Control - Orlando for the management of the performance of the ICA, and Taiwan's Industrial Development Bureau (IDB), Industrial Cooperation Program (ICP) Office for their support of this ICP Project. The Sandia team sincerely appreciates the support of Dr. Terry Sullivan of Brookhaven National Laboratory with the BLT-MS and DUST software codes, and the assistance of Mr. Ralph Cady of the U.S. Nuclear Regulatory Commission (NRC) in facilitating the transfer of NRC codes to the Institute of Nuclear Energy Research, Taiwan (INER). The Sandia team also would like to express great appreciation to the management and technical staff at INER for their generous support during Sandia's visits to INER and their effort in providing technical reports to Sandia.

Sandia National Laboratories is a multiprogram laboratory operated by Sandia Corporation, a Lockheed Martin Company, for the United States Department of Energy under Contract DE-AC04-94AL85000.

CONTENTS

FIGURES

TABLES

NOMENCLATURE

ABWR	Advanced Boiling Water Reactor
AEC	Taiwan Atomic Energy Council
AIT	U.S. American Institute in Taiwan
BLT-MS	Breach, Leach, and Transport - Multiple Species code
BWR	Boiling Water Reactor
CFR	U.S. Code of Federal Regulations
Ci	Curies
DCF	dose conversion factor
DOE	Department of Energy
DUST-MS	Disposal Unit Source Term – Multiple Species code
FCMA	Fuel Cycle and Materials Administration
FEHM	Finite Element Heat and Mass Transfer code
FEP	features, events, and processes
GCD	Greater Confinement Disposal
GTCC	Greater Than Class C
HELP	Hydrologic Evaluation of Landfill Performance model code
IAEA	International Atomic Energy Agency
IDB	Industrial Development Bureau, Ministry of Economic Affairs, Taiwan
ICP	Industrial Cooperation Program
ICRP	International Commission on Radiological Protection
INER	Institute of Nuclear Energy Research
LLW	Low-Level Radioactive Waste
MOGP	member of the general public
NAS	U.S. National Academy of Sciences
NPP	nuclear power plant
NRC	U.S. Nuclear Regulatory Commission
PWR	Pressurized Water Reactor
SNL	Sandia National Laboratories
TECRO	Taiwan Taipei Economic and Cultural Representative Office
TEDE	Total Effective Dose Equivalent
WIPP	Waste Isolation Pilot Plant
YMP	Yucca Mountain Project

This page intentionally blank.

1. INTRODUCTION

Taiwan Power Company, regulated by the Fuel Cycle and Materials Administration (FCMA) of the Taiwan Atomic Energy Council (AEC), is planning to: (1) evaluate and select a LLW final disposal site for Taiwan, (2) complete a performance assessment using site characterization data and design information to satisfy regulatory requirements, and (3) construct and begin disposal operations by around 2014 (Note: The schedule is delayed, and the current plan is to confirm a site around 2011). It is anticipated that several of Taiwan's research institutions, including the Institute of Nuclear Energy Research (INER), will support this effort. Among the responsibilities for Taiwan's LLW final disposal program, INER has been assigned responsibility to perform a regulatory analysis and an independent safety assessment of the LLW final disposal system through a total system performance assessment.

Original near-term milestones for INER were to: (1) complete preliminary independent performance assessments of two potential LLW disposal sites in 2005, and (2) complete a refined independent performance assessment using more detailed design and site data for a selected site by December 2006. These milestones have been somewhat delayed, and Taiwan has postponed selection of a disposal site. However, INER still intends to complete the preliminary performance assessments for two different site and design concepts to demonstrate their capability and support eventual resolution of the LLW disposal problem.

Sandia National Laboratories (Sandia) and INER have been exchanging technical information in geologic repository experience since 1998, through a collaboration under purview of the mutual agreement of the U.S. American Institute in Taiwan (AIT) –Taiwan Taipei Economic and Cultural Representative Office (TECRO) Joint Standing Committee on Civil Nuclear Cooperation. Beginning in February 2005 and funded through the Lockheed Martin Industrial Cooperation Program (ICP), Phase I of the Technology Transfer for Low-Level Radioactive Waste Final Disposal was completed in July 2006. Through this project, Sandia transferred technology to assist INER in developing their capabilities in conducting performance assessments for the low-level radioactive waste (LLW) final disposal system planned in Taiwan. Sandia has a long record of involvement with radioactive waste management and disposal and considerable experience that may be useful to Taiwan in strengthening their technical capabilities in assessing system performance.

The main objectives of Phase I were to assist INER in: (1) regulatory analysis of LLW final disposal, (2) development of LLW performance assessment capabilities using NRC-sponsored codes and other computational tools, and (3) conducting performance assessments for two potential LLW final disposal sites using available site and initial conceptual design information.

During Phase I, several meetings and workshops were held at INER as shown in Table 1.

Table 1. Meetings and Workshops Held at INER

Dates	Meeting Topics
6/13-14/2005	Data Needs/Initial Regulatory Analysis Results
7/28-8/8/2005	Workshops on FRAMES/MEPAS, DUST, FEHM, BLT-MS
10/11-14/2005	Regulatory Analysis/ FEP Screening/Scenario Development
12/12-20/2005	Performance Assessment Framework Workshop
4/3-13/2006	Follow-up Performance Assessment Framework Workshop

Sandia also obtained several software codes for INER and provided various documents requested by INER. Similarly, INER provided copies of Taiwan's regulatory documents and responded to Sandia requests for information on site and design characteristics. Throughout Phase I, Sandia and INER communicated regularly via e-mail and discussions held during visits to INER and have developed a strong, collaborative relationship.

This report describes the work performed by Sandia under Phase I and summarizes the results of the preliminary analysis of the long-term system performance for the two different site and design concepts selected for the study of LLW disposal in Taiwan. Chapter 2 provides some background information on Taiwan and its low-level radioactive waste disposal program and an overview of the performance assessment methodology. Chapter 3 describes the performance assessment framework and models developed for this work. Chapter 4 presents the preliminary assessment modeling of a near-surface disposal facility. Chapter 5 presents the preliminary assessment modeling of the performance of a mined cavern disposal facility. Chapter 6 summarizes and compares the results for the two disposal concepts. Chapter 7 provides recommendations for future work. Chapter 8 lists references cited in this report.

2. BACKGROUND

2.1. Low-Level Radioactive Waste Program Status

Taiwan generates radioactive waste from a variety of commercial, medical, industrial, and educational activities. Low-level radioactive waste (LLW) generated by commercial nuclear power generation is stored on-site at the nuclear power plants and at the Lanyu Storage Site on Lanyu (Orchid) Island (see Figure 1.). The building in the middle of Figure 1 is a moveable temporary building for inspections, repairing, or re-packaging of LLW drums. The Lanyu Storage Site includes solid LLW produced primarily (~80%) by nuclear power plants and all medical, agricultural, industrial, education and research sectors (~20%) in Taiwan. Figure 2 shows on-site LLW interim storage at Chinshan Nuclear Power Plant.

Figure 1. Lanyu Island Low-Level Radioactive Waste Storage Facility.

Figure 2. Interim on-site storage at Chinshan Nuclear Power Plant

Overall, Taiwan currently has ~130,000 drums of LLW. Assuming 40 years of operation of all four nuclear power plants, the total quantity of LLW estimated to 2045 will be nearly 966,000 drums, including nuclear facility decommissioning wastes. Full capacity of 98,112 drums at Lanyu was reached in 1996 and additional wastes are now stored at the nuclear power plants and INER. Although Taiwan has not yet selected a site for final disposal of LLW, the Taiwan Power Company has narrowed consideration down to four representative potential sites from an initial list of 30 regions around Taiwan. Figure 3 shows the locations of these four potential sites.

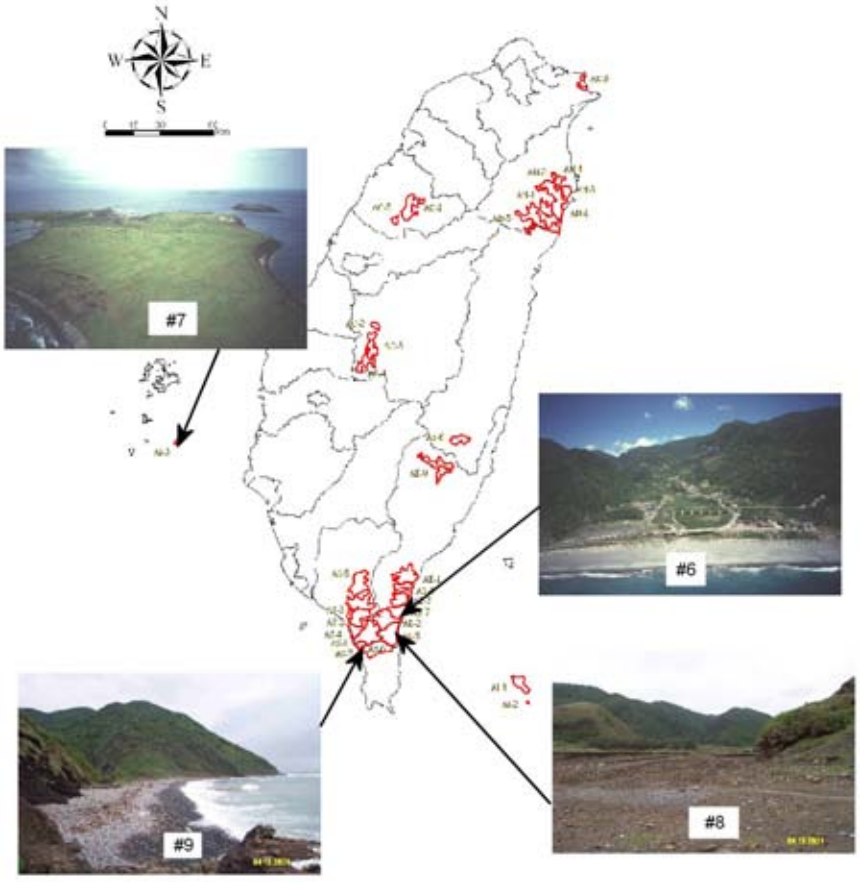

Figure 3. Locations of the Four Potential Candidate Sites

Two of these sites (Site #6 and Site #7) were selected for the current study and involve quite different disposal concepts and disposal environments.

One representative site (Site #7) is located on a small island off the western coast of Taiwan and uses a near-surface (shallow land burial) disposal design, which has an engineered cover system to limit infiltration. This site has basalt bedrock and interbedded sedimentary rocks. Figure 4 shows the preliminary layout and a cross-section for the disposal facility.

A second representative site (Site #6) is along the southeastern coast of the main island and uses a mined cavern design with a tunnel system located about 500 to 800 m below the surface.

Bedrock at this site consists of argillite and meta-sedimentary rocks. Figure 5 shows the layout and a cross-section for the facility at this site.

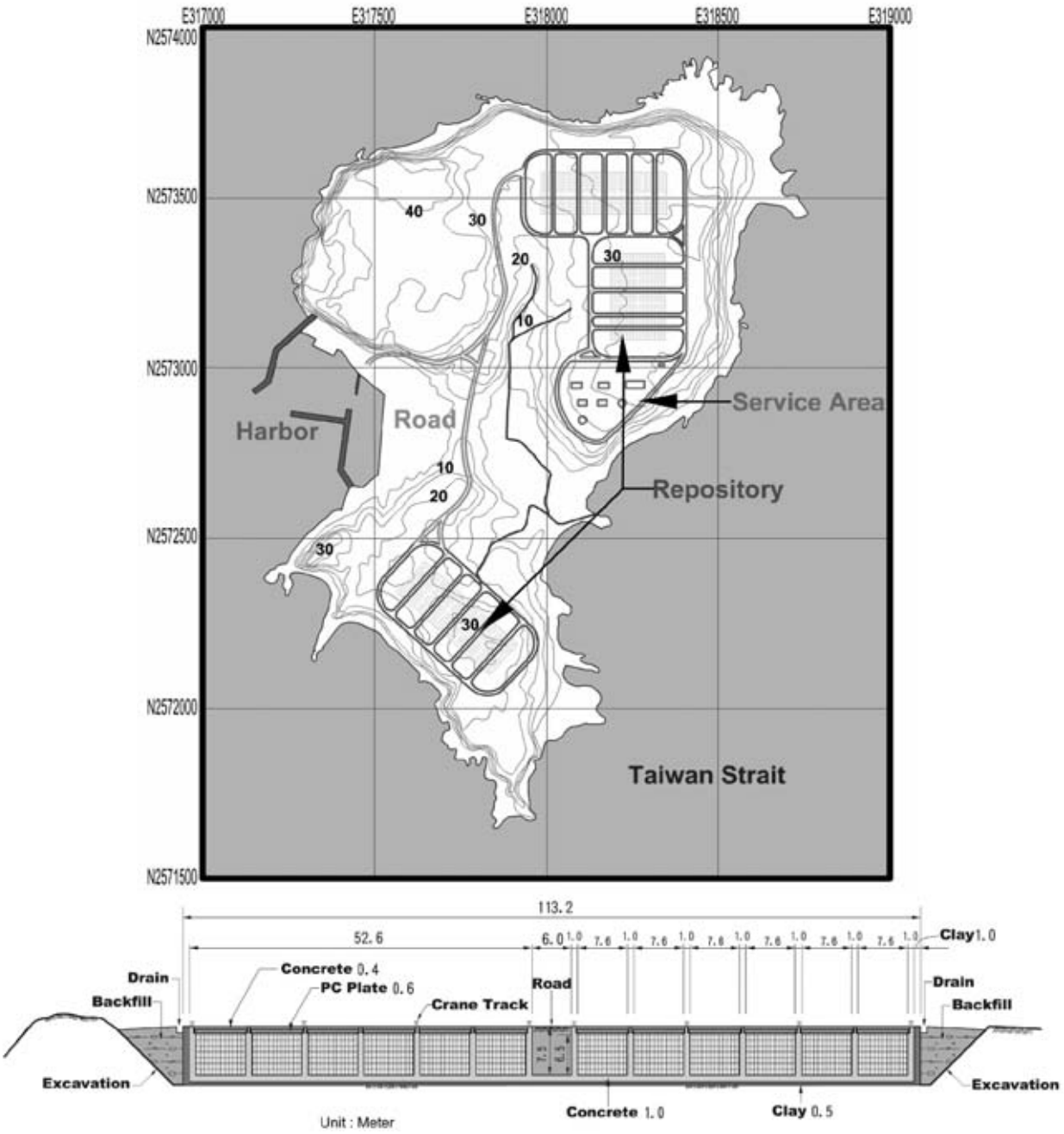

Figure 4. Island Site for Near-Surface Disposal System Concept and Cross Section of Disposal Cell

2.2. Taiwan Environmental Overview

The Republic of China (Taiwan) has a total area of approximately 35,980 square kilometers (13,892 square miles), including the main island of Taiwan and a number of much smaller islands, and is roughly the size of Maryland and Delaware combined. The main island is 394 kilometers (245 miles) long and 144 kilometers (89.5 miles) wide at its broadest point. Close to 23 million people live in Taiwan, which has one of the highest population densities in the world. (For comparison, the combined population of Maryland and Delaware is ~ 6 million.) Most of the population lives on the western and northern parts of the main island, with the eastern two-thirds mostly rugged mountain terrain.

Taiwan's climate is subtropical in the north and tropical in the south, with average temperatures ranging from 14ºC (57ºF) in January to 28ºC (82ºF) in July. Summer, which starts in May and lasts through September, is usually hot and humid. Short, mild winters last from December through February, with scattered snowfall only occurring on the island's highest mountains. Numerous typhoons affect Taiwan every year. The average annual precipitation is about 4,000 mm (about 160 in).

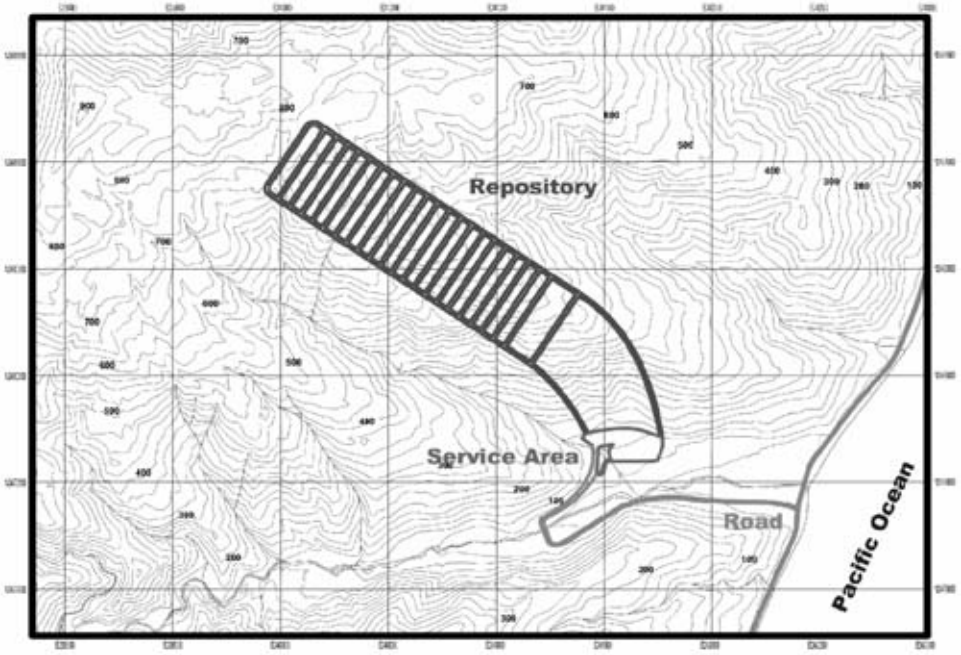

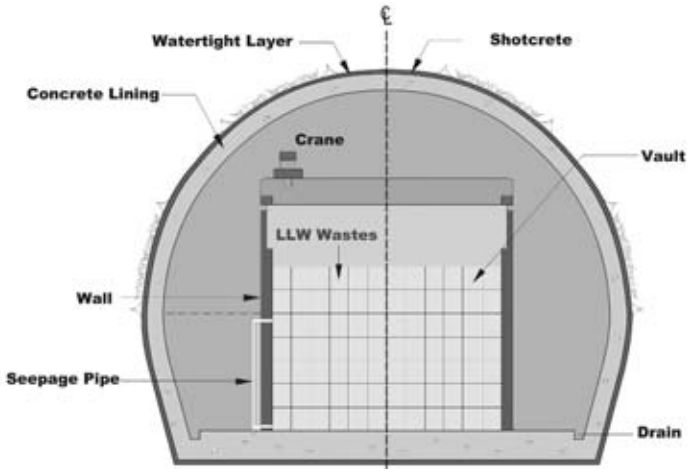

Figure 5. Site for Mined Cavern Disposal System Concept and Cross Section of Disposal Tunnel.

Taiwan lies in an extremely active tectonic region, near the junction of the Eurasian and Philippine Sea tectonic plates. This region experiences seismicity and rates of crustal motion among the highest in the world. The last century saw several large damaging earthquakes, including the 7.3 magnitude Chi-Chi (Jiji) earthquake on September 21, 1999.

In addition to six commercial nuclear power reactors (four Boiling Water Reactors (BWRs) and two Pressurized Water Reactors (PWRs)) at three power plants with a combined capacity of 4884 MW(e), there are two Advanced Boiling Water Reactors (ABWRs) currently under construction (2600 MW(e)). In addition IAEA's Research Reactor Database (RRDB) indicates that Taiwan has several research reactors (IAEA, 1999). Radioactive waste produced during operations and decommissioning activities will need to be included in the total inventory.

2.3. Performance Assessment Methodology Overview

Assessing the long-term performance of a disposal system to determine its safety involves considerable uncertainty and multiple assumptions. Iterations on the assessment are useful as lessons are learned from analysis of model results, additional data become available, and assumptions are revised and refined. An overview of the general process of performance assessment is shown in Figure 6 (NRC, 2000).

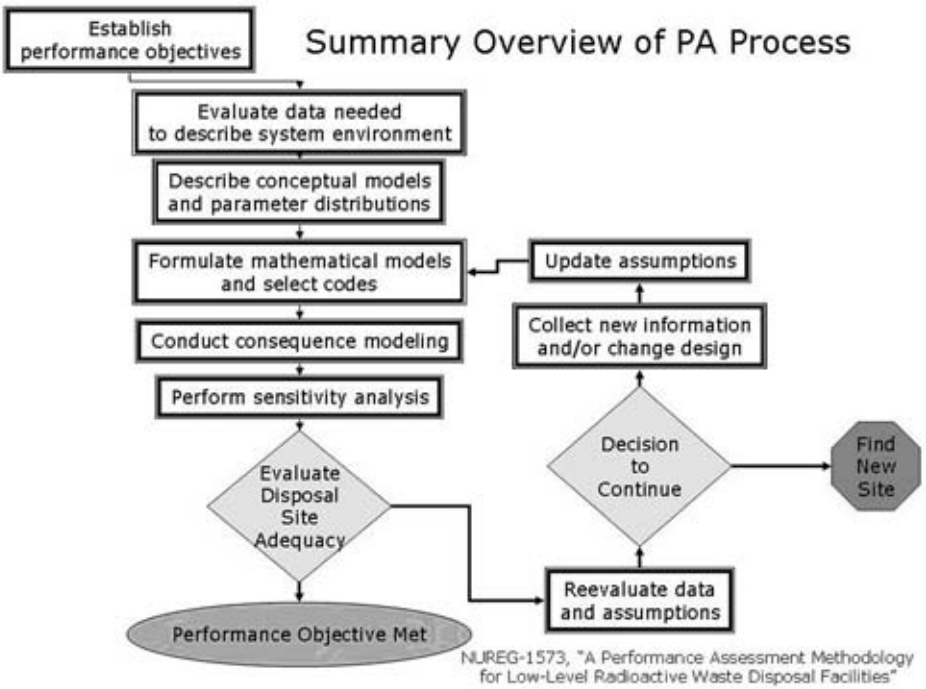

Figure 6. Flowchart of the Performance Assessment Process.

A first step is the establishment of performance objectives, which define measures against which the system performance can be compared. Having identified quantitative performance objectives, the next step is to evaluate the data needed to fully describe the system environment. This includes data on the natural environment of the site, performance characteristics of the waste and its containers, and features of the design of the facility and any engineered barriers contributing to system performance. Where data are limited or unavailable, assumptions and expert judgments are needed to ensure the results are both conservative and defensible.

Having developed a general understanding of the system environment and performance characteristics, the next step in the PA methodology is to generate descriptions of how the system functions, i.e., to establish conceptual models of how various components of the system operate over time. This step may also require specifying distributions for important parameters that will be used in modeling system behavior.

Information developed from the earlier steps then forms the basis for selecting mathematical models used to represent system behavior, which are then implemented through the use of software codes. These codes, along with parameter distributions and assumptions, are then used to model system performance and compliance with the performance objectives.

This methodology represents an ideal approach. In reality, some of these steps tend to occur in parallel or in a slightly different order. Performance assessment is an iterative process, however, and each of these steps will be regularly revisited and updated in the course of analysis.

3. PERFORMANCE ASSESSMENT FRAMEWORK

To develop the framework for conducting the performance assessment for the two Taiwan design concepts, the first four steps in the methodology described above were performed. That is, an effort was first undertaken to identify and quantify performance objectives against which the system performance is measured. Second, available data and information needed to describe the system behavior were compiled and evaluated and, where data were insufficient, assumptions made to allow the analysis to proceed. Third, conceptual models of the system and system processes were developed along with distributions for various parameters needed to model system behavior. Fourth, using the information compiled in the earlier steps, mathematical models represented by several software codes were selected and integrated into a computational framework, which was subsequently used to perform the probabilistic assessment of the long-term behavior of the two systems. A summary of the work performed during Phase I for each of these four steps is provided in the following sections.

3.1. Specification of Performance Objectives

An important step in the methodology of performance assessment is the establishment of quantitative performance objectives, which establish metrics against which regulatory compliance is determined. An introductory presentation on this topic was given at INER in June 2005, followed by a more thorough discussion in October 2005.

To identify performance objectives applicable to Taiwan, Sandia first performed an evaluation and comparison of Taiwan LLW regulations against the U.S. regulations on which they were based, and made a number of observations and recommendations, which are summarized below. A more complete description is contained in SAND2005-6336P, which was provided to INER in November 2005 (SNL, 2005).

In the United States, LLW disposal facilities are regulated by the Nuclear Regulatory Commission (NRC). Regulations for safety and licensing of these facilities are contained in Title 10 of the U.S. Code of Federal Regulations (CFR) Part 61, which specifies three post-closure performance objectives for near-surface LLW disposal facilities in 10 CFR 61.41, 61.42, and 61.44:

- Concentrations of radioactive material which may be released to the general environment in ground water, surface water, air, soil, plants, or animals must not result in an annual dose exceeding an equivalent of 25 mrem to the whole body, 75 mrem to the thyroid, and 25 mrem to any other organ of any member of the public. Reasonable effort should be made to maintain releases of radioactivity in effluents to the general environment as low as is reasonably achievable.(10 CFR 61.41)
- Design, operation, and closure of the land disposal facility must ensure protection of any individual inadvertently intruding into the disposal site and occupying the

site or contacting the waste at any time after active institutional controls over the disposal site are removed. (10 CFR 61.42)

- The disposal facility must be sited, designed, used, operated, and closed to achieve long-term stability of the disposal site and to eliminate to the extent practicable the need for ongoing active maintenance of the disposal site following closure so that only surveillance, monitoring, or minor custodial care are required. (10 CFR 61.44)

Taiwan's regulations on the licensing of LLW final disposal facilities are based on the NRC regulations, but from the documentation provided appear to have a few potentially significant differences. The evaluation focused on two of the Taiwan regulatory documents. A primary reference is the document "Regulations on Final Disposal of Low Level Waste and Safety Management of the Facilities" (INER, 2003a). A second reference used in the evaluation is the document "Safety Standards for Protection against Ionizing Radiation" (INER, 2003b). Because the U.S. requirements were written generically for anticipated waste streams and broad applicability to diverse near-surface disposal designs, however, care should be taken to understand the implicit assumptions in these regulations in applying them to other situations. The comparison between Taiwan and U.S. regulations, and some of the considerations used to establish each of the three performance objectives are summarized below. Following that discussion, Table 6 summarizes recommendations made by Sandia with respect to the quantification of the three performance objectives.

Performance Objective 1 - Protection of the General Public

With one exception, Taiwan regulations for the first performance objective for protection of the general public are quite similar to the U.S. regulations, as shown in Table 2.

Table 2. Taiwan and U.S. Public Protection Performance Objective.

Taiwan	U.S.
The design of low level disposal facilities shall ensure the annual effective equivalent dose caused to a general public outside the facilities are not more than 0.25 mSv, and confirm to the as low as reasonably achievable principle. (from Chapter 3, Article 8)	Concentrations of radioactive material which may be released to the general environment in ground water, surface water, air, soil, plants, or animals must not result in an annual dose exceeding an equivalent of 25 mrem to the whole body, 75 mrem to the thyroid, and 25 mrem to any other organ of any member of the public. Reasonable effort should be made to maintain releases of radioactivity in effluents to the general environment as low as is reasonably achievable. (10 CFR 61.41)

Minor differences include the use in Taiwan's regulations of international (SI) units and eliminating explicit specification of dose pathways. U.S. regulations identify specific pathways

(i.e., ground water, surface water, air, soil, plants, or animals), while the Taiwan regulations imply consideration of "all" potential pathways.

A potentially more significant difference requiring clarification is the term "effective equivalent dose" in the Taiwan disposal regulations. The NRC in NUREG-1573 (NRC, 2000) recommends use of International Commission on Radiological Protection (ICRP) 20 methodology for calculation of Total Effective Dose Equivalent (TEDE); whether or not "Effective Equivalent Dose" is also based on ICRP 20 or is calculated using a different methodology should be verified (Note that the Taiwan "Safety Standards for Protection against Ionizing Radiation" has a definition of "Effective Dose Equivalent," but not "Effective Equivalent Dose.").

Performance Objective 2 – Protection of the Inadvertent Human Intruder

Some potentially significant differences in regulations between those of Taiwan and the U.S. were identified, which may require additional clarification. Comparison between the Taiwan and U.S. regulations is shown in Table 3.

Table 3. Taiwan and U.S. Inadvertent Human Intrusion Performance Objective.

Taiwan	U.S.
Solidifying and packing shall be performed for Class C waste, and the waste shall meet the provisions of both Article 5 and Article 6. Additionally, the engineering design of the disposal area shall be strengthened to ensure the safety of those inadvertent intruders after the institutional control period. (Article 4.3) The security and alarm design of low level disposal facilities shall be able to prevent any individual inadvertently intruding into the disposal site and occupying the site. (from Chapter 3, Article 12)	Design, operation, and closure of the land disposal facility must ensure protection of any individual inadvertently intruding into the disposal site and occupying the site or contacting the waste at any time after active institutional controls over the disposal site are removed. (10 CFR 61.42)

In the U.S., the inadvertent human intruder is protected by the use of the waste classification system and requirements to ensure the waste is recognizable until after the wastes decay to safe levels. These requirements are summarized in Table 4.

The waste classification system limits the specific activity of the disposed wastes, and was developed independent of site-specific characteristics and based on a standard set of surrogate intrusion exposure conditions. Container integrity and intrusion barrier requirements were established to further protect the intruder. Note that compliance to these requirements implies that a site-specific safety assessment is not necessary to demonstrate protection of the inadvertent intruder (NUREG-1573, p.1-13, footnote 7) (NRC, 2000).

Table 4. U.S. Protection Requirements for the Inadvertent Human Intruder.

Waste Class	Basis for Concentration Limits	Disposal Requirement in 10 CFR 61
A	Safe for intrusion after 100 years	Class A inventory limits (10 CFR 61.55) and institutional controls for 100 years following closure (10 CFR 61.59)
B	Recognizable up to 300 years and safe for intrusion after 300 years	Class B inventory limits (10 CFR 61.55) and Class B and C waste forms or containers designed to be recognizable for 300 years (10 CFR 61.7 (b) (2))
C	Recognizable up to 500 years and safe for intrusion after 500 years	10 CFR 61.55 Class C inventory limits (10 CFR 61.55), 300 year waste form, and intruder barriers for 500 years or waste > 5 m deep (10 CFR 61.52 (a) (2))
GTCC	Not safe for intrusion even after 500 years	Not typically appropriate for near-surface burial (10 CFR 61.55 (a) (3) (iii))

Assumptions used by the NRC in developing regulations associated with this performance objective include:

1. Assuming an institutional control period of 100 years as an appropriate length of time a government could be expected to provide custodial care;
2. Establishing the dose standard for the intruder at 500 mrem/yr to the whole body or the bone or 150 mrem/yr to other organs, 20 times larger than the 25 mrem/yr limit to the general member of the public under the assumption that intrusion would be a temporary exposure to only a few individuals;
3. Conservatively assuming intrusion to occur at the end of institutional control (100 years) due to a temporary, bureaucratic error;
4. Conservatively assuming a unit probability of the intrusion occurring (i.e., intrusion occurs);
5. Defining the point in time at which the waste becomes unrecognizable, e.g. 100 years for Class A, 300 years for Class B, and 500 years (the assumed lifetime of readily implemented intrusion barriers) for Class C;
6. Establishing three surrogate intruder exposure scenarios for determining dose consequences - defined: intruder-discovery; intruder-construction; and intruder-agriculture; and
7. Specifying waste classification limits by calculating dose consequences for the three exposure scenarios and then performing a series of back calculations to establish appropriate concentration limits.

In developing the waste classification system the NRC considered a large, but not entirely comprehensive, number of radionuclides based on anticipated waste streams. In particular, Taiwan may want to conduct their own analyses of uranium, radon and thorium because the NRC did not analyze these radionuclides in developing the 10 CFR 61 Class limits. The NRC notes in Footnote 7 of NUREG-1573 that separate intruder analyses may be necessary in cases where disposed waste characteristics differ from those considered in the technical analyses underlying 10 CFR 61, e.g., anomalous quantities and concentrations of certain long-lived radionuclides that waste classification and intruder barrier requirements of 10 CFR 61 may not reasonably protect the inadvertent intruder (NRC, 2000).

Taiwan adopted the Class A, B and C waste classification system (Chapter 2, Articles 3 and 4), but it does not appear that Taiwan has fully adopted the corresponding requirements for waste integrity and intruder barriers.

Performance Objective 3 – Long-term Post-closure Stability

Taiwan regulations do not appear to consider the need to minimize void spaces and waste compressibility to ensure long-term waste package and site stability. Because of a history of post-closure site instability and performance problems identified in pre-1982 LLW disposal practices in the U.S., the NRC in 10 CFR 61 set criteria for waste packages and waste emplacement. While it appears Taiwan adopted waste form stability requirements similar to those of the U.S., Taiwan regulations do not include explicit requirements to eliminate future subsidence by eliminating voids inside and between containers (see Table 5).

Table 5. Taiwan and U.S. Long-Term Stability Performance Objective.

Taiwan	U.S.
The waste of the low level disposal facilities… (Chapter 2, Article 5) The homogeneous solidifying waste… (Chapter 2, Article 6)	A cornerstone of the system is stability - stability of the waste and the disposal site (10 CFR 61.7(b) (2)) The disposal facility must be sited, designed, used, operated, and closed to achieve long-term stability of the disposal site and to eliminate to the extent practicable the need for ongoing active maintenance of the disposal site following closure so that only surveillance, monitoring, or minor custodial care are required. (10 CFR 61.44) Void spaces between waste packages must be filled with earth or other material to reduce future subsidence within the fill. (10 CFR 61.52(a) (5))

Quantification of Performance Objectives

In order to demonstrate that a disposal facility satisfies the imposed performance objectives necessary for licensing, it is important to be able to translate the objectives into a set of quantifiable measures. Missing from the regulations, for example, is certain key information such as the time periods or locations at which compliance is to be demonstrated. Based on experiences in the U.S., additional interpretation or supplemental guidance is needed in the following areas:

- Point of compliance;
- Timeframe of compliance;
- Nature of future exposure scenarios;
- Consideration of low probability features, events and processes;
- Assessing compliance with deterministic and probabilistic analyses;
- Applicability of 10 CFR 61 to a Mined Cavity; and
- Reasonable Assurance

The focus of this discussion is on the demonstration of compliance to the first performance objective for long-term protection of the member of the general public. Compliance with the remaining performance objectives, as mentioned above, is through demonstration that waste classification, design, and operational requirements are satisfied.

Point of Compliance

The point of compliance for calculating dose to the member of the general public is generally assumed to be the point of maximum exposure 100 m beyond the edge of the disposal cell, a concept developed in the U.S. (DOE, 1994; p. 21). Importantly, if groundwater advective rates are fairly fast (meters per year or faster), moving the point of compliance closer to the edge of the disposal cell (e.g., 20 m), or further from the edge of the disposal cell (e.g., 300 m) does not significantly alter doses to the Member of the General Public (MOGP).

Timeframe of Compliance

U.S. regulations require that the waste packages be stable for 300 years and that the intruder barriers must last 500 years (or the Class B/C wastes must be buried more than 5 m deep), but do not specify a timeframe of compliance for meeting the dose standard specified in 10 CFR 61.41. Similarly, Taiwan regulations do not specify a compliance timeframe.

In NUREG-1573 (NRC, 2000) and SECY-96-103 (NRC, 1996c), the NRC recommends limiting the timeframe of safety assessment calculations to 10,000 years. The NRC conducted

simulations to study the time to peak dose and found that 10,000 years is sufficiently long to: (a) evaluate performance of both engineered barriers and the site; (b) capture the peak doses from the most mobile, long-lived radionuclides; and (c) bound the potential peak doses at longer times. Setting the timeframe of compliance at 10,000 years also limits unnecessary speculation about events in the extremely distant future.

For disposal systems that may contain large quantities of uranium (>1000 Ci) and/or transuranics, however, the NRC found that the peak dose may not occur in 10,000 years and recommends that the calculations be continued, using the same models and input parameters, until the peak dose is reached. Such long-lived LLWs include mobile radionuclides (e.g., ^{14}C, ^{36}Cl, ^{129}I, and ^{99}Tc), large quantities of uranium (with the ingrowth of mobile daughter products), and large inventories of transuranics (^{239}Pu). The NRC recommends that information on simulated doses that may occur beyond 10,000 years be used for "informational purposes" and not for the purposes of determining regulatory compliance.

Nature of Future Exposure Scenarios

U.S. and Taiwan regulations do not specify the exposure scenario used for calculating dose to the member of the general public. Because the nature of any future human activities is uncertain, the U.S. National Academy of Sciences (NAS) concluded "that there is no scientific basis for making projections over the long-term of either the social, institutional, or technological status of future societies." (NAS, 1995). Given this uncertainty, the NRC assumes the living habits of current society are representative of the future. The NRC therefore recommended in NUREG-1573 that calculations of radiological exposures to any member of the general population should be made in terms of the average member of the critical group, where the critical group is defined as "the group of individuals reasonably expected to receive the greatest exposure to radiological releases from the disposal facility over time based on conservative but reasonable exposure assumptions and model parameter values. Similarly, ICRP-81 (ICRP, 1998) recommends calculation doses to the average individual in the critical group. Article 2 of Taiwan's Safety Standards for Protection against Ionizing Radiation defines "critical group" as referring to the general population who receive a rather uniform dose and whose members receive the maximum dose; Article 11.2 states that standards for protection of the general population are applicable "to the critical group in the population."

NRC, ICRP and Taiwan regulations all recommend use of the current average member of the critical group to define the general public exposure scenario. Modelers in Taiwan will need to define the characteristics of their "average member of the critical group. In the U.S., the average member of the critical group is sometimes taken to be the subsistence farmer living 100 m downgradient of the LLW disposal facility and has many of the characteristics described in the intruder-agriculture scenario used to develop 10 CFR 61's waste classification system (see NUREG- 0782 (NRC, 1981), p. G-57 for details).

Consideration of Low Probability Features, Events and Processes

To assess potential doses to the general public, it is necessary to identify and quantify the features, events and processes (FEPs) that may affect the long-term movement of radionuclides in a LLW disposal system. The NRC recommends the FEPs analysis be conducted as a part of the LLW siting process and not as part of the safety assessment process. In 10 CFR 61.50, the NRC establishes disposal site suitability requirements for land disposal, which specify minimum characteristics for an acceptable near-surface disposal site. By following the NRC's 10 CFR 61.50 criteria, "disruptive" FEPs are eliminated in the site selection process and the NRC recommends modeling long-term system performance as a continuation of the "reference natural processes." The reference natural processes would include such processes and events as waste form degradation, flooding (100, 500 and 1000 year floods), and seismic events. Taiwan has similar requirements in Chapter 3, Article 7; however if a different siting process is used, it is recommended a FEPs analysis is done as part of the safety assessment.

Additionally, the NRC states that consideration of societal changes in the FEPs analysis would result in unnecessary speculation and should not be included in the safety assessment. The NRC also does not recommend including inadvertent human intrusion as a disruptive event (NUREG-1573, p.1-11) (NRC, 2000). However, some international guidance recommends an analysis to demonstrate that inadvertent human "puncturing" does not significantly alter long-term performance of the facility. To help demonstrate robustness and defense in depth, following this international guidance is recommended.

Whether the FEPs analysis is utilized in the site selection process or the safety assessment process, it is useful to establish a probability metric below which very low probability FEPs can be excluded. In NUREG-1573 (footnote 12) the NRC recommends inclusion of FEPs with a probability of occurrence of > 0.0001/yr, excluding FEPs with a lower annual probability of occurrence. This cut-off will ensure the inclusion of very low probability events (one chance in 10,000 years), without the inclusion of speculative and extremely low probability FEPs.

Assessing Compliance with Deterministic and Probabilistic Analyses

Uncertainty is inherent in all safety assessments, whether deterministic or probabilistic. NUREG-1573 recommends two different approaches for addressing uncertainty. One approach is to provide a single bounding estimate of system performance, supported by data and assumptions that clearly demonstrate the conservative, bounding nature of the analysis. The other approach is to conduct an unbiased probabilistic safety assessment where uncertainty in key models and parameters is translated into uncertainty in system performance with a distribution of potential doses to the member of the general public.

When measuring performance by a single estimate, uncertainty is addressed by providing reasonable assurance that the single estimate conservatively bounds performance. Because large uncertainties are inherent in a safety assessment, such bounding analyses may use simple

modeling approaches and parameters that can be demonstrated as being conservative; selection of appropriate models and parameter values, however, may be difficult.

An alternative approach is to conduct an unbiased probabilistic safety assessment. Through a probabilistic analysis, effects of uncertainties in the system are translated into effects on the potential general public doses. Probabilistic analyses are also amenable to sensitivity analysis. A sensitivity analysis is a powerful safety assessment tool for guiding the iterative safety assessment methodology recommended by the NRC and the IAEA (NUREG-1573 (NRC, 2000) p. 3-2 and IAEA, 2003, Figure 1).

If the safety assessment uses a single, conservative performance estimate to bound potential doses, then the doses must be below 0.25 mSv/yr. If the assessment uses an unbiased probabilistic approach, the NRC recommends that the distribution of potential doses have a mean of < 0.25 mSv/yr and that the 95th percentile of distribution be <1 mSv/yr. (NUREG-1573 (NRC, 2000), p. 3-19)

Applicability of 10 CFR 61 to a Mined Cavity

10 CFR 61 primarily applies to near-surface land disposal, but was written to accommodate alternative methods of disposal, indicating that technical requirements for alternative methods may be added in the future. Therefore, the procedural requirements and the performance objectives of 10 CFR 61 are considered applicable to disposal in a mined cavity, but the existing Part 61 technical requirements may or may not be appropriate. For example, the technical requirement for a 500 year intruder barrier may or may not be applicable to disposal in a mined cavity 100 m below the land surface.

Reasonable Assurance

A safety assessment uses observations about what is known to simulate what might occur in the future. The process is fundamentally a science-based process that uses quantitative analysis based on quantitative and qualitative input. Because the results of a safety assessment process cannot be directly verified, the "standard" for an NRC safety assessment is that of "reasonable assurance," which the NRC describes as demonstrating that facility siting, design, operation, closure, and post-closure control provide reasonable assurance that exposures to humans are within the limits established in the performance objectives.

Table 6. Recommended Quantitative Performance Objectives for LLW Disposal in Taiwan.

Performance Objective	Dose Standard	Point of Compliance	Period of Compliance	Nature of Future Exposure for Calculating Doses	Consideration of Features, Events and Processes (FEPs)	Discussion/Comment
Protection of the Member of the General Public	(1) < 0.25 mSv/yr EED for deterministic bounding analysis or (2) mean value of distribution < 0.25 mSv/yr and 95th percentile < 1 mSv/yr. U.S. uses TEDE per ICRP 20 method	100 m down gradient of edge of the disposal system	10,000 years	All pathways to average member of critical group in Taiwan In U.S., average member critical group may be subsistence farmer using groundwater 100 m downgradient	Consider all reasonably foreseeable FEPs that could effect movement of radionuclides over period of compliance with a probability > 0.0001 in a year	Requires site-specific safety assessment of potential doses to average member of critical group in Taiwan. Safety assessment must provide a "reasonable assurance" that dose standard is met.
Protection of the Inadvertent Human Intruder	To develop Class limits U.S. used 5 mSv whole body and 15 mSv to other organs, because inadvertent intrusion a temporary accident and few people involved	To develop Class limits U.S. assumed intrusion directly into the wastes	U.S. assumed: (1) loss of container integrity (loss of waste recognition) at 100 years to define Class A limits and (2) loss of container integrity at 300 years and loss of intruder barrier at 500 years for Class B/C	To develop Class limits U.S. assumed: three stylized, reasonable, but conservative intruder scenarios: discovery; intruder-construction; and intruder-agriculture; no drinking water pathway	To develop Class limits U.S. assumed continuation of current processes, such as radioactive decay and waste container degradation , but no evolution, such as sea level rise or volcanism	The U.S. does not require a site-specific safety assessment for protection of intruder if following 10 CFR 61 Class A, B, C requirements. U.S. requires 300-year container integrity and 500-year intruder barrier (or 5 m burial) for Class B/C wastes. Taiwan may require analysis of U, and Th and Ra because U.S did not analyze these for 10 CFR 61 Class limits.
Waste Stability						Must defend assumptions about long-term anti-infiltration, and container integrity and multiple barriers.

3.2. Analysis of Data Needs

Early in the project, INER provided several preliminary documents in response to Sandia requests for information on the geologic setting, environmental characteristics, waste inventory and characteristics, facility design information, and relevant regulations. The information provided was evaluated for use in developing the framework for the assessment. As expected due to the very early state of the program and limitations imposed on the program, information was quite sparse for most parameters and other questions were raised about the appropriateness and applicability of some of the information. However, because the goal of the project was a preliminary system performance assessment, it was possible to identify these situations and to make assumptions to allow the analysis to proceed.

Observations on Waste Inventory

The "Inventory of Low-Level Radioactive Waste in Taiwan" report contains a summary of the inventory of low-level radioactive waste (LLW), which will be used as a planning basis for selecting a site and designing a final disposal facility in Taiwan (INER, 2005a). The report concludes that the total anticipated activity of operating and decommissioning LLW is approximately $2.54 \times 10^{+4}$ Ci contained in about 966,000 fifty-gallon drums. Although inventory estimates involve significant uncertainty and a large number of assumptions, Sandia made an observation that the total activity seemed unusually low and performed a quick review of the document and its underlying assumptions. The following summary observations were made and communicated (in more detail) to INER for their use:

- Operational waste volumes were based on historical data and are assumed reasonable.
- Limited detail was provided to enable evaluation of decommissioning waste volumes from the research reactors, Lanyu storage site, and Volume Reduction Center.
- For NPP decommissioning waste volumes, updated U.S. estimates of NPP decommissioning waste volumes suggest a potentially much smaller volume of waste may be generated (425,000 drums vs. 634,000 drums).
- Simplistic calculations were made, which indicate it likely activated metal components (such as the reactor shroud containing the bulk of the decommissioning activity) were excluded from the NPP decommissioning inventory.
- Radionuclide inventories shown for operational wastes stored at INER appear lower than expected from typical national medical and industrial sources, and it was suggested the national inventory for Taiwan be further investigated.

- No activity estimates from operations and decommissioning of the Lanyu facility or the Volume Reduction Center appeared to be included, and no reference provided for activity estimates of research reactor decommissioning.

Waste Volume

Four waste streams were specified for developing estimates of the decommissioning waste inventory, including:

- NPP decommissioning waste (634,000 drums)
- INER and Tsing-Hua University research reactor decommissioning (33,000 drums)
- Lanyu LLW storage site decommissioning (11,000 drums)
- Volume Reduction Center decommissioning (2,000 drums).

For the three smaller streams, insufficient detail was provided to evaluate the estimated volumes, and it was assumed they are also reasonable realistic. Estimates of the volume of decommissioning wastes for the NPPs, however, are described as based on NUREG/CR-0672 (NRC, 1980) for BWRs and NUREG/CR-0130 (NRC, 1978) for PWRs. These two reports provide estimates of decommissioning inventories for particular NPPs selected as reference plants. The values of 16.4m^3/MW(e) for BWRs and 15.2 m^3/Mw(e) for PWRs for estimating decommissioning waste volume used in the INER report were traceable to the reference reports. It was noted, however, that those original analyses were revised in NUREG/CR-6174 (NRC, 1996b) for BWRs and in NUREG/CR-5884 (NRC, 1995) for PWRs. The revised values of 12.4 m^3/MW(e) for BWRs and 5.9 m^3/MW(e) for PWRs (as shown in the Integrated Database, DOE/RW-0006, Rev. 11 (DOE, 1995)) used much lower estimates of concrete debris volumes and higher packaging densities and would result in a smaller overall volume of NPP decommissioning waste (i.e., 84,930 m^3 vs. 126,539 m^3, or equivalently, approximately 425,000 drums vs. 634,000 drums).

Waste Activity

Approaches similar to that used to estimate waste volume were applied in the INER report to the estimates of waste activity, i.e., activity estimates for operating wastes from NPPs and INER were derived from historical records and extrapolated, while NUREG/CR-0130 and NUREG/CR-0672 were again used as a basis for estimating activity inventories from NPP decommissioning.

NPP Decommissioning

A total of 14,900 Ci at 2070 is estimated in the INER report for the NPP decommissioning waste from the four NPPs operating for 40 years. From Table 3.1 of the INER report, this implies a post-operation decay time of approximately 50 years for the three NPPs currently in operation and of about 25 years for the NPP under construction.

For comparison purposes against the following calculations, Table 4-3 of the INER report shows a decommissioning inventory of 107 Ci for NPP Unit 1, a 636 MW(e) BWR. From Table D.34 of the Draft Environmental Impact Statement (EIS) for 10 CFR 61 (NUREG-0782 (NRC, 1981), Vol. 3) and the Integrated Data Base (DOE/RW-0006 (DOE, 1995), Rev. 11), one can estimate values of ~5,700 Ci/MW(e) and ~4,200 Ci/MW(e) for BWRs and PWRs, respectively, for decommissioning waste following prompt decommissioning. Of these totals, Table D.34 implies only 263 Ci/MW(e) for BWRs and 32.8 Ci/MW(e) for PWRs fall into Classes A, B, or C --- the bulk of the radioactivity is in activated metals at concentrations requiring disposal as GTCC. Also, from Table-D.34 of NUREG-0782 (NRC, 1981), excluding the activated metal inventory leaves the remaining inventory as 46 Ci/MW(e) BWR and 45 Ci/MW(e) PWR.

Without attempting to estimate individual radionuclide decay fractions, a very rough estimated value of 0.0222 is used for the following. (The 0.0222 value is the fractional decay factor for activated stainless steel for 50 years from NUREG/CR-0672 (NRC, 1980) Table E.1-1 and is dominated by the relatively slow decay of Ni-63. Similarly, values of 0.00342 for carbon steel and 0.00476 for contaminated steel, the other neutron-activated components comprising the bulk of the activity are also dominated by the slow Ni-63 decay):

- Case 1 (Entire decommissioning inventory – Class A, B, C, and GTCC):
  (5700 Ci/MW(e) * 636 MW * .0222 decay fraction = 80,479 Ci)
- Case 2 (Inventory limited to LLW – Class A, B, and C):
  (263 Ci/MW(e) * 636 MW(e) * .0222 decay fraction = 3,713 Ci)
- Case 3 (Inventory excludes activated metal):
  (46 Ci/MW(e) * 636 MW(e) *.0222 decay fraction = 649 Ci)

Based on these simplistic calculations, it is suspected that the radionuclide inventories shown in Table 4-3 of the INER report (107 Ci for NPP Unit 1) probably exclude large activated metal components (e.g., the reactor core shroud). Although small in volume (NUREG-0782 (NRC, 1981) Table D.34 shows volumes of 138 m^3 and 418 m^3 for the reference 1155 MW(e) BWR and 1175 MW(e) PWR, respectively.), these materials constitute the overwhelming fraction of the total activity of the decommissioning waste inventory.

As a second example, consider the effect of removing just the core shroud from the inventory. Table E.1-6 of NUREG/CR-0672 indicates that the stainless steel core shroud of the reference 1155 MW(e) BWR at shutdown is 3.75 m^3 in volume and contains ~6.3 x 10^{+6} Ci, corresponding to a volumetric concentration of 1.68 x 10^{+6} Ci/m^3. Table E.1-1 shows a volumetric concentration of 2.85 x 10^{+6} Ci/m^3 for neutron activated stainless steel, implying the shroud

represents ~59% (1.68/2.85) of the stainless steel activity. At 50 years, the radioactivity concentration initially present ($2.85 \times 10^{+6}$ Ci/m^3) for neutron activated stainless steel has decreased by a factor of 0.0222 to $6.3 \times 10^{+4}$ Ci/m^3, of which 59% is due to the core shroud, i.e., at 50 years, the core shroud volumetric activity is $3.7 \times 10^{+4}$ Ci/m^3, which is equivalent to 140,000 Ci in the 3.75 m^3 volume. Applying a scaling factor for the power difference (636 MW(e)/1155MW(e) = 0.55), reduces this value to 77,000 Ci. Finally, from Table E.1-1 at 50 years, the total fractional decay factor of 0.0222 is dominated by that of Ni-63 of 0.0217, i.e., 98% of the total radioactivity or 75,460 Ci at 50 years is due to Ni-63 in the core shroud. This value is significantly larger than the 3.51 Ci shown for Ni-63 in INER Table 4-3 for NPP Unit 1, again suggesting the exclusion of neutron-activated material from the inventory shown in the INER report.

Other than NPP Decommissioning

A total of 2,090 Ci is estimated in the INER report for the operations waste accumulated at INER from 1977 to 2045 and corrected for decay to 2070. Assumedly, this estimate includes the LLW generated by INER's research reactor, hospitals, industry, and other research institutions as mentioned in Section 3.1.6 of the INER report. If that assumption is true, the estimate of 2,090 Ci seems rather low and clarification of what is included in this total is needed. A more typical national inventory of sealed sources, for example, would have significantly higher activity than this estimate. [An evaluation of a report (Vicente et al., 2004) on the sealed source inventory in Brazil (a country of ~186 million people) gives a (corrected) estimate of $7.13 \times 10^{+5}$ Ci --- using that ratio for the 23 million people in Taiwan, one estimates ~9,000 Ci from sealed sources alone.] It is not clear if the inventory of medical and industrial waste in the INER report represents all such waste in Taiwan, or for example, perhaps only represents a small fraction of orphan material which ends up in storage at INER, while the majority of the medical and industrial inventory remains in storage at the owning locations or is returned to the original manufacturer outside of Taiwan.

An estimate of 144 Ci is given for the activity resulting from INER and Tsing-Hua University research reactor decommissioning, but no reference is provided for the estimate. Activity estimates from operations and decommissioning of the Lanyu interim storage site or the Volume Reduction Center are not provided or described.

Observations on Other Data Needs

Early in Phase I, Sandia was provided some preliminary site and design data and asked for comment. Sandia identified several areas in the areas of hydrology, subsurface geology, and design where additional data would be important to the performance assessment work. Well data, streamflow data, hydraulic conductivity data, fracture orientations, surface topography, details of the cover design, waste container and disposal cell material characteristics, and more detailed inventory information (e.g., radionuclide distribution over waste forms, disposal locations of different waste types) are examples of such data needs, which were discussed during the initial Phase I visit to INER in June 2005. In response, INER provided additional

information and assumptions where available, but also emphasized that very little site specific data were available and that design information was quite preliminary.

3.3. Performance Assessment Model

The purpose of constructing a performance assessment model is to evaluate the potential performance of a waste disposal site against regulatory requirements and the needs of the decision makers. Performance criteria may include such information as: the potential dose to an exposed population over some specified time period; the magnitude of the peak dose; the time at which the peak dose occurs; identification of the key radionuclides contributing to dose; the time it takes for initial failure of the waste packages; the importance of engineered barrier materials to impeding radionuclide transport; etc. For preliminary scoping analyses, the performance assessment model might be rather simplistic, employing such tools as analytical models for rapid analyses of the sites. As more information becomes available, the models are likely to become more sophisticated. Likewise, the processes that are simulated may be rather limited when first configuring a model, and become more representative of site conditions as more data becomes available.

Two types of modeling analyses are considered: deterministic and probabilistic. Deterministic analyses are single realizations of a model. They may be used to gain understanding of different conceptual model designs or different parameter specifications. Probabilistic analyses provide much more information about the site performance. Uncertainties in the input parameters are translated into uncertainties in the performance of the model. Statistical analysis of the model output can be made from uncertainty analyses in order to assess confidence in the model results. A probabilistic model provides the data that can be used to support a more comprehensive sensitivity analysis. The sensitivity analysis provides a means of evaluating the importance of the input parameters compared to selected outputs, such as dose. This information may be helpful in prioritizing characterization needs, for instance.

One of the key performance measures that these analyses are concerned with is the dose limit to an exposed population, which is 25 mrem/yr. The performance assessment considers a hypothetical drinking water well located 100 meters down-gradient of the waste disposal facility as the main point of compliance. Other exposure scenarios may be evaluated as well.

Features, Events, and Processes

U.S. and international guidance suggest developing a comprehensive list of features, events, and processes (FEPs) considered in modeling performance of a radioactive waste disposal system. As decisions are made on whether or not to include an individual factor in the model of the system, the disposition of each of these entities should be documented to provide traceability and enhance defensibility of the overall assessment. This methodology has been used at Sandia for the Waste Isolation Pilot Plant (WIPP), Yucca Mountain Project (YMP), Greater Confinement Disposal (GCD) and other projects, and adopted internationally on a number of high-level waste programs. Screening arguments used to include or exclude a factor or set of factors may be

based on probability of occurrence, consequence of impacts, relevance, and regulatory exclusion. FEPs which are retained ("screened in") then provide a basis for developing conceptual models and scenarios reflected in the system model for the assessment and focus data collection efforts. Sandia made a presentation on this methodology at INER in October 2005 and recommends its use on the LLW disposal program. INER has made some progress on adopting the concept, but may defer full implementation to future stages of the program.

3.3.1. General Conceptual Model and Specifications

Figure 7 shows a very high-level depiction of the overall conceptual model of the LLW disposal system. Water enters the system through the engineered surface cap in the shallow land disposal concept or percolates through the overburden of the mined cavern disposal concept. Infiltrating water contacts the waste, following the eventual failure of the concrete containment and waste containers due to corrosion processes. Radionuclides in the waste form are leached out and transported through either an unsaturated and/or saturated hydrologic regime to groundwater. In the model, a drinking water well at 100 m down gradient is assumed, and potential dose exposures are due to consumption of water contaminated by the released radionuclides along drinking water and food consumption pathways. As this high-level conceptual model is refined and more detail added, a much greater level of specificity is established based on known and assumed characteristics and processes associated with each site and design concept, as described below.

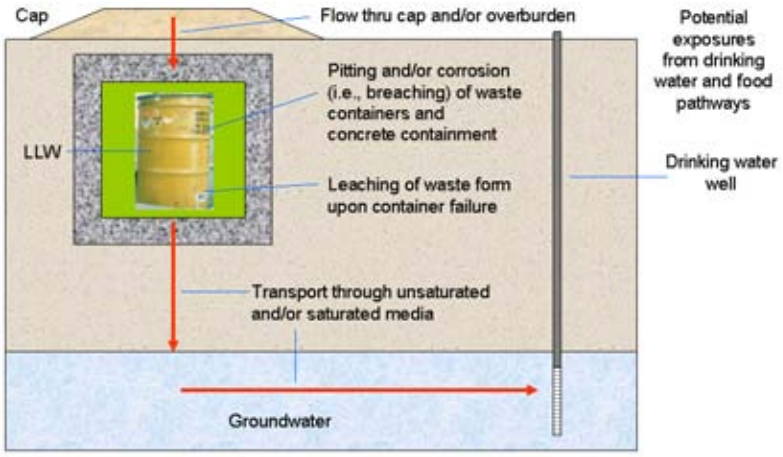

Figure 7. Illustration of the Conceptual Model of the Release and Migration of Contaminants from a LLW disposal system.

Alternative Conceptual Models for Transport

Two alternative conceptual models are considered for radionuclide transport processes:

- Advective-Dispersive Transport – modeled in the near-field with BLT-MS breach and leach processes and in the far-field with 2-D finite element transport processes of BLT-MS; and
- Matrix Diffusion Transport – also modeled in the near-field with BLT-MS breach and leach processes, but in the far-field modeled with three separate 1-D pipe segments for matrix diffusion processes in GoldSim.

Mathematical Models and Code Representations

The following software codes were selected for use in the performance assessment:

1. **GoldSim** (to implement a probabilistic analysis that will explicitly address uncertainties, and to simulate one-dimensional matrix-diffusion transport);
2. NRC's Breach, Leach, and Transport – Multiple Species (**BLT-MS**) code (to simulate waste-container degradation, waste-form leaching, and advective-diffusive transport through the host rock);
3. Finite Element Heat and Mass Transfer code (**FEHM**) (to simulate groundwater flow and estimate flow velocities);
4. Hydrologic Evaluation of Landfill Performance Model (**HELP**) code (to evaluate infiltration through the disposal cover);
5. **AMBER** code (to evaluate human health exposures); and
6. NRC's Disposal Unit Source Term – Multiple Species (**DUST-MS**) code (to screen applicable radionuclides).

The following model assumptions are embodied in the mathematical models and structure of the performance assessment model:

1. BLT-MS can model most of the desired processes, including: breaching of the containers, e.g. by localized and general corrosion; leaching of the waste form, e.g., by rinse, diffusion, and dissolution processes; and transport in the host rock, e.g., by advective-dispersive transport.
2. The flow system can be modeled separately with the FEHM code and Darcy flow velocities abstracted for input to BLT-MS.
3. Infiltration through the cover for the near-surface disposal concept can be simulated with the HELP code and input to FEHM.

4. Matrix diffusion is considered an alternative conceptual model for transport in the host rock, and is employed in this process within GoldSim.
5. Biosphere effects will be modeled with AMBER to produce Dose Conversion Factors (DCFs) and input to GoldSim. (Currently, DCFs are derived from other studies.)
6. Probabilistic analysis using the GoldSim code is desired to quantify uncertainties.
7. It is further assumed that both the near-surface disposal concept and the mined cavern disposal concept will have similar source term inventories, i.e., radionuclides of concern, types of waste containers, and types of waste form leaching processes.
8. For both design concepts, the point of compliance is assumed to be a domestic drinking water well 100m down-gradient from the disposal facility.
9. Release of radionuclides in the gas phase is not considered in this preliminary performance assessment model. The depth below ground surface of the mined cavern disposal system precludes significant releases via the gas phase. For the near-surface disposal system, the low permeability of the cover design would limit the upward migration of gas; however, ^{3}H and ^{14}C are significant components of the inventory and have the potential to migrate in the gas phase.
10. Differences considered between the two design concepts include: different host rocks, different flow fields, different disposal cell layout configurations, and the presence of an engineered cover only for the near-surface disposal concept.

Additional Assumptions

Source Term – limited to a selection of 10 radionuclides selected based on sufficiently long half-life, contribution to total source activity, and mobility.

Container Types – Carbon steel drums, galvanized steel drums, and concrete overpacked drums.

Waste Form Release Mechanisms – Arithmetic distribution over four mechanisms: partitioned rinse, diffusion, uniform degradation, and solubility-limited release. Allocation of release mechanisms reflects relative proportions of different waste types, e.g., solidified operational waste, decommissioning waste, non-solidified wastes, etc.

Waste Inventory

A screening analysis was performed on the waste inventory to determine which radionuclides and which waste forms would be included in the performance assessment analysis. A number of factors and assumptions were considered in developing the waste inventory, such as:

- Only radionuclides with a half-life greater than one year were considered;
- The waste is segregated according to several types, operational and decommissioning waste, and solidified (i.e., grout added to waste form) versus non-solidified waste;

- Only ten radionuclides were considered for this preliminary analysis due to a dimensioning limitation in the BLT-MS code;
- Eight radionuclides with the highest activities were selected for inclusion in the source term;
- Two radionuclides with little sorptive capacity, long half-lives, and high mobility were also included in the inventory.

The activities of each of the selected radionuclides were determined from the inventory for each of the waste type designations selected. The waste type categories and their release mechanisms are: non-solidified operational waste subject to rinse and diffusion release; solidified operational waste subject to diffusion release; non-solidified decommissioning waste subject to rinse and diffusion release; and non-solidified decommissioning waste (i.e., metals) subject to dissolution or a prescribed degradation rate. The activities associated with each radionuclide for each waste type are shown in Table 7. Dissolution was assumed to occur over a 1000 year time frame. Diffusion rates were selected from the literature (NRC, 1989). INER staff pointed out that the final nature of the waste forms has not been established. If the performance assessment modeling were to show that stabilizing or solidifying the waste forms prior to disposal would improve performance then they might consider doing so. Alternate analyses would be run to evaluate this potential. Each of the radionuclides was also subject to solubility limits as well, which could control the timing of the releases.

Table 7. Radionuclide Inventory for the Performance Assessment Model.

Radio-nuclide	Waste type 1 – non-solidified operational waste subject to rinse and diffusion [Ci]	Waste type 2 – solidified operational waste subject to diffusion [Ci]	Waste type 3 – non-solidified decommissioning waste subject to rinse and diffusion [Ci]	Waste type 4 – non-solidified decommissioning waste subject to dissolution [Ci]
Ni-63	$1.64 \times 10^{+2}$	$2.50 \times 10^{+2}$	0	$5.18 \times 10^{+2}$
Cs-137	$1.07 \times 10^{+2}$	$1.63 \times 10^{+2}$	$3.79 \times 10^{+2}$	0
C-14	$2.51 \times 10^{+1}$	$3.83 \times 10^{+1}$	0	0
H-3	$9.78 \times 10^{+0}$	$1.49 \times 10^{+1}$	0	0
Co-60	$6.04 \times 10^{+0}$	$9.23 \times 10^{+0}$	0	2.19×10^{-1}
Sr-90	$3.41 \times 10^{+0}$	$5.21 \times 10^{+0}$	$4.62 \times 10^{+1}$	0
Pu-240	$5.50 \times 10^{+0}$	0	0	0
Pu-239	$6.53 \times 10^{+0}$	0	0	0
Tc-99	6.58×10^{-1}	$1.00 \times 10^{+0}$	1.58×10^{-3}	0
I-129	4.93×10^{-1}	7.53×10^{-1}	1.70×10^{-10}	0

Performance Assessment Model Structure

Infiltration through the engineered cover for the near-surface disposal concept is modeled by the HELP code, which feeds boundary conditions to the FEHM flow model. For the mined cavern

disposal concept, the FEHM flow model alone is used to model hydrologic flow. The BLT-MS code was selected for modeling the release of radionuclides from the waste and their transport to the accessible environment under the influence of the FEHM flow fields. The GoldSim code was used to perform the probabilistic variations of the BLT-MS code under the FEHM-driven flow conditions. Concentrations of radionuclides reaching the 100-m system boundary as a function of time were then converted to dose for determining compliance with the performance objective for protection of the general member of the public.

In the preliminary performance assessment, a base case analysis was first performed for the two site design concepts. The conceptual model for the analysis incorporated the models and assumptions described above. It is important, however, to recognize the limitations of the analysis and the large number of factors excluded from the system, some of which may significantly enhance performance if incorporated into the model. For example, additional details can be added to the system model to incorporate and represent in more realistic detail the performance of engineered barriers. Design configuration details such as the distribution and packaging of various waste forms and dimensional characteristics of disposal cells may also contribute to performance. Many of these parameters, however, will remain unknown quantities until characteristics of a specific site are determined and advanced design details become available. Sensitivity and uncertainty analyses on the system may also provide significant information useful in focusing site characterization and design activities.

To gain some initial insight into the effects of potential improvements in performance, in addition to the base case analysis, alternative case analysis was also performed. The alternative case analysis incorporated somewhat different conceptual models of the system (e.g., additional or different engineered features, varied repository elevation) and different assumptions (e.g., different flow domains and release mechanisms).

3.3.2. Groundwater Infiltration Model

For the near-surface disposal system concept the infiltration of precipitation can play an important role in the potential release of contaminants from the system. An engineered cover or cap is designed to limit infiltration into the disposal cell by the lateral diversion of downward percolating moisture or by enhancing evapotranspiration from the upper layers of the cover. The preliminary cover design for the near-surface disposal system at potential Site #7 is shown in Figure 8.

A numerical model of infiltration is constructed to estimate the rate of infiltration for use in groundwater flow and transport simulations in the performance assessment model. This model is implemented with the HELP software code (EPA, 1994) for the climatic conditions and the preliminary cover design at potential Site #7. Climatic conditions are simulated using both average values of input parameters and site-specific weather data. Reasonable values for the cover material parameters, based on engineering judgment, are used in the infiltration model, given the lack of measured values.

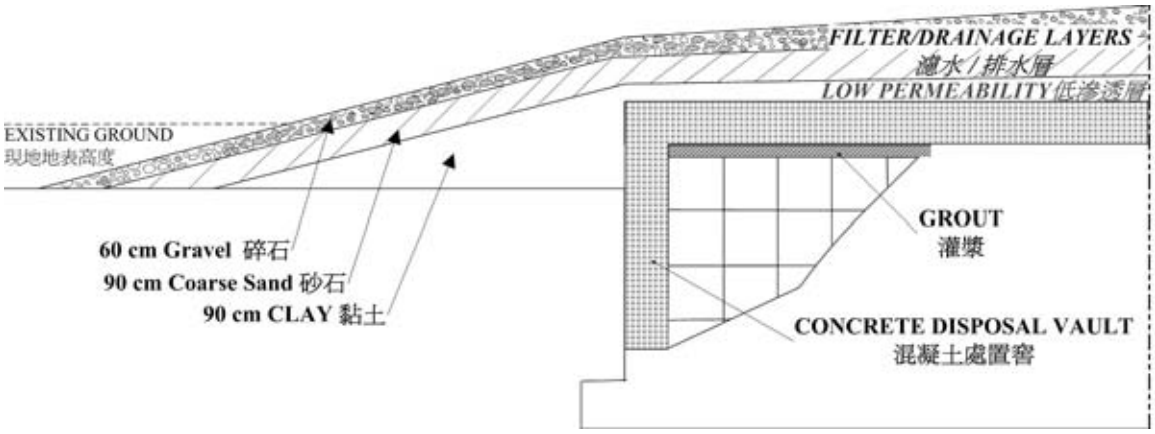

Figure 8. Cross Section of the Cover System for the Near-Surface Disposal System.

3.3.2.1. HELP Software Code

The Hydrologic Evaluation of Landfill Cover Performance (HELP) model is a software code developed primarily at the U.S. Army Corps of Engineers Waterways Experiment Station that has been used since the early 1980s to assist designers and regulators to evaluate the performance of proposed landfill cover designs. The HELP code accounts for numerous processes associated with the water balance of covers, including variability in weather, surface runoff, infiltration, evapotranspiration, vegetative growth, soil moisture storage, unsaturated percolation, lateral subsurface drainage, and leakage through geomembrane liners, as illustrated in Figure 9. HELP can also be used to simulate water movement through waste and the collection of leachate by sub-waste liner systems. Version 3 of the HELP software is used here.

The HELP code is a quasi-two-dimensional, deterministic, water-routing model for determining water balances. Numerous simplifying assumptions are used in the simulation of the physical processes included in the model. Although these simplifications may provide adequate approximations of water movement for typical environmental conditions and design configurations, the user of the software must exercise caution in model construction and interpretation of the results. Favorable comparisons between HELP results and field observations have been obtained for humid climatic settings, but the software is probably less suitable for use under arid conditions. The engineering documentation for the HELP software contained in the accompanying data archive has detailed discussions of the mathematical models used and the assumptions made in the code.

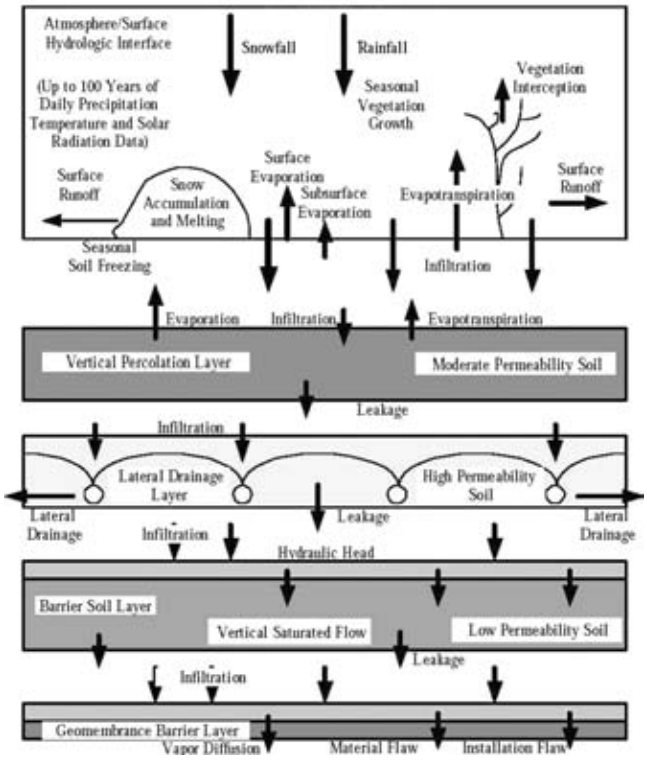

Figure 9. Illustration of Hydrologic Processes in the HELP Software Code.

The HELP software incorporates a database of weather data (e.g., precipitation, temperature, and average wind speed) for numerous locations in the United States. These inputs can be edited to be consistent with site-specific information. Daily weather records can be used directly as input boundary conditions for the HELP model or a synthetic (stochastic) weather record can be generated based on local weather statistics. The software also includes a database of material properties (e.g., saturated hydraulic conductivity, porosity, field capacity, and wilting point) for different soil types.

3.3.2.2. Example Infiltration Model and Results

A preliminary example model for infiltration and percolation through the fictitious cover design at Site #7 was constructed for the HELP software code. Information used in the construction of the example model was taken from the report on "Supplementary Data for LLW-ICP Project", LLW-ICP-I-INER-DOC-007 (INER, 2005b) and from the report "Description of Near Surface Disposal Concept of Low-Level Radioactive Waste Repository in Taiwan", LLW-ICP-I-INER-DOC-005 (INER, 2005c). Several assumptions, interpolations, and approximations were required, but an attempt was made to use reasonable values in the example model.

Weather data from Orlando and Miami, Florida taken from the HELP software database were used as the starting point of the climatic modeling. These locations were chosen because of their sub-tropical climate and presumed similarity to Site #7 in Taiwan. However, the monthly average values for precipitation and temperature were altered to match the information on potential Site #7. The monthly average values of precipitation used in the model are shown in Table 8. Note that the average monthly values of precipitation were interpolated between the values given for June and December, but the total annual average value of precipitation is approximately equal to the value of 950 mm given for Site #7. The approximate weighted average wind speed for the site of 18.6 km/hr was also specified in the example model. Approximate quarterly average values of relative humidity are shown in Table 9 and were also used in the example model. These inputs were used to generate a synthetic daily weather record using the HELP code.

Table 8. Monthly Average Values of Precipitation and Temperature for Potential Site #7.

Month	Precipitation (mm)	Temperature (°C)
January	15	16
February	20	16
March	30	20
April	50	23
May	100	26
June	209	28
July	180	30
August	150	30
September	100	28
October	60	24
November	22	20
December	12	17

Table 9. Quarterly Average Values of Relative Humidity for Potential Site #7.

Quarter	Relative Humidity (%)
First	83
Second	85
Third	87.5
Fourth	80.5

The waste cell configuration, cover design, and materials were specified in the example model as follows. The approximate dimensions of one of the waste cells shown for potential Site #7 is about 200 m by 400 m and the drainage layer of the cover was assumed to drain over a distance of 200 m with a slope of 2%. The example model consists of six layers from top to bottom: 1) 60 cm of riprap, 2) 30 cm of gravel, 3) 30 cm of pea gravel, 4) 30 cm of sand, 5) 90 cm of

compacted clay, and 6) 60 cm of gravelly sand. Layers 2, 3, and 4 constitute a lateral drainage layer; however, it should be noted that the HELP code treats only the bottom of the three layers as a lateral drainage layer in the simulations. Combining these three layers into a single layer of intermediate texture does not seem to have a large impact on the simulation results, but may be important for some of the sensitivity analyses. Material properties for these layers are taken from the database in HELP and the values used in the example model are shown in Table 10.

Table 10. Layer Properties Used in the Example Model for Potential Site #7.

Layer #	Soil Type	Saturated Hydraulic Conductivity (cm/s)	Porosity	Field Capacity	Wilting Point
1	Gravel	3.0×10^{-1}	0.397	0.032	0.013
2	Gravel	3.0×10^{-1}	0.397	0.032	0.013
3	Coarse Sand	1.0×10^{-2}	0.417	0.045	0.018
4	Sand	5.8×10^{-3}	0.437	0.062	0.024
5	Compacted Clay	1.0×10^{-7}	0.451	0.419	0.332
6	Coarse Sand	1.0×10^{-2}	0.417	0.417	0.018

There are some aspects of the fictitious cover design that are problematic with regard to using the HELP software to model percolation through the cover. The upper layer consists of riprap and the HELP database does not contain parameters for a material that is this coarse. Gravel is used in the example model for the upper layer of the cover. It is difficult to know the appropriate values of evaporative zone depth and vegetative cover for riprap. Upon initial emplacement, infiltration would occur very rapidly through such coarse grained material, no vegetation would be present, and evapotranspiration would be limited. Within some period of time, windblown sediment would probably accumulate in the riprap and vegetation would be established on the cover. The example HELP model assigns a value of 50 cm to the evaporative zone depth to the upper layer as a compromise value. As mentioned earlier, multiple adjacent drainage layers cannot be directly simulated using the HELP code and only the bottom sand layer acts as a drain in the example model.

The preliminary example HELP model was run for a simulation time of 100 years and the average percolation flux through the fictitious cover design was simulated to be 45.0 mm/year. Figure 10 shows the simulated daily precipitation and percolation through the cover over the first five years of the simulation. Seasonal variation in precipitation intensity and highly damped seasonal variation in simulated percolation flux is apparent in the plot in Figure 10. The plot also shows that the annual variations in simulated percolation through the cover are not large. Consequently, the 100 year simulation duration used in the analyses is adequate for estimating the average percolation flux through the cover.

It should be noted that the results from this model are preliminary and need to be examined in more detail to verify self-consistency and adequacy. The intended purpose of the preliminary HELP model is to introduce a template for HELP software inputs and to form a basis for percolation model refinement.

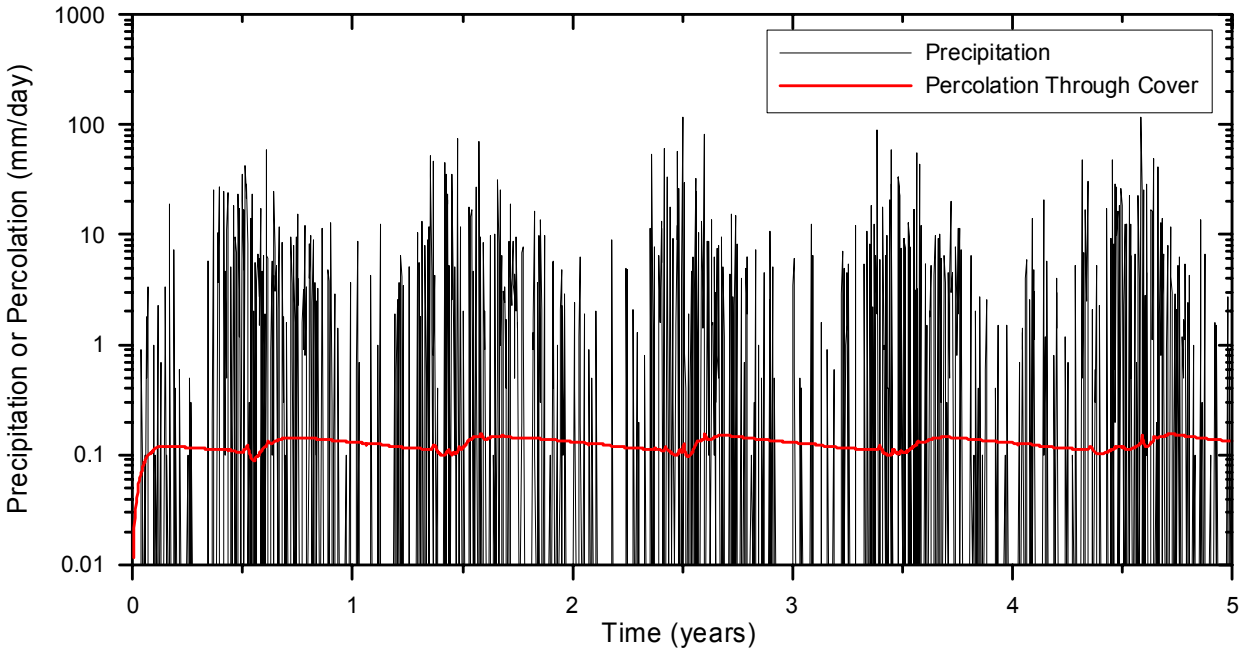

Figure 10. Simulated Precipitation and Percolation through the Cover for Potential Site #7.

3.3.2.3. Infiltration Model Sensitivity Analyses

Several modifications to the preliminary example model of infiltration and percolation were made to examine the sensitivity to model parameters and cover design features. These sensitivity analyses include: 1) uncertainty in the saturated hydraulic conductivity of the compacted clay layer, 2) variations in the slope of the drainage layer, 3) modification of the upper layer to be a soil that enhances moisture storage and encourages evapotranspiration, and 4) incorporation of a high-density polyethylene (HDPE) geomembrane layer below the lateral drainage layer.

Results of the sensitivity to saturated hydraulic conductivity in the compacted clay layer are shown in Figure 11. The simulated percolation flux is relatively highly sensitive to the saturated hydraulic conductivity of the clay, particularly for values above 1.0×10^{-7} cm/s. It is noteworthy that the HELP software database has a default value of saturated hydraulic conductivity for compacted clay of 6.8×10^{-7} cm/s, suggesting that it may be difficult to achieve a value as low as 1.0×10^{-7} cm/s for the field emplacement of the compacted clay layer.

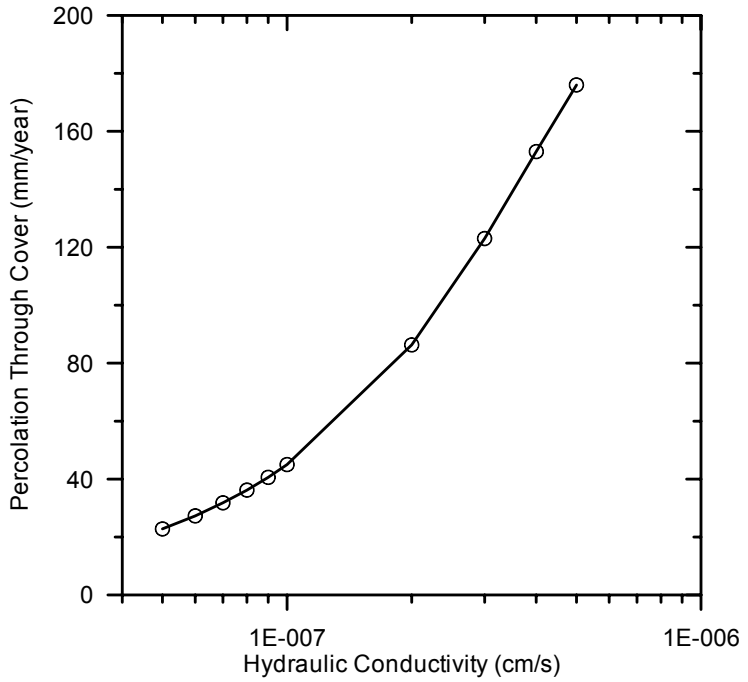

Figure 11. Simulated Percolation Through the Cover as a Function of Saturated Hydraulic Conductivity of the Compacted Clay Layer.

Results of the sensitivity to the slope of the drainage layer are shown in Figure 12. The simulated percolation flux is significantly, but not highly, sensitive to this design characteristic of the fictitious cover design. This conclusion could be conditional on the limitation in the way in which the drainage layer is represented in the preliminary example HELP model, as described above.

The fictitious cover design was modified by changing the upper layer to a fine sandy loam soil and the HELP model was also changed to a maximum evaporative zone depth of 90 cm and a maximum leaf area index of 4, accordingly. This sensitivity run examines the impacts of a vegetated cover with greater evapotranspiration potential, relative to the riprap upper layer. The results of this modified example model indicate a simulated percolation through the cover of 30.9 mm/year, which is significantly lower than the 45.0 mm/year simulated for the fictitious cover design with the riprap upper layer.

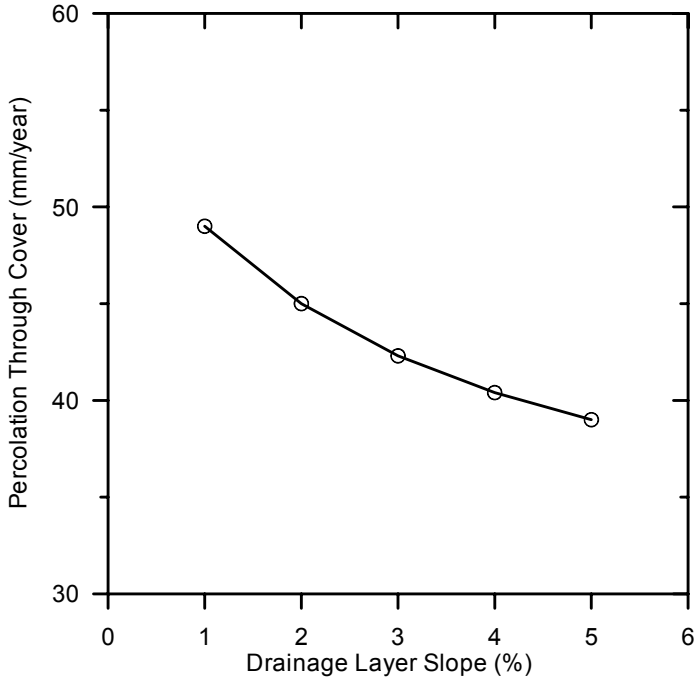

Figure 12. Simulated Percolation through the Cover as a Function of the Slope of the Drainage Layer.

The fictitious cover design was modified in the final sensitivity analysis by adding a HDPE geomembrane layer below the lateral drainage layer to illustrate the impact of such a design feature. Furthermore, the alternative design was simulated for variations in the integrity of the geomembrane by varying the number of barrier defects. The results of this sensitivity analysis are shown in Figure 13. These results indicate dramatically lower percolation through the cover for low density of defects in the geomembrane, with the simulated percolation flux approaching the value from the preliminary example HELP model for values of greater than a few thousand defects per hectare. The plot in Figure 13 gives some indication of the possible evolution of performance over time for a cover with a HDPE geomembrane, because of degradation of the geomembrane. Degradation of HDPE is not well understood, but expert opinion suggests significant degradation after 200 years following emplacement.

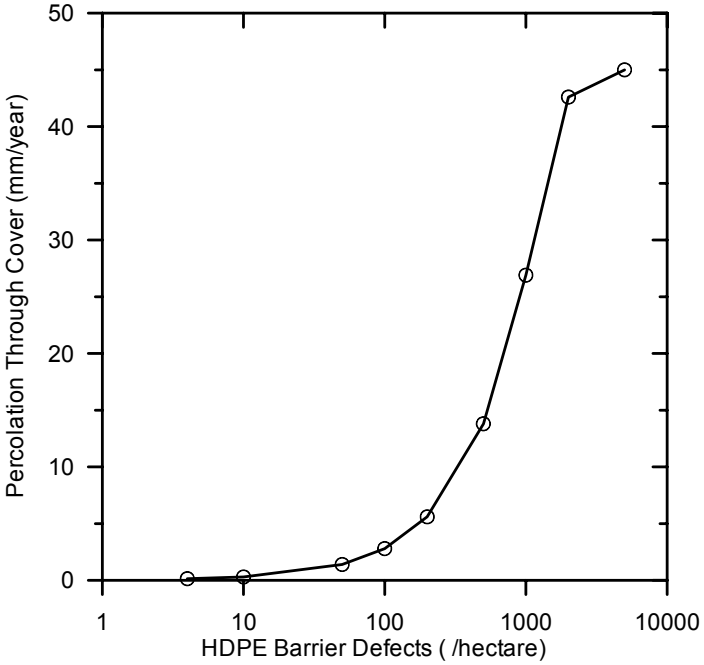

Figure 13. Simulated Percolation Through the Cover as a Function of Defect Density in the HDPE Geomembrane Barrier.

Following the development of the preliminary example HELP model of infiltration, staff at INER obtained weather data for 2001 through 2005 from potential Site #7. The HELP model was revised to use these site-specific data on precipitation and temperature from this time period to simulate infiltration through the cover design. In addition, the HELP model was simplified to three layers, consisting of gravel, a sand drainage layer, and a compacted clay barrier. The infiltration model results from this five-year period indicate percolation through the cover of 49.4 mm/year without a geomembrane barrier and 3.3 mm/year with the geomembrane. These results are somewhat higher than those obtained using the synthetic weather generator in HELP with sites in Florida as proxies for potential Site #7. However, the results using the site-specific weather data are comparable to those from the preliminary HELP model, considering other uncertainties in the simulations.

An additional sensitivity study was conducted using the HELP model with the site-specific weather data along with Monte Carlo sampling of uncertain parameters (SNL, 2000). Latin Hypercube Sampling (LHS) (SNL, 1998) was used to produce 50 realizations with three uncertain parameters (saturated hydraulic conductivity, field capacity, and wilting point) in three materials (gravel, sand, and compacted clay). The uncertainty distributions used in the sampling are shown in Table 11. A positive correlation between field capacity and wilting point was specified in the LHS method, using a correlation coefficient of 0.88 (SNL, 2002).

Table 11. Uncertainty Distributions for Material Properties in the Infiltration Model.

Parameter	Soil Type	Uncertainty Distribution
Saturated Hydraulic Conductivity (cm/s)	Gravel	Log Normal (geometric mean: 0.30, geometric standard deviation: 0.50)
Field Capacity	Gravel	Uniform (lower bound: 0.012, upper bound: 0.052)
Wilting Point	Gravel	Uniform (lower bound: 0.003, upper bound: 0.023)
Saturated Hydraulic Conductivity (cm/s)	Sand	Log Normal (geometric mean: 1×10^{-2}, geometric standard deviation: 0.50)
Field Capacity	Sand	Uniform (lower bound: 0.025, upper bound: 0.065)
Wilting Point	Sand	Uniform (lower bound: 0.008, upper bound: 0.028)
Saturated Hydraulic Conductivity (cm/s)	Compacted Clay	Log Normal (geometric mean: 1×10^{-7}, geometric standard deviation: 0.50)
Field Capacity	Compacted Clay	Uniform (lower bound: 0.35, upper bound: 0.451)
Wilting Point	Compacted Clay	Uniform (lower bound: 0.30, upper bound: 0.36)

The results of the Monte Carlo realizations with the HELP infiltration model (without the geomembrane layer) indicate considerable uncertainty in the percolation flux through the cover at potential Site #7, given the uncertainty in the underlying parameters. These results for the 50 realizations are shown in Figure 14 with the histogram of percolation flux as the red bars of frequency on the left axis. The cumulative probability function (CDF) is plotted as the blue line in the same figure. The median value of simulated percolation flux from the Monte Carlo analysis is about 50 mm/year, which is similar to the value from the base case HELP model. The Monte Carlo results also indicate a wide range of uncertainty, with a small probability that the percolation flux could be greater than 200 mm/year. Conversely, there is a significant probability that the percolation flux would be lower than the expected value of about 50 mm/year.

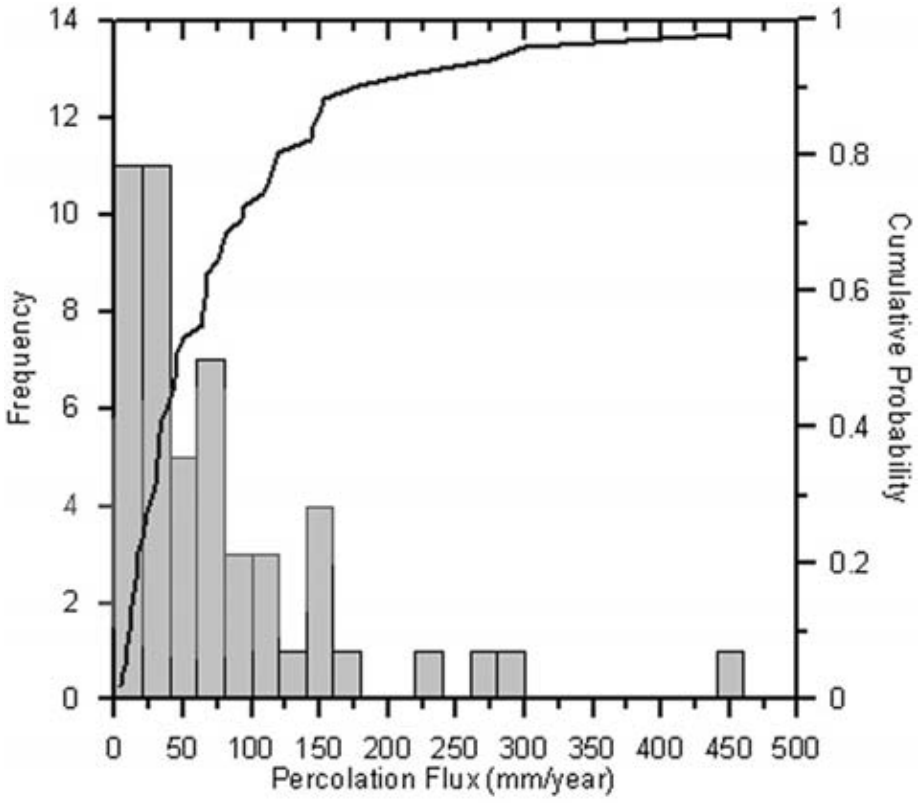

Figure 14. Histogram and CDF of Simulated Percolation Flux from the Monte Carlo Analysis of Infiltration through the Cover.

The results of the Monte Carlo realizations with the HELP infiltration model indicate the greatest sensitivity of simulated percolation flux to the uncertainty in the saturated hydraulic conductivity of the compacted clay layer. This relationship is illustrated in the scatter plot of simulated percolation flux and corresponding sampled value of saturated hydraulic conductivity for clay shown in Figure 15. The positive correlation shown in this figure is consistent with expectations, given the function of the compacted clay layer as a barrier to downward percolation of groundwater within the cover.

It should be noted that the assessment of uncertainty in percolation flux through the cover shown here is preliminary in nature. Data on the properties of materials to be used in construction of a cover system would presumably reduce the uncertainty in parameter values (e.g., saturated hydraulic conductivity of the compacted clay) and lead to a reduction in the uncertainty in percolation flux through the cover.

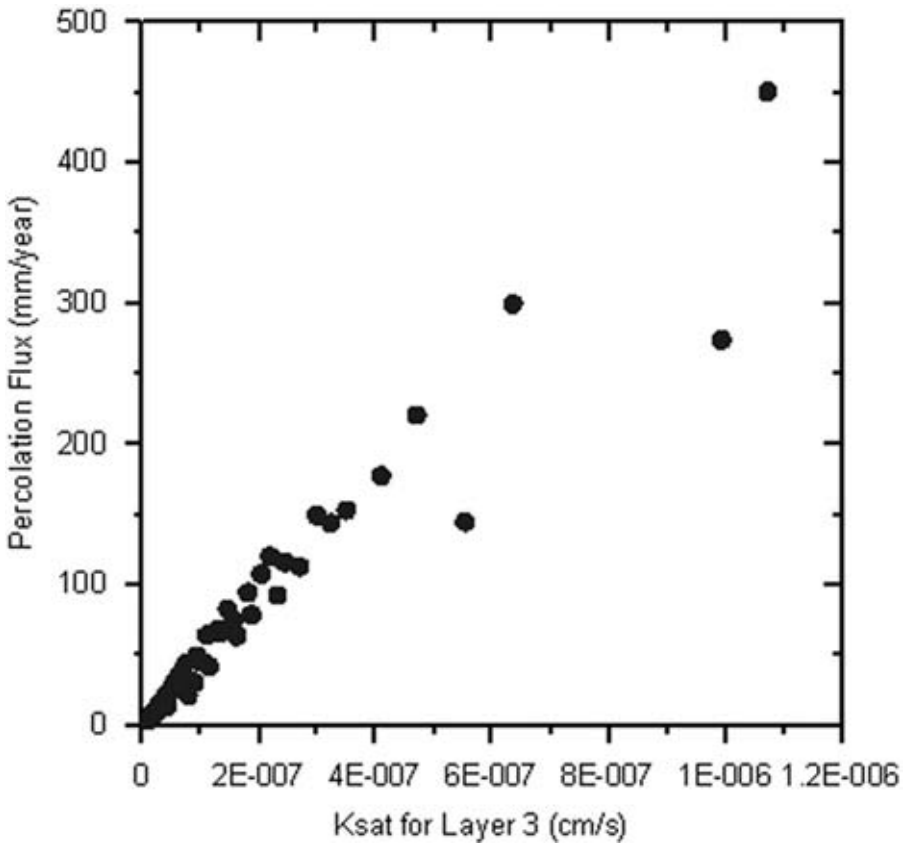

Figure 15. Simulated Percolation Flux Versus Sampled Value of Saturated Hydraulic Conductivity for the Compacted Clay Layer.

3.3.3. Groundwater Flow Model

3.3.3.1. Near-Surface Disposal System Site

A preliminary three-dimensional, site-scale flow model for potential Site #7 has been developed to simulate groundwater flow on the island site. The preliminary site-scale groundwater flow model is implemented with the FEHM software code (Zyvoloski et al., 1997) and is used to estimate the flow vectors along a cross section down gradient of one of the disposal cells on the island. These groundwater flow vectors are exported to the BLT-MS code for radionuclide simulations in the performance assessment model.

It is important to emphasize that both the base case and alternative site-scale flow models for Site #7 were developed with very limited data from the site. There is a large degree of uncertainty regarding the quantitative results produced by these models; however, qualitative comparisons between these alternative conceptual models are of greater reliability. It is possible that site-specific data, if and when it becomes available, would allow researchers to identify the most reasonable interpretation of the hydrogeologic system.

The site-scale flow model for Site #7 was constructed to include the entire island (as shown in Figure 16) and implemented using the FEHM software code. The three-dimensional model domain extends from the assumed interface between fresh water and underlying sea water below the island up to the topographic surface. In the base case site-scale model, the basalt is conceptualized as a homogeneous (but vertically anisotropic) fractured continuum and the sedimentary unit is conceptualized as a porous medium. Although it is recognized that tidal fluctuations and seasonal variations in recharge may cause transience in the groundwater flow system, this preliminary site-scale flow model assumes steady-state flow conditions. The preliminary model also represents the flow system as a confined aquifer, with the topographic surface as the upper boundary. This representation as a confined aquifer is a significant simplification of the groundwater flow system, if the water table is far below the topographic surface, as the model results suggest it may be.

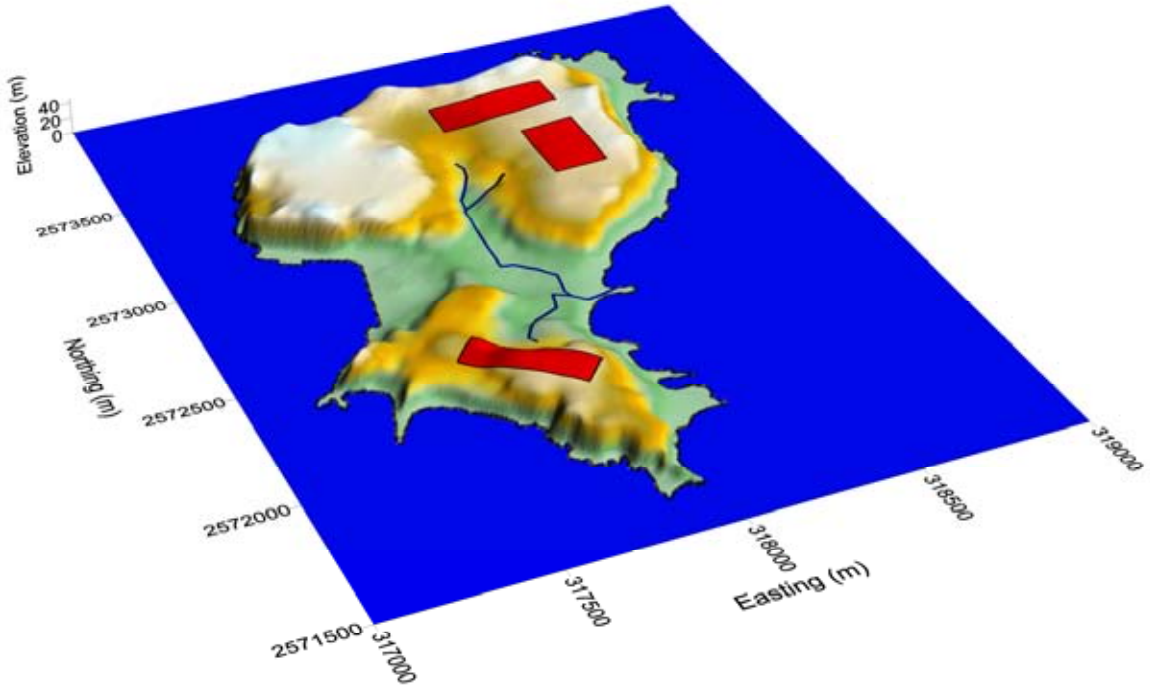

Figure 16. Topography and Low-Level Waste Disposal Cell Locations (Red) of Potential Site #7.

The boundary conditions of the site-scale flow model at Site #7 consist of constant head boundary at the ocean shoreline, no-flow at the lower boundary of the model, and specified recharge flux on the upper surface of the model. The constant head boundary conditions along the shoreline are applied along the margins of the model domain to a depth of 20 m below sea level. The recharge flux in areas other than below the LLW disposal cells is assumed to be 100 mm/year, which is about 10% of the average precipitation at Site #7. The groundwater recharge

flux beneath the disposal cells is specified to be 45 mm/year, based on preliminary calculations of infiltration through the cover design conducted with the HELP software code (see Section 3.3.2).

FEHM Numerical Model

The numerical grid for the Site #7 site-scale flow model consists of three-dimensional triangular prisms and was generated to approximately conform to the shape of the island, as shown in Figure 17. The two-dimensional triangular grid was generated with the Easymesh software code and higher resolution was specified in the areas of the three LLW disposal cells and along the streams. The two-dimensional triangular mesh was projected in the vertical dimension using a FORTRAN routine. The grid was truncated along a sloping lower surface representing the interface between fresh water and sea water and was truncated at the topographic upper surface. A perspective view of the three-dimensional finite-element grid used in the site-scale flow model is shown in Figure 18.

The base case site-scale flow model for Site #7 includes an approximately lenticular shaped zone for the sedimentary unit near the middle of the island. The horizontal permeability assigned to the sedimentary unit is 2×10^{-13} m^2, which is more than an order of magnitude higher than the permeability assumed for the basalt (5×10^{-15} m^2). The ratio of horizontal to vertical permeability in the basalt is specified as 5.0 and this anisotropy ratio is assigned a value of 20.0 in the sedimentary unit.

The recharge boundary conditions are applied in the site-scale flow model by first defining zones with the nodes under each of the LLW disposal cells that occur on the upper surface of the model domain (zones 11, 12, and 13). The other nodes on the upper surface of the model are assigned to zone 6. The total mass rate input to each of these zones (in units of kg/s) is calculated based on the infiltration rate and the total area of the zone. These values are specified in the "boun" macro of the FEHM code and the groundwater inflow is automatically distributed among the nodes within each zone in proportion to the area associated with each node.

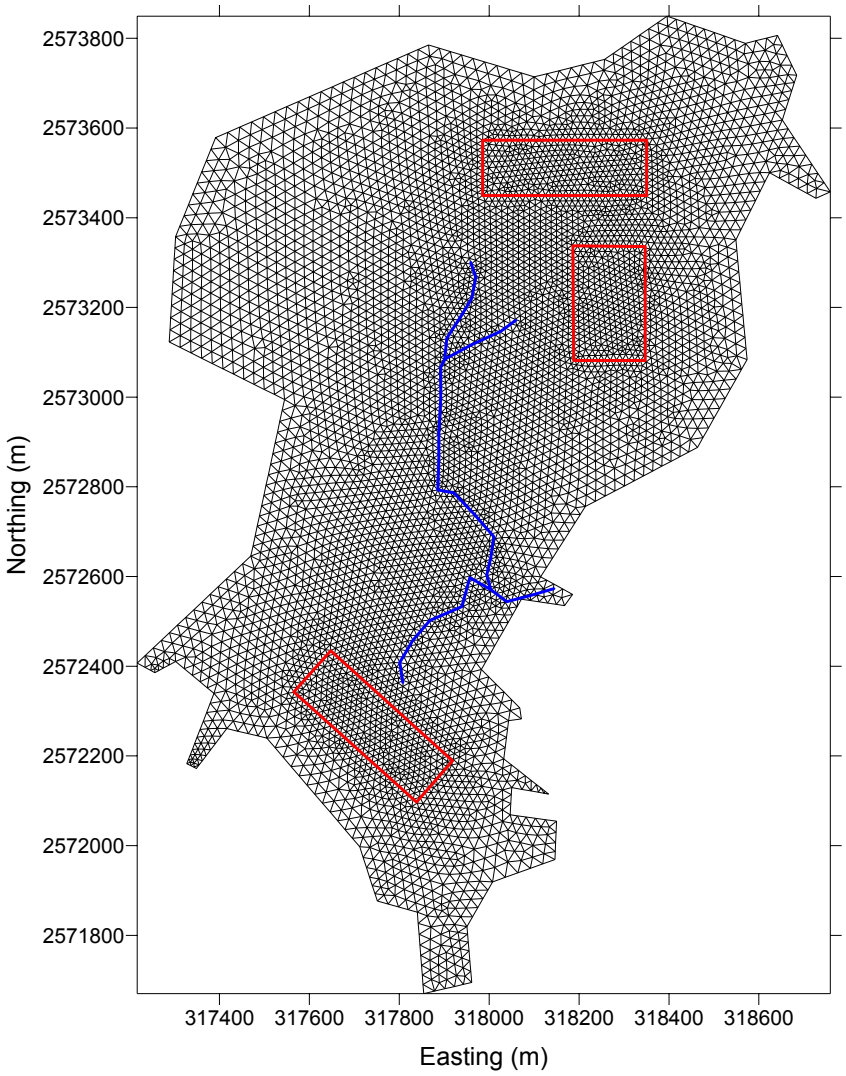

Figure 17. Two-Dimensional Finite-Element Grid for Site #7 with Low-Level Waste Disposal Cells Shown in Red and Intermittent Streams Shown in Blue.

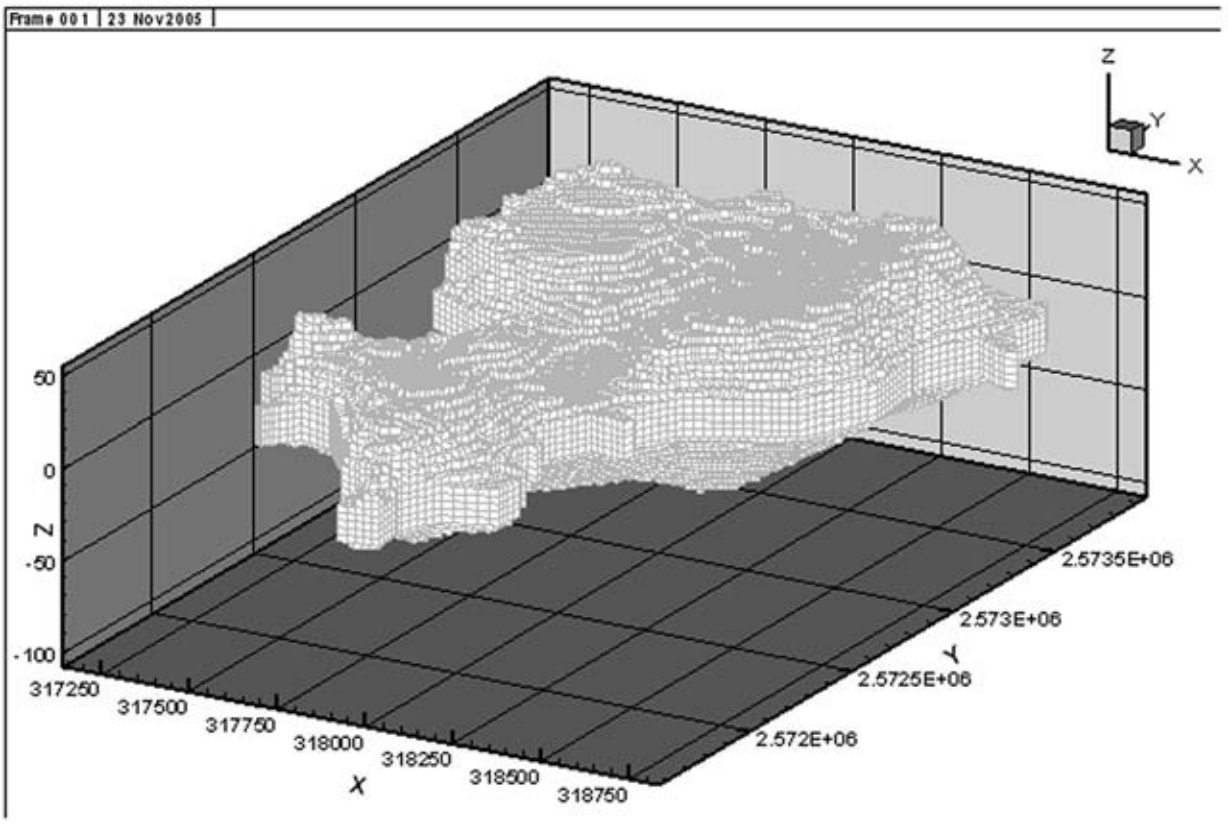

Figure 18. Three-Dimensional Finite-Element Grid for Site #7.

The simulated steady-state hydraulic head at sea level within the base case site-scale flow model for Site #7 is shown in the contour plot of Figure 19. The horizontal gradients in head indicate that groundwater flows generally outward from the more central parts of the island toward the ocean shoreline. The highest values of simulated head (between 3 and 4 m) occur in the north-central part of the island and simulated head is generally much lower than the local topographic elevation.

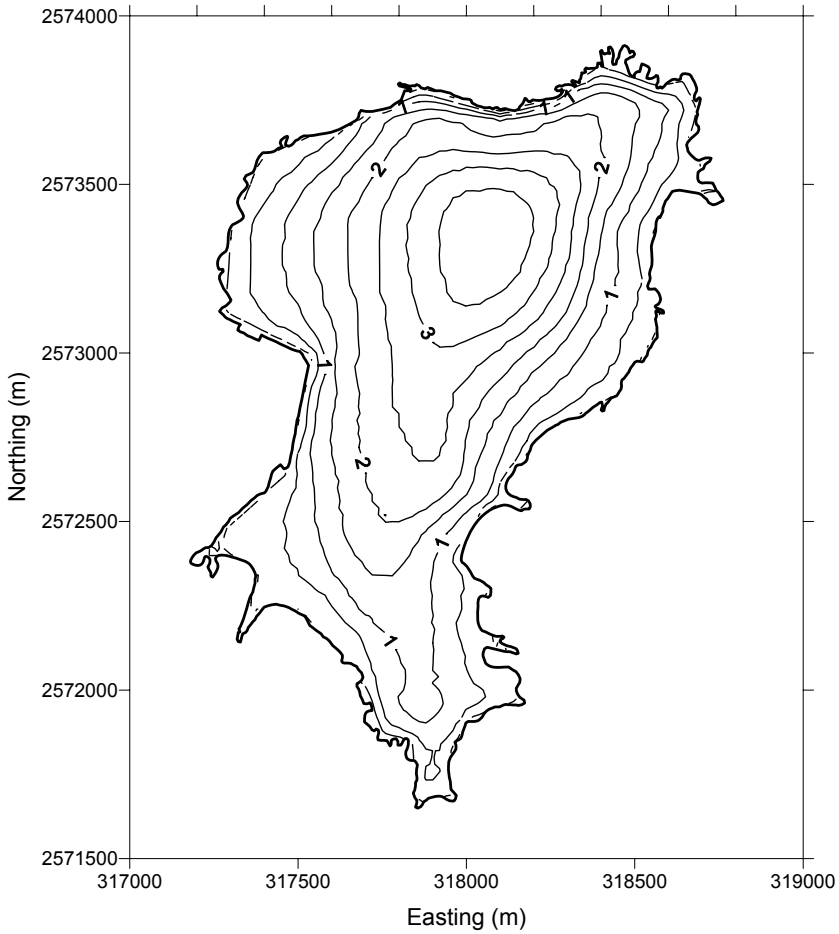

Figure 19. Simulated Hydraulic Head Contours (Meters) at Sea Level for the Base Case Site-Scale Flow Model.

Alternative FEHM Site-Scale Flow Model

The base case site-scale flow model includes the sedimentary unit mapped near the middle of the island as a separate hydrogeologic unit and assumes a higher permeability for this unit than the basalt bedrock elsewhere on the island. This sedimentary unit is also assumed to be roughly lenticular in shape and interbedded between basalt units in the base case flow model. The suggested alternative conceptual model is that the sedimentary unit be assigned the same permeability as the basalt unit. A plausible alternative site-scale flow model was developed for this analysis and the simulated flow vectors were extracted along the previously defined cross section for potential use in the performance assessment model.

The alternative site-scale flow model was produced by simply setting the values of permeability within the sedimentary unit equal to the lower values assigned to the basalt unit. The resulting distribution of simulated steady-state hydraulic head at sea level is plotted in Figure 20. The resulting values of simulated head are significantly higher than in the base case model, with the highest values of greater than 14 m occurring near the center of the island. The higher values of

head and gradient in head are expected, given the reduction in permeability specified for the sedimentary unit in the alternative model. It is also noteworthy that the highest values of simulated head extend southward into the middle portion of the island. In the base case model, the higher-permeability sedimentary unit occurs in this area of the model and tends to drain groundwater away, preventing the build-up of head in the middle part of the island.

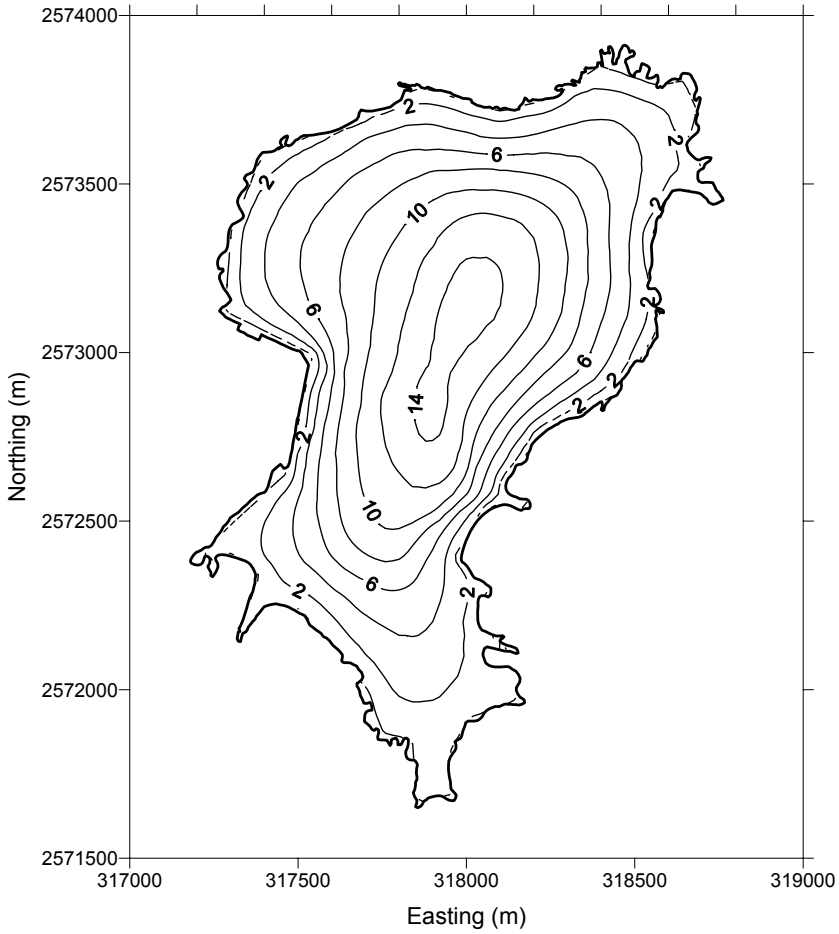

Figure 20. Simulated Hydraulic Head Contours (Meters) at Sea Level for the Alternative Site-Scale Flow Model.

No water level measurements in wells are available to constrain the site-scale flow model for Site #7, but there is some information that is useful. The streams in the middle part of the island are reported to flow only during precipitation events and are therefore not likely to be areas of significant groundwater discharge. There are also no reported locations of natural groundwater discharge in the middle part of the island. Consequently, it is not expected that the hydraulic head in the middle part of the island would be higher than the topographic elevation because this would likely result in some discharge of groundwater to the surface. These inferences place a limit on how high the simulated head can be in the site-scale flow model and still be consistent with the apparent lack of surface water discharge.

Figure 21 shows a contour plot of the difference between the simulated head in the alternative site-scale flow model and the topographic elevation. A positive value of this difference indicates that the simulated hydraulic head is higher than the topographic elevation. The areas with blue shading in Figure 21 show where the simulated head is more than one meter higher than the topographic surface, indicating a strong simulated potential for discharge to the surface. Since no groundwater discharge is reported in the middle part of the island, the simulated head in the alternative site-scale flow model for Site #7 is unrealistically high in this area.

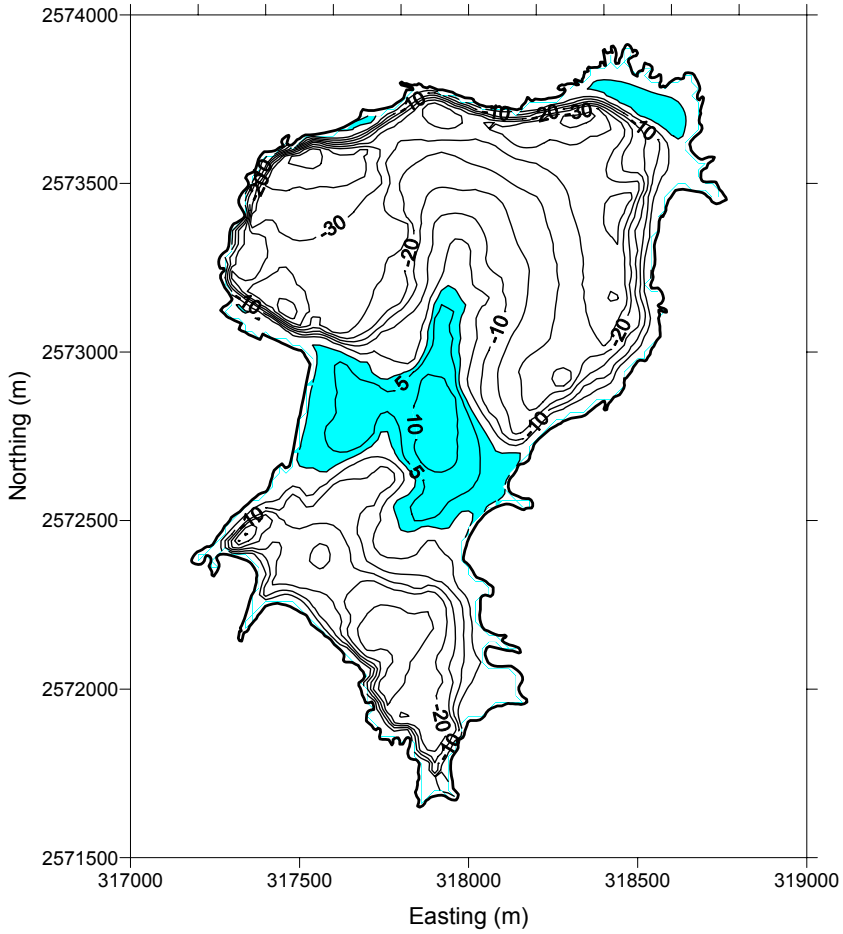

Figure 21. Contours of Difference (Meters) Between Simulated Head from the Alternative Site-Scale Flow Model and the Topographic Elevation with Blue Shading Indicating Areas Where Simulated Head is Higher Than the Topographic Surface.

Based on the inferences described above, a modified alternative site-scale flow model was developed to be consistent with the observed lack of groundwater discharge in the middle part of the island. In the modified alternative site-scale flow model, the sedimentary unit is assigned the same permeability as the basalt unit, but the permeability of both units is increased by a factor of 6 (to 3×10^{-14} m^2 for horizontal permeability). This value of permeability is the approximate minimum value that results in simulated heads in the middle portion of the island that are lower

than the topographic elevation, and thus consistent with observations. The contours of simulated head at sea level from the modified alternative site-scale flow model are shown in Figure 22.

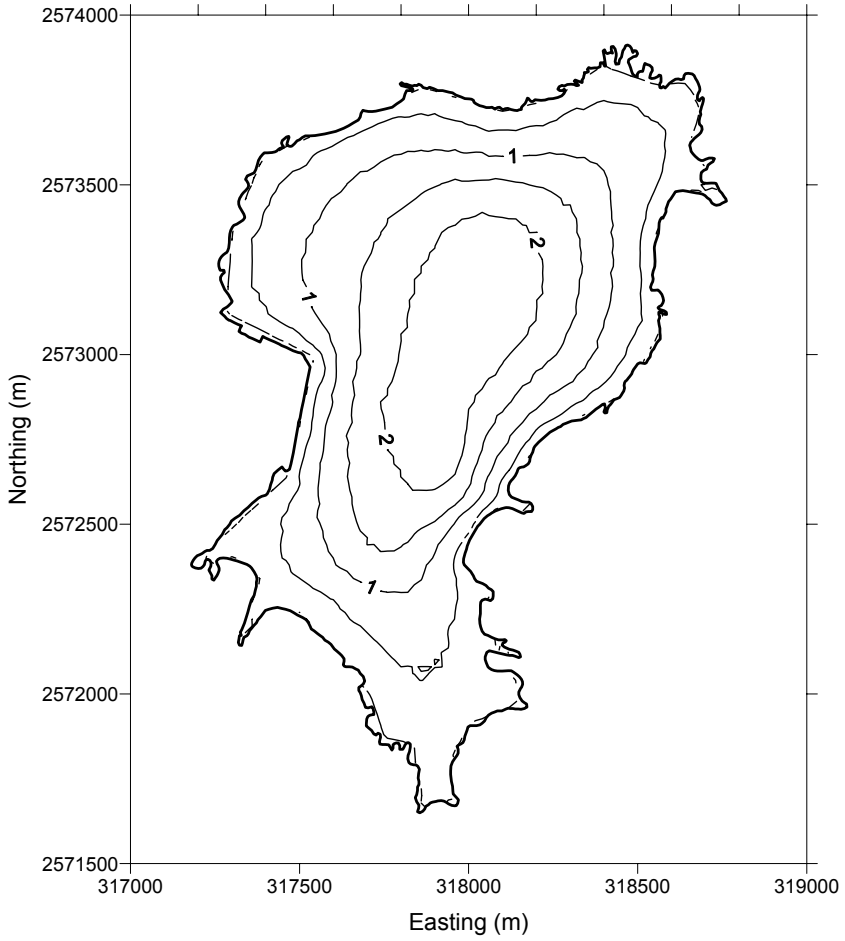

Figure 22. Simulated Head Contours (Meters) at Sea Level for the Modified Alternative Site-Scale Flow Model.

Abstraction of Groundwater Flow Vectors for Radionuclide Transport Simulations

The groundwater flow simulated by the three-dimensional FEHM site-scale flow model for Site #7 is used in the BLT-MS radionuclide transport model for performance assessment analyses. Because the BLT-MS code is limited to two-dimensional simulations, the groundwater flow simulated by the site-scale flow model is extracted along a cross-section through the repository. Although the projection of the groundwater flow vectors onto the cross section is an abstraction of the three-dimensional flow field, it is reasonably accurate because the cross section is oriented approximately parallel to flow below the disposal cell.

The extraction of groundwater flow velocities from the site-scale flow model and their projection onto the cross section is accomplished as follows. The nodes from the flow model that are

located within a specified distance of the cross section are identified and the simulated values of flow velocity are extracted from the FEHM output file. The location of the cross section and nodes extracted from the site-scale flow model are shown in Figure 23. The x and y components of the simulated groundwater flow are combined into a single horizontal component of the flow vector oriented along the cross section. The resulting groundwater flow vectors along the cross section are plotted in Figure 24. Note that the flow vectors in Figure 24 are in units of m/s and the location of the repository is shown by the red rectangle. The plot of the flow vectors indicates that there is generally flow toward the ocean to the right. Vertical groundwater flow is inferred to occur through the repository and in the vadose zone above the water table. The magnitude of downward vertical flow below the repository is estimated from the analysis of infiltration through the cover, using the HELP code (see Section 3.3.2).

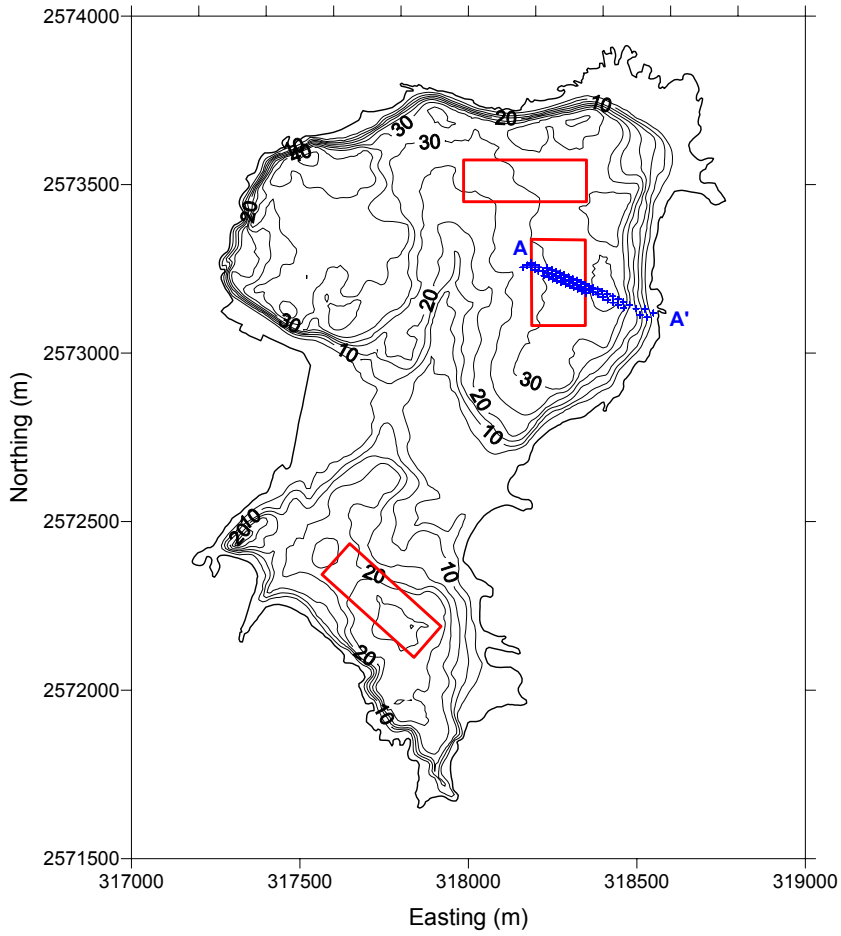

Figure 23. Topographic Contour Map (Meters) of the Site #7 Model Domain and FEHM Nodes Within 20 m of the Cross Section.

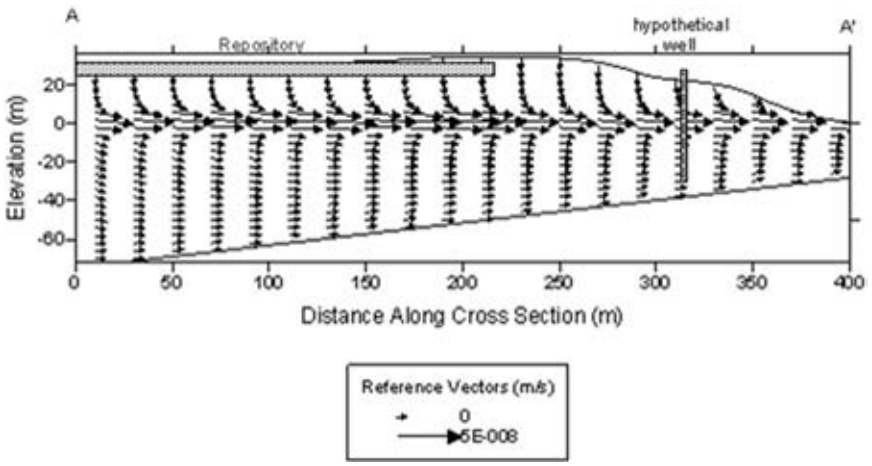

Figure 24. Simulated Groundwater Flow Vectors Along the Cross Section from the Base Case Site-Scale Flow Model.

The simulated groundwater flow vectors along a cross section from one of the LLW disposal cells were also extracted from the modified alternative site-scale flow model for comparison to the base case and potentially for incorporation into the BLT-MS model of radionuclide transport for the performance assessment. The groundwater flow vectors along cross section A-A' are shown for the modified alternative flow model in Figure 25.

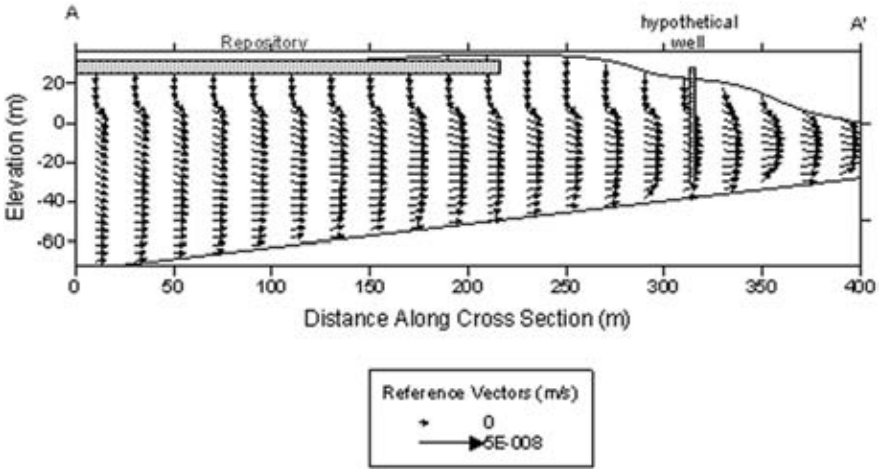

Figure 25. Simulated Groundwater Flow Vectors Along the Cross Section from the Modified Alternative Site-Scale Flow Model.

Comparison of the simulated groundwater flow vectors along the cross section from the base case (Figure 24) and the modified alternative (Figure 25) site-scale flow models indicates that the simulated flow rates are significantly higher within the narrow width of the sedimentary unit of the base case model. However, deeper in the cross section the average simulated flow rate in the modified alternative flow model is somewhat greater than the flow rates in the same areas of the

base case model. The patterns of flow vectors also indicate that flow paths beneath the water table from the LLW repository would be primarily confined to the sedimentary unit in the base case site-scale flow model and would pass through both the sedimentary unit and the deeper basalt unit in the modified alternative site-scale flow model.

The modified alternative site-scale flow model for Site #7 constitutes a credible alternative conceptual model of the flow system for use in the analyses of LLW disposal system performance. The base case flow model and the modified alternative flow model differ primarily with regard to the relative distribution of flow between the hydrogeologic units along the flow path from the LLW disposal cell evaluated.

3.3.3.2. Mined Cavern Disposal System Site

A preliminary three-dimensional, site-scale groundwater flow model for potential Site #6 was developed for use in the performance assessment modeling of the mined cavern disposal system. The preliminary site-scale FEHM flow model calculates the average groundwater flow rate through the proposed repository level at Site #6 and also simulates the groundwater flow vectors down gradient of the repository to the hypothetical well that is the point of release to the biosphere in the performance assessment analyses.

It should be noted that the preliminary Site #6 site-scale flow model was constructed with very limited data from the site. Neither water level measurements from wells nor stream flow data are available for use in calibration of the flow model. Consequently, there is a high degree of uncertainty in the quantitative modeling results. Conceptual insights derived from the preliminary site-scale flow model are presented with somewhat higher confidence, but should be utilized with caution.

The FEHM site-scale flow model for Site #6 was constructed in three dimensions to represent the groundwater flow system in the steep terrain around the repository location, including the ocean shoreline and major streams as probable boundaries. The fractured argillite bedrock is conceptualized as a homogeneous single continuum and it was assumed that the flow system is approximately in steady state. Boundaries of the model domain are located along the ocean and major topographic ridge crests, as shown in the plot of surface topography and stream locations in Figure 26.

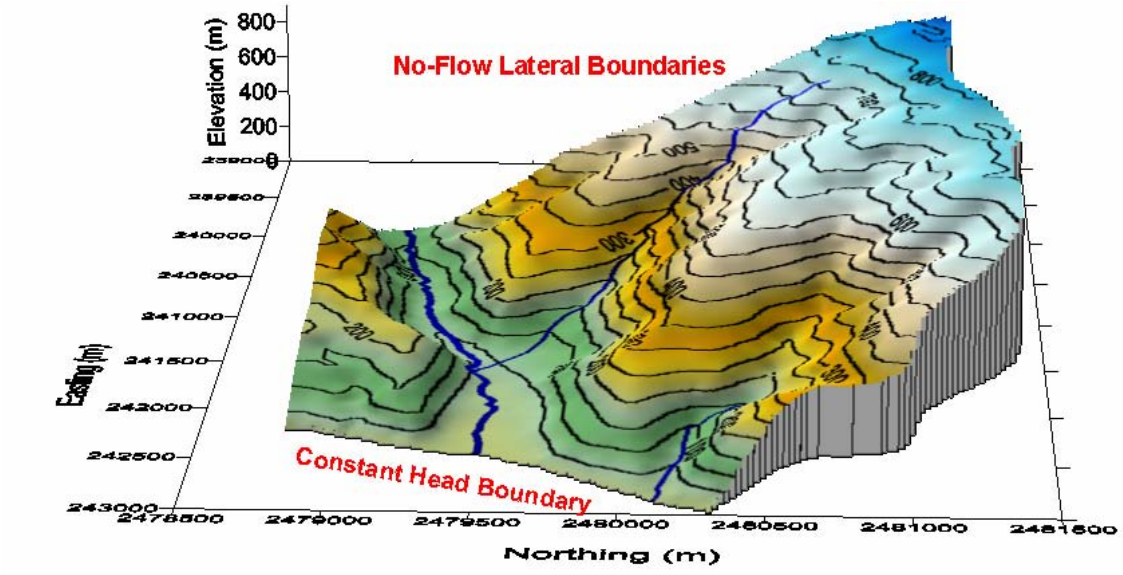

Figure 26. Site-Scale Flow Model Domain and Boundary Conditions for Site #6.

The boundary conditions of the site-scale flow model consist of a constant head boundary at the ocean shoreline, no-flow boundary conditions along the sides and the base of the model, and specified recharge flux on the upper surface of the model. In addition, the streams are represented as head-dependent flux boundaries, in which the flow into or out of the model is controlled by the difference in head in the stream and in the underlying aquifer. The recharge flux is assumed to be 500 mm/year, which corresponds to about 20% of the precipitation at Site #6. The water table is assumed to be not deep in this area (relative to the overall topography) and the flow system is consequently approximated as a confined aquifer.

Contaminant transport simulations with the site-scale flow model were conducted assuming a single continuum for the aquifer (i.e., no matrix diffusion). Since these simulations were conducted to delineate contaminant pathways and discharge locations, this assumption has no impact on the results presented here. The repository was represented as a planar, "smeared" source of contaminants in which the concentration of the source was held constant at a relative value of 1.0.

FEHM Numerical Model

The numerical grid for the Site #6 site-scale flow model was generated as an unstructured triangular finite-element mesh and projected in the vertical direction to produce a three-dimensional grid consisting of triangular prisms. The grid was refined along streams to more accurately represent these features as flow boundaries. The two-dimensional triangular finite-element grid that formed the basis of the three-dimensional grid was generated with the Easymesh software code. A FORTRAN routine was used to generate the three-dimensional grid,

which has a lower surface at -500 m elevation and was truncated at the topographic surface along the upper surface of the grid, as shown in Figure 27.

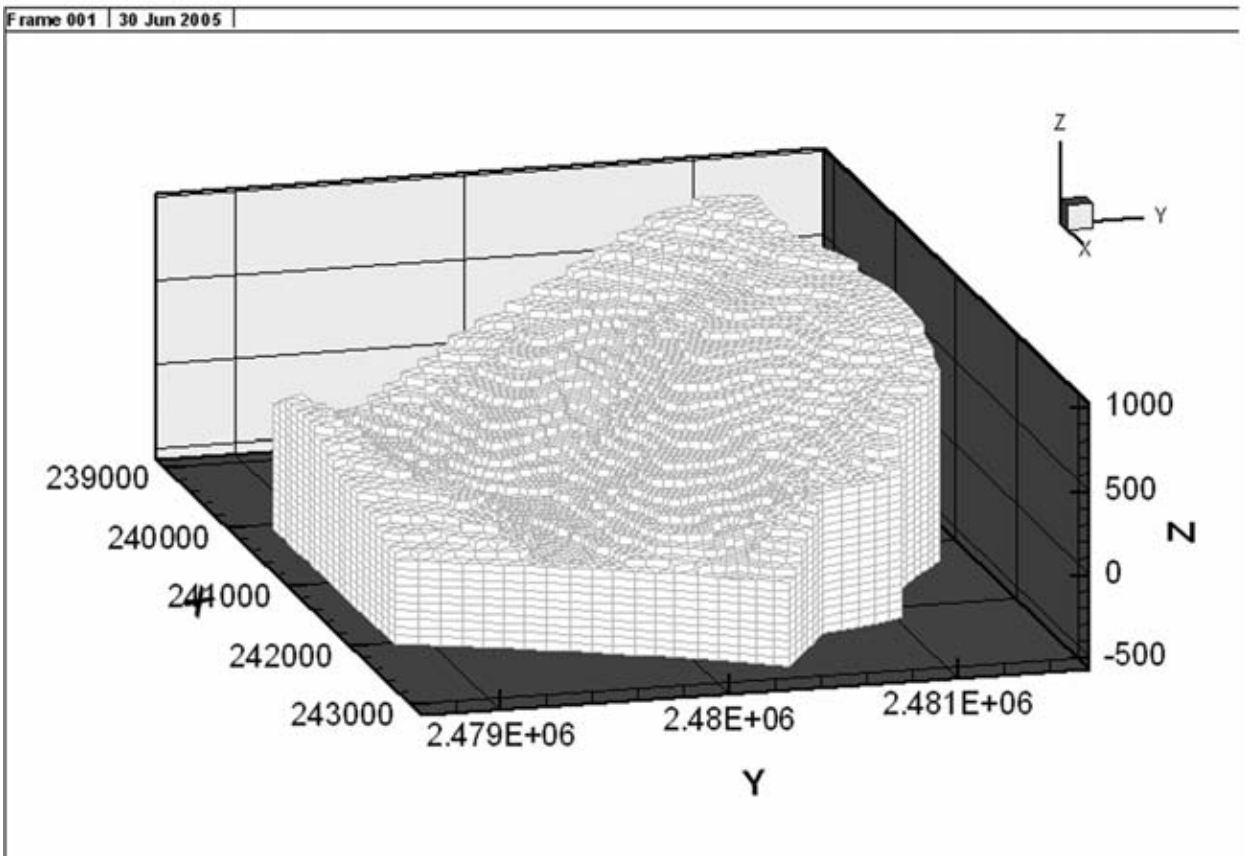

Figure 27. Finite-Element Grid for the FEHM Site-Scale Flow Model.

The resulting steady-state groundwater flow solution from the Site #6 site-scale flow model is shown with the simulated head at sea level within the model domain in Figure 28. The contours of simulated head shown in Figure 28 indicate that horizontal flow occurs generally toward to the ocean shoreline boundary of the model domain. At elevations near sea level, the groundwater flow direction is altered significantly by the presence of the streams, with flow converging toward the stream channels. This indicates that groundwater is simulated to discharge into the streams at these locations. Examination of cross-sectional plots of simulated groundwater flow vectors indicates that groundwater flow is generally downward in areas of higher topographic relief around the repository and is upward locally near the streams.

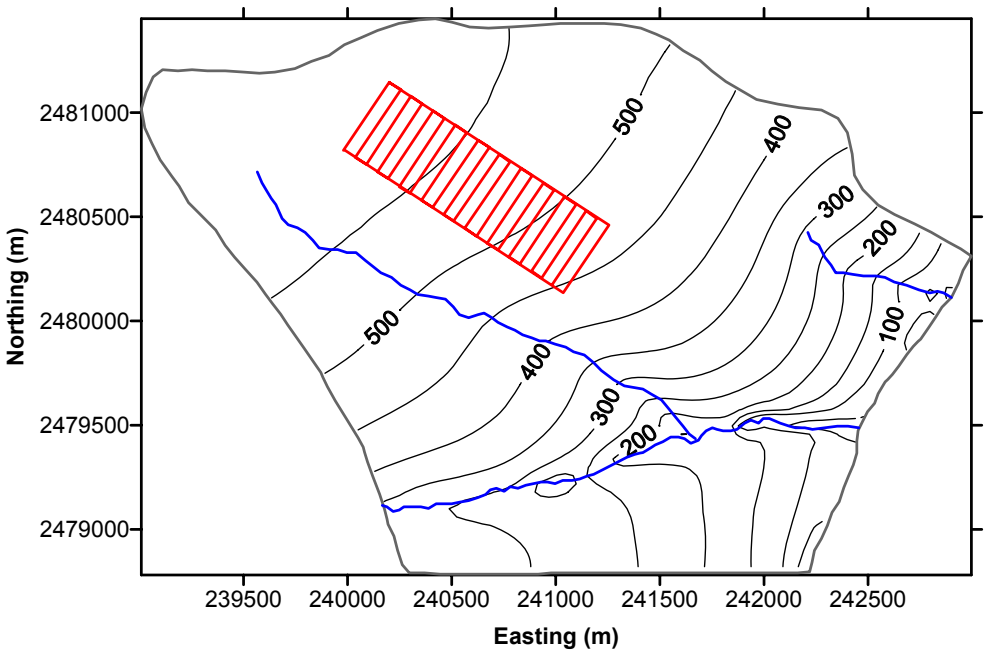

Figure 28. Simulated Hydraulic Head at Sea Level in the Site-Scale Flow Model for Site #6. Streams Are Shown in Blue and Repository Tunnels Are Shown in Red.

Contaminant transport simulations have been conducted with the Site #6 site-scale model to determine the pathways taken by radionuclides potentially released from the LLW repository. These simulations indicate that contaminants from the repository could be released to the streams down gradient of the repository and to the ocean, depending on the point of release from the repository and the amount of transverse dispersion occurring in the contaminant plume. Figure 29 shows the simulated contaminant concentrations in the upper nodes of the site-scale model domain, projected onto the surface plot of topographic relief. This plot shows that contaminants are simulated to be discharging from the groundwater and into sections of JJL Creek and JJL0101 Creek. Other three-dimensional visualization plots show that the simulated contaminant plume also discharges to the constant-head boundary of the model at the ocean shoreline. Note that the results shown in Figure 29 are for the base case, in which the repository is located at an elevation of about 100 m above sea level.

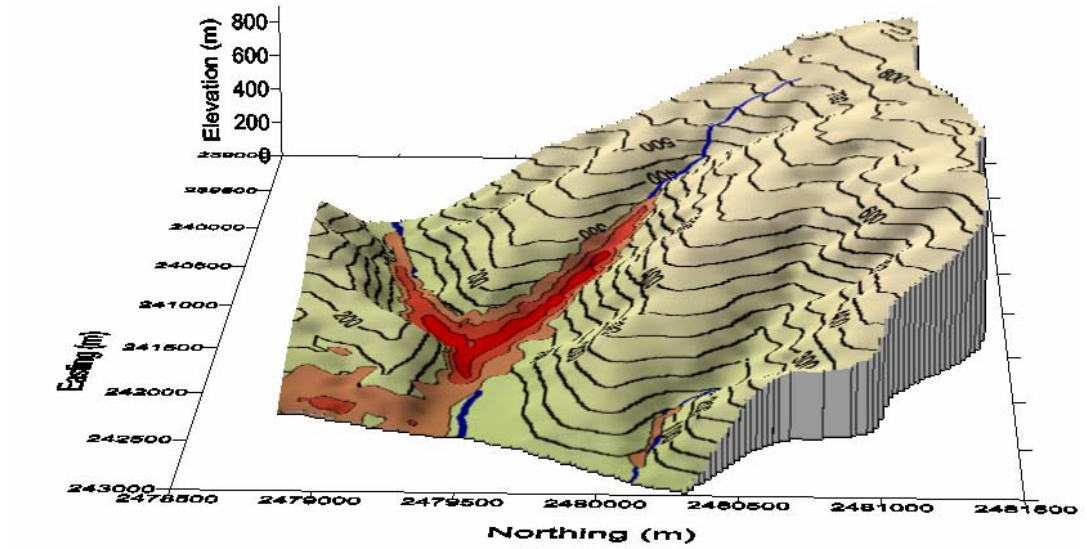

Figure 29. Simulated Concentration of a Contaminant Released from the Site #6 Repository in the Upper Elements of the Site-Scale Flow and Transport Model.

The groundwater flow rate through the repository and the location of discharge of contaminants would vary as a function of the elevation of the repository. Alternative vertical placement of the LLW repository was considered in variations of the site-scale flow and transport model. The steady-state solution for groundwater flow in the site-scale flow model was used to evaluate the average groundwater flux through the repository horizon for the base case (repository elevation of about 100 m above sea level), repository elevation of 0 m, and repository elevation of -100 m. The x, y, and z vector values of groundwater flow were combined to calculate a total value of groundwater flux at each node and the values were averaged among all the nodes within the repository horizon. The amounts of contaminant simulated to discharge to the streams relative to the releases to the ocean were quantitatively evaluated for variations in repository elevation. This was accomplished in the FEHM model by obtaining the groundwater outflow rate at each node along the streams and multiplying that outflow rate by the steady-state contaminant concentration at that node. The resulting contaminant mass discharge for each node along the streams was then summed and compared to the total contaminant mass release from the repository.

The results of the analysis are shown in Table 12 and indicate that the average simulated groundwater flux in the three cases considered does not vary by a large amount. The average flux through the repository decreases from 1.51 m/year for the base case to 1.39 m/year for the case in which the repository is located 100 m deeper, and decreases further to 1.31 m/year for a repository elevation of 200 m deeper. The results also show that about 62% of the contaminant mass released from the repository would be discharged to the streams for the base case, in which the repository elevation is about 100 m. The percentage of contaminant mass discharged to the streams decreases to about 53% and 42% for simulations in which the repository elevation is 0 m and -100 m, respectively.

Table 12. Flow Rates and Solute Discharge to Streams for Different Vertical Locations of the Repository at Site #6.

Repository Elevation (m)	Average Groundwater Flux at Repository (m/year)	Solute Discharge to Streams (mol/s)	Total Solute Release from Repository (mol/s)	Percentage Solute Release to Streams
100	1.51	3.13	5.08	62%
0	1.39	2.20	4.16	53%
-100	1.31	1.43	3.37	42%

The results of the analysis of repository elevation indicate that the simulated average groundwater flow rate through the repository horizon is not very sensitive to the vertical location of the repository. The average flow rate decreases by only about 13% (1.31 m/year versus 1.51 m/year) for a repository elevation 200 m lower than the base case. Lower average groundwater flow rate with greater depth in the flow system is consistent with general principles of hydrogeology, in which the shallower portion of the groundwater flow system is expected to be the more active part of the system. It should be noted that there are differences in average flow direction, as a function of depth, in the Site #6 site-scale flow model. At higher elevations, there is a larger vertical component to simulated flow and at lower elevations the groundwater flow tends to be more horizontal.

The contaminant transport simulations indicate that there is a larger impact to the percentage of mass discharge to streams with variations in the elevation of the repository. The decreasing discharge of contaminants to streams with lower elevation of the repository is also consistent with hydrogeological expectations, because shallower parts of groundwater flow systems have greater interactions with surface water than do the deeper parts of flow systems.

Finally, it is important to note that these conclusions are based on a preliminary, uncalibrated site-scale flow model. Consequently, the quantitative results have a high degree of uncertainty. However, the qualitative conclusions are probably valid, given their consistency with conceptual expectations of groundwater flow systems.

Abstraction of Groundwater Flow Vectors for Radionuclide Transport Simulations

The groundwater flow simulated by the three-dimensional FEHM site-scale flow model for Site #6 is used in the BLT-MS radionuclide transport model for performance assessment analyses. Because the BLT-MS code is limited to two-dimensional simulations, the groundwater flow simulated by the site-scale flow model is extracted along a cross-section through the repository. Although the projection of the groundwater flow vectors onto the cross section is an abstraction of the three-dimensional flow field, it is reasonably accurate because the cross section is oriented approximately parallel to flow through the repository.

The extraction of groundwater flow velocities from the site-scale flow model and their projection onto the cross section is accomplished as follows. The nodes from the flow model that are located within a specified distance of the cross section are identified and the simulated values of flow velocity are extracted from the FEHM output file. The location of the cross section and nodes extracted from the site-scale flow model are shown in Figure 30. The x and y components of the simulated groundwater flow are combined into a single horizontal component of the flow vector oriented along the cross section. The resulting groundwater flow vectors along the cross section are plotted in Figure 31. Note that the flow vectors in Figure 31 are in units of m/s, the outline of the preliminary BLT-MS transport model domain is shaded gray, and the location of the repository is shown by the red rectangle. The plot of the flow vectors indicates that there is generally flow toward the ocean to the right with a significant downward component of flow at the repository and above. At the right side of the cross section there is a strong upward component to flow toward discharge locations along the streams.

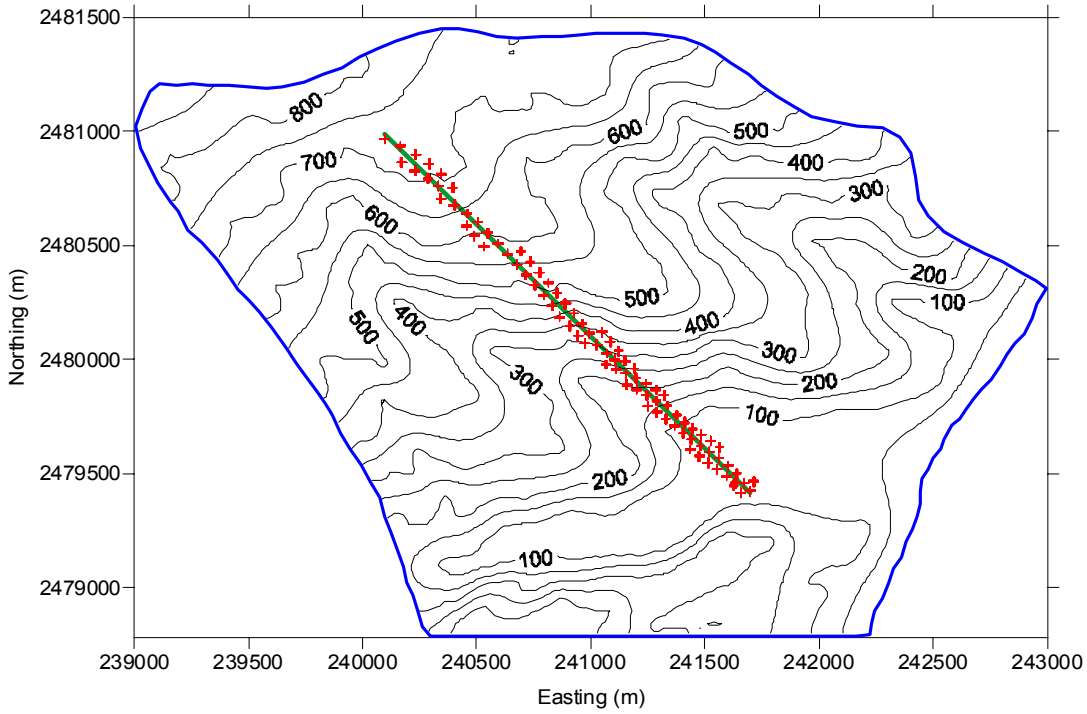

Figure 30. Topographic Contour Map of the Site-Scale Flow Model Domain and FEHM Nodes Within 50 m of the Cross Section.

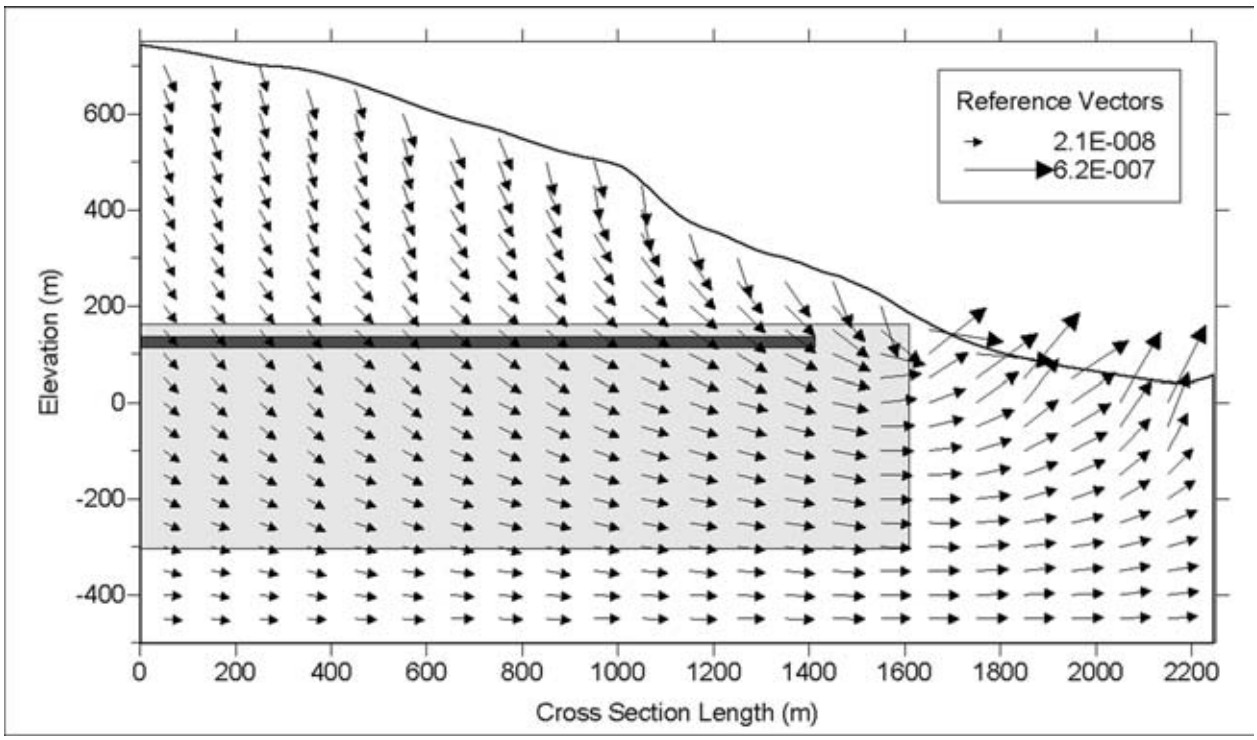

Figure 31. Groundwater Flow Vectors Along the Cross Section.

The vertical and horizontal components of groundwater flow vectors along the cross section are interpolated onto a regular grid using kriging. These components of the flow vectors are exported for input to the BLT-MS model grid at the node locations defined for that grid. In addition, the magnitudes of the groundwater flow vectors are scaled to lower values for those grid node locations within the engineered system of the drifts. The technical basis for the scaling of flow velocities is explained in the following section on the FEHM drift-scale flow modeling.

FEHM Drift-Scale Flow and Transport Model

Using the average ambient groundwater flow rates through the repository level from the site-scale flow model probably overestimates the flux through the LLW. This is because materials within the engineered system of the drift would likely have lower permeability than the host rock and would divert groundwater flow around the drift. Consequently, INER requested that a higher-resolution, drift-scale flow model be constructed to assess the impacts of the disposal drifts on the groundwater flow field. The preliminary drift-scale flow and transport model using the FEHM software was developed to address this request.

Because of the different objectives in the Site #6 drift-scale flow model, relative to the site-scale model and due to the higher resolution required, the conceptual model was changed significantly. The drift-scale flow model with FEHM was constructed with a two-dimensional (2-D), cross-sectional domain perpendicular to a single drift. The 2-D representation of the flow system is adequate because groundwater flow simulated by the three-dimensional site-scale flow model is

approximately perpendicular to the drift alignment in the region of the repository. The model domain in the drift-scale flow model is 100 m by 100 m and centered around a single drift. The specified groundwater flux boundary conditions are assigned to the outside of the model domain to approximate the magnitude and direction of groundwater flow near the center of the repository, as simulated by the site-scale flow model. The boundaries are located sufficiently far from the drift to minimize impacts on the simulated groundwater flow within or near the drift.

The conceptual model of groundwater flow in the drift-scale flow model with FEHM is that the flow occurs in a homogenous continuum within the host rock. Although flow in the host rock probably occurs primarily through fractures, this continuum assumption is acceptable at spatial scales larger than the fracture network through which flow occurs. It should be noted that the acceptability of this assumption may be questionable at small scales, such as in the numerical grid near the drift. Homogeneous material properties are also assumed for the engineered system within the drift (i.e., for the drift wall and floor, backfill, container walls, and waste).

The numerical grid for the Site #6 drift-scale flow model in the FEHM code was generated as an unstructured triangular finite-element mesh. The grid was refined at the drift location and made to conform to the material boundaries shown in the engineering drawing of the profile of the disposal tunnel. Figure 32 shows the finite-element grid of the entire drift-scale flow model domain and Figure 33 shows a blowup of the grid within the drift.

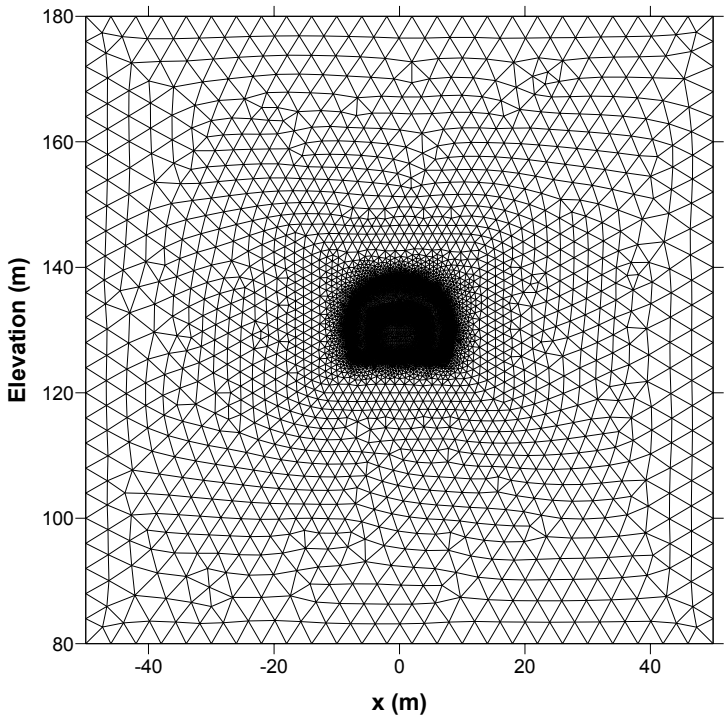

Figure 32. Finite Element Grid for the Entire Drift-Scale Flow Model Domain.

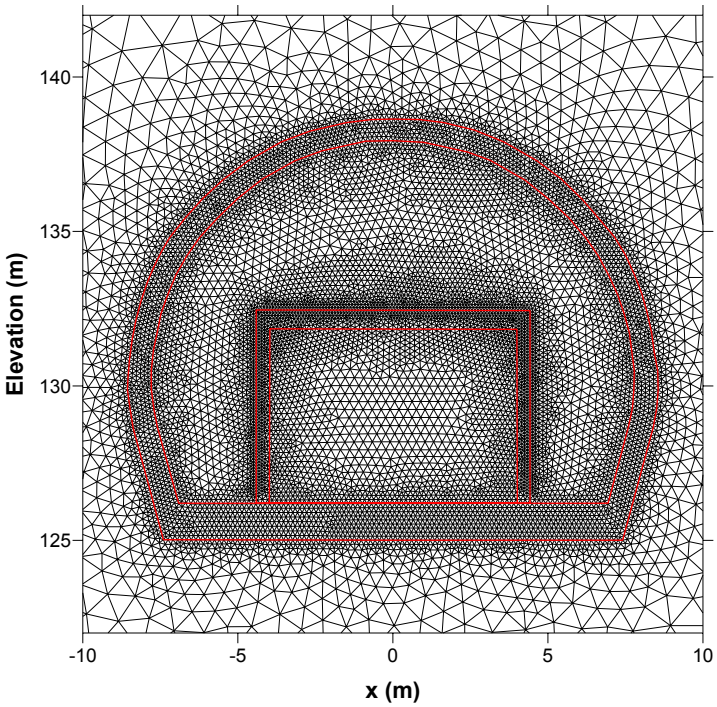

Figure 33. Finite Element Grid for the Central Part of the Drift-Scale Flow Model Domain.

This 2-D triangular finite-element grid was generated with the Easymesh software code, in which all of the elements satisfy the Delaunay criterion of gird quality. This grid criterion is required for the translation of the grid into the finite-volume representation used in the FEHM software to solve for flow. The grid consists of 11527 nodes and 22951 elements. Refinement of the grid near and within the drift was accomplished by defining features of the engineered system with series of line segments. The largest grid node spacing of 4 m occurs along the boundaries of the model domain. A square area around the drift reduces the node spacing to 1.5 m. Node spacing along the drift walls, floor, and waste container walls is specified to be 0.15 m and the spacing within the backfill and waste is somewhat coarser at 0.3 m.

Material properties are assigned to the nodes in the FEHM software and separate zones are assigned for the drift walls and floor, drift backfill, waste container walls, and waste. Figure 34 shows nodes assigned to each of these zones by color, superimposed on the Voronoi mesh corresponding to the finite-element grid. Figure 34 verifies that the proper nodes are assigned to each of these zones used to specify material properties for the engineered system components in the FEHM drift-scale flow model.

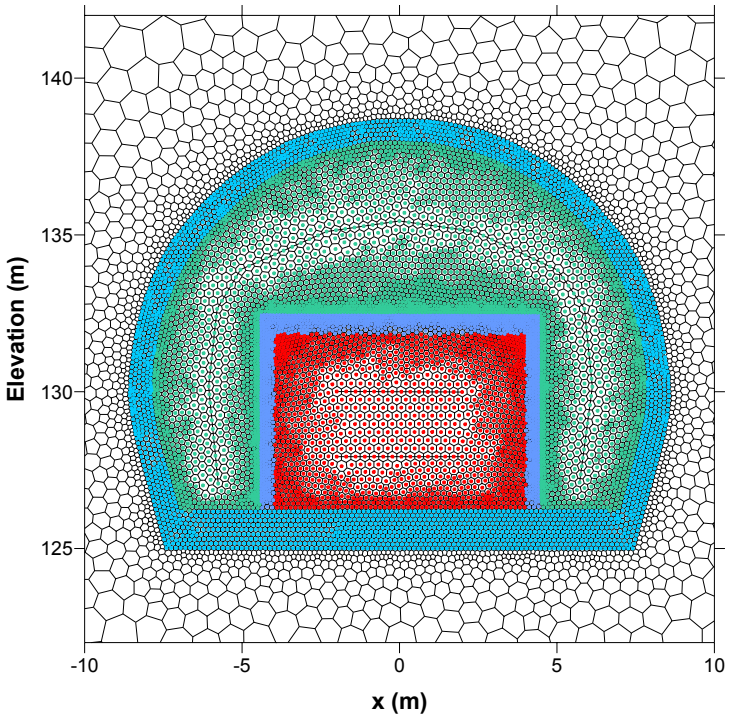

Figure 34. Voronoi Mesh for the Central Part of the Drift-Scale Flow Model Domain. Filled colored circles indicate nodal assignments to zones corresponding to the drift wall and floor (light blue), backfill (green), container walls (blue), and waste (red).

The boundary conditions for the Site #6 drift-scale flow model are taken from the site-scale flow model and applied as follows. The average simulated groundwater flux in the vertical direction from the site-scale flow model is 3.3×10^{-8} m/s downward. Converted to mass flow rate and applied over the 100 m length of the upper boundary of the drift-scale flow model, this is an inflow rate of 3.3×10^{-3} kg/s. An identical value of specified mass flux is applied as outflow from the lower boundary of the model domain. Similarly, the average horizontal groundwater flux from the site-scale model is 4.0×10^{-8} m/s, which translates to an inflow of 4.0×10^{-3} kg/s along the right boundary and equal outflow along the left boundary of the model domain. A representative value of 500 m for specified hydraulic head is applied at a single node in the lower left part of the model domain to allow the FEHM flow model to calculate a unique steady-state pressure solution.

The groundwater flow simulations with FEHM assume steady-state conditions in a fully saturated medium. The flow solution is formulated in terms of hydraulic head, so heat transport is not considered in the simulations.

Four cases were developed to assess the sensitivity of the Site #6 drift-scale flow model with regard to groundwater flow within and near the drift. These cases are summarized below:

- Case #1: Permeability of all components of the engineered barrier system is equal to the host rock. Permeability of all nodes is 1×10^{-13} m^2.

- Case #2: Permeability of the concrete drift walls, drift floor, and waste container walls is 1 x 10^{-15} m^2. Permeability of host rock, backfill, and waste is 1 x 10^{-13} m^2.
- Case #3: Permeability of the concrete drift walls, drift floor, and waste container walls is 1 x 10^{-15} m^2. Drift is backfilled with bentonite-amended backfill with a permeability of 1 x 10^{-18} m^2. Permeability of host rock and waste is 1 x 10^{-13} m^2.
- Case #4: Permeability of the concrete drift walls, drift floor, container walls, and the waste is 1 x 10^{-15} m^2. Drift is backfilled with bentonite-amended backfill with a permeability of 1 x 10^{-18} m^2. Permeability of host rock is 1 x 10^{-13} m^2.

The value of permeability for the bentonite-amended backfill is approximately the same as the value obtained for a 30% bentonite and 70% granite mixture investigated by the Swedish repository program.

The results for Case #1, in which the permeability of all drift components is equal to the host rock permeability, are shown in Figure 35. As expected, the simulated hydraulic gradient and the groundwater flow vectors are approximately uniform throughout the host rock and within the drift.

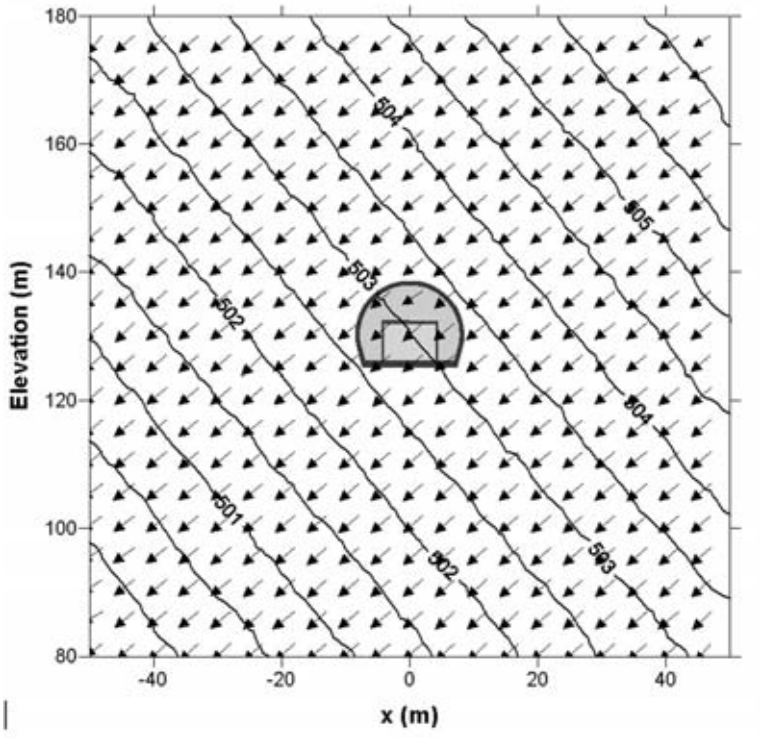

Figure 35. Simulated Head Contours and Groundwater Flow Vectors for Case #1 of the Drift-Scale Flow Model.

The results for Case #2, in which the permeability of the drift wall, drift floor and, waste container walls are less than the host rock permeability, are shown in Figure 36. The groundwater flow vectors are diverted around the drift because of the lower permeability in the concrete drift walls and container walls. The simulated head contours in Figure 36 indicate that distribution of hydraulic gradient has also been altered around and within the drift, as anticipated. Note that the changes in simulated flow vectors and the hydraulic head do not extend farther than about 10 to 20 m from the drift walls. This observation about how far from the drift these impacts extend also applies to Cases #3 and #4.

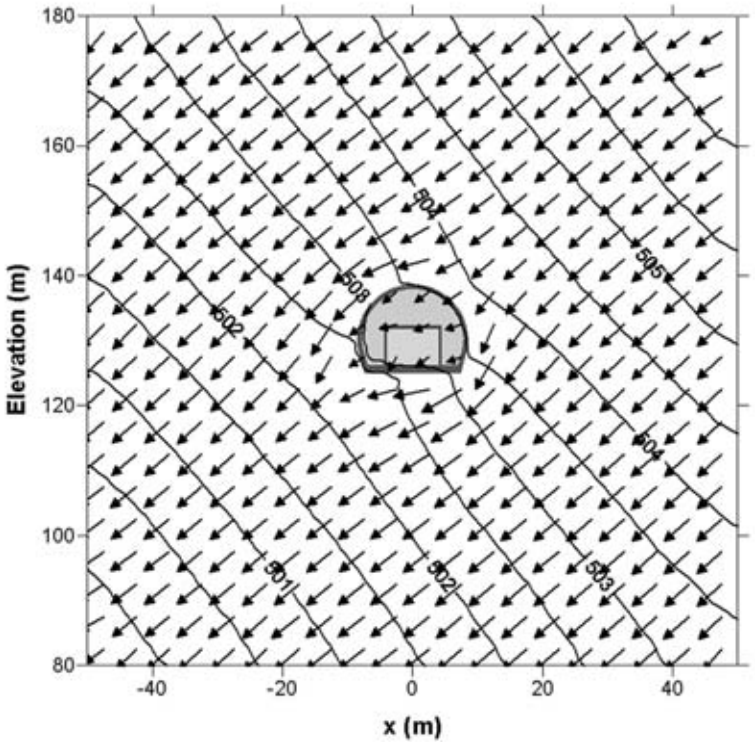

Figure 36. Simulated Head Contours and Groundwater Flow Vectors for Case #2 of the Drift-Scale Flow Model.

The simulated flow vectors and head contours for Case #2 are shown in more detail within and around the drift in Figure 37. The simulated head gradient within the lower-permeability drift wall and floor in the lower left part of the drift is higher than in the host rock. The diversion of flow around the drift and the acceleration of the diverted groundwater flow, particularly around the lower right corner of the drift, are evident in Figure 37. Simulated groundwater flow within the waste (light brown color in the figure) is still primarily downward and to the left, but with a significantly lower magnitude than in the surrounding host rock.

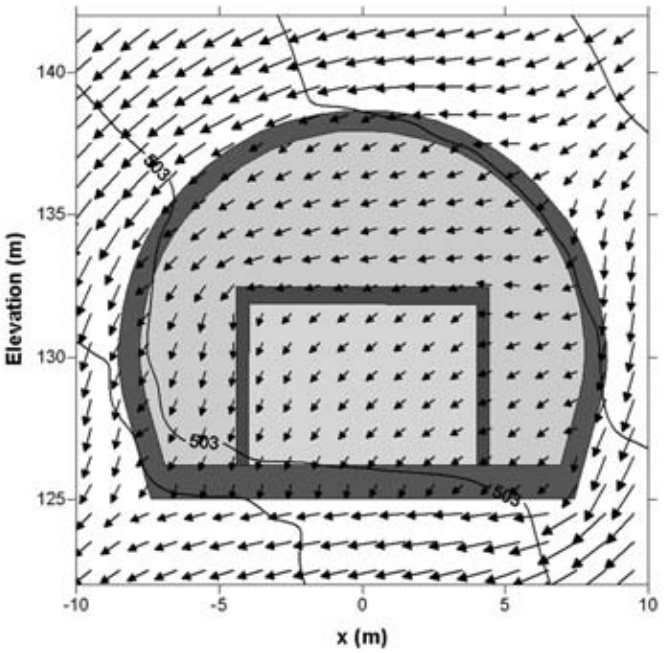

Figure 37. Simulated Head Contours and Groundwater Flow Vectors for Case #2 of the Drift-Scale Flow Model for the Area Within and Near the Drift.

The simulated flow vectors and head contours for Case #3, in which the backfill is assigned a value of permeability much lower than the host rock, are shown in the area within and around the drift in Figure 38. A significant increase in the gradient in hydraulic head in the backfill is evident from the close spacing of head contours in the upper right area of the drift. The flow vectors in Figure 38 also show a strong diversion of groundwater flow around the drift. The simulated magnitude of groundwater flow within the waste is significantly lower than the ambient flow rate in the host rock and the pattern of flow within the waste has an interesting pattern. Flow occurs into the waste, through the container wall, from the surrounding backfill on the upper and right sides of the waste container. Also, more significant flow is simulated to occur up through the floor of the drift on the right side of the waste and downward out of the waste on the left side. This flow pattern occurs because the permeability in the floor of the drift is lower than the host rock, but still significantly higher than in the backfill.

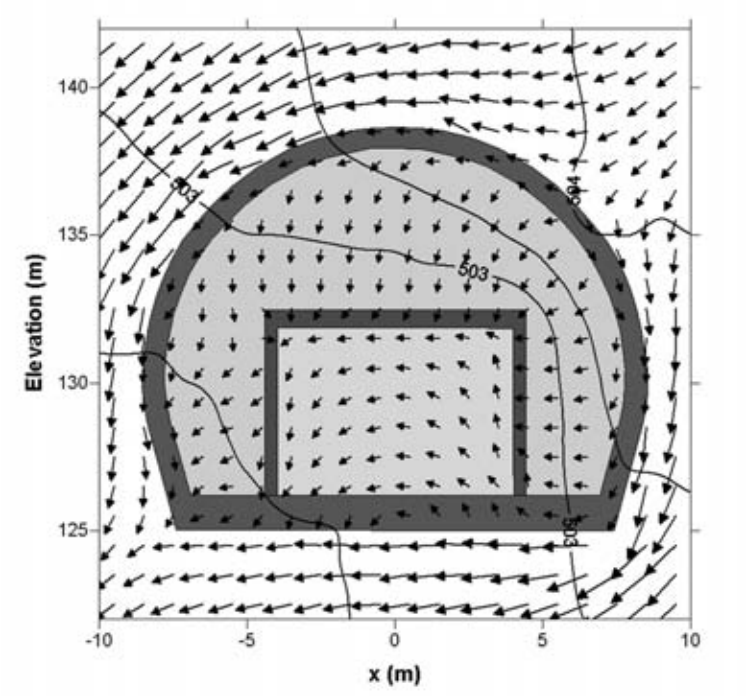

Figure 38. Simulated Head Contours and Groundwater Flow Vectors for Case #3 of the Drift-Scale Flow Model for the Area Within and Near the Drift.

Case #4 corresponds to a disposal method that includes more effective grouting within and around waste drums inside the waste container. The flow simulation results for Case #4 are similar to those for Case #3, but the magnitude of groundwater flow vectors in the waste is smaller in Case #4 and the circulation pattern of flow up and downward through the drift floor is not as strong.

The average magnitude of groundwater flow within the waste zone of the Site #6 drift-scale flow model is an indication of the effectiveness of the engineered system at diverting groundwater flow around the waste. The average flow rates in the waste for the four cases examined in this sensitivity study are shown in Table 13. The ratio of the average flow rate in each case to the ambient flow rate in the host rock is also shown in Table 13. These results indicate that the simulated average groundwater flow rate in the waste is reduced from about one order of magnitude to greater than two orders of magnitude for Cases #2 through #4, relative to the flow rate in the surrounding host rock.

Table 13. Average Flow Rates in Waste for Sensitivity Cases.

Case #	Average Flow Rate in Waste (m/year)	Ratio of Average Flow Rate to Case #1
Case #1	2.57	1.00
Case #2	0.209	0.0813
Case #3	0.0442	0.0172
Case #4	0.0115	0.00447

The Site #6 drift-scale flow model for each of the four cases was modified to simulate solute transport from the waste zone in the steady-state flow fields. Two sets of transport simulations were conducted for the four cases. In the first set, the concentration of the contaminant was held constant at a relative concentration equal to 1.0 and the resulting steady-state contaminant plume was plotted for the purpose of visualization. This first set of transport simulations corresponds to the transport of a radioelement with a low solubility limit in the system, such as plutonium or americium. The low solubility of such a contaminant would result in a constant concentration source at the waste that would persist until the inventory in the waste is exhausted. In the second set of transport simulations, the initial concentration of the contaminant in the waste is set to a relative concentration of 1.0 and the contaminant is then flushed from the waste as a pulse release. The release rate of the contaminant is then tracked at the drift-scale flow model boundary in order to compare these breakthrough curves for the four cases. This second set of transport simulations corresponds to the transport of a highly soluble radioelement, such as tritium or iodine.

The transport simulations documented here assume a porosity of 0.15 in all components of the system and also assume transport in a single-continuum medium. Although the transport processes in the fractured host rock may be more realistically represented using a dual-porosity approach, these simulations are intended to illustrate the differences in the release of contaminants within and near the drift and not to accurately portray transport in the far field.

The simulated steady-state contaminant plume for Case #1 is shown in Figure 39. The figure indicates that the simulated concentrations are swept to the left and downward from the waste zone by groundwater flow. Transverse dispersion spreads the simulated plume in the directions lateral to flow and also reduces the concentration along the centerline of the plume in the longitudinal direction. It should be noted that numerical dispersion in the FEHM solute transport solution also contributes significantly to the simulated dispersion, particularly in the areas of the contaminant plume near the model boundaries, where the grid is coarser.

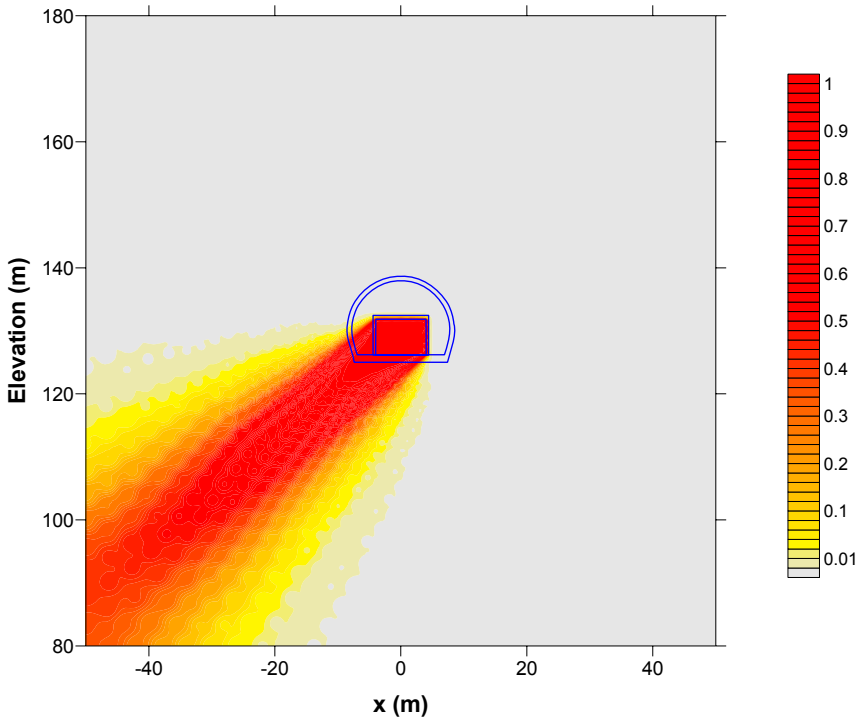

Figure 39. Simulated Concentration for Transport from a Constant-Concentration Source for Case #1 of the Drift-Scale Flow Model.

The simulated contaminant plumes for the drift-scale flow model Cases #2, #3, and #4 indicate that the simulated contaminant concentrations within the plumes decrease among these cases as the amount of groundwater flow diversion around the drift increases. The simulated contaminant plume for Case #4 is shown in Figure 40. For the cases with lower permeability zones within the drift, the groundwater flow rate through the waste is lower and the corresponding advective transport of contaminant mass out of the waste is lower. This lower mass of contaminants is then diluted in the flow of groundwater that has been diverted around the drift when it leaves the drift, resulting in lower concentrations in the simulated plume down gradient of the drift.

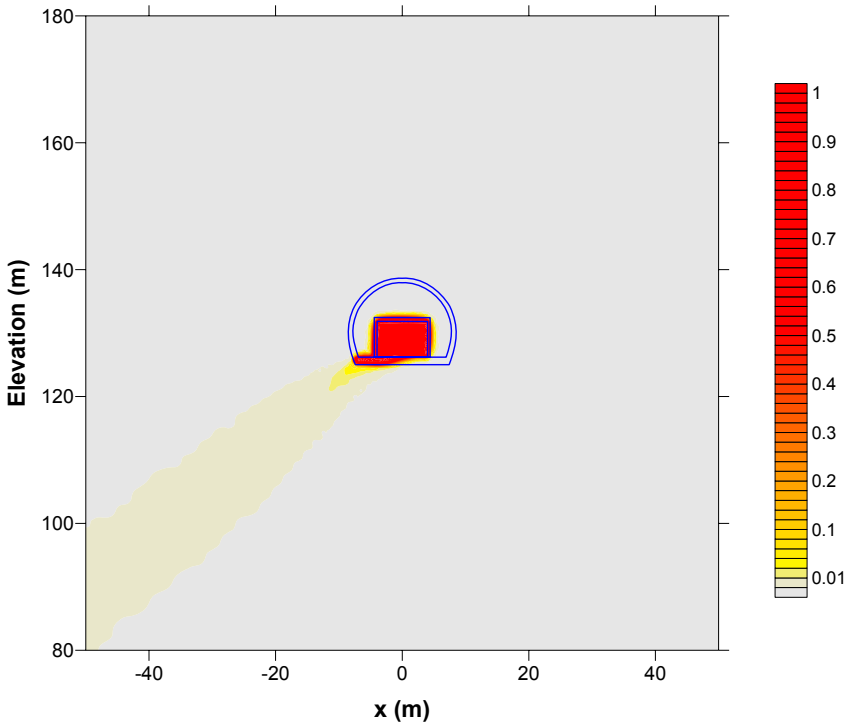

Figure 40. Simulated Concentration for Transport from a Constant-Concentration Source for Case #4 of the Drift-Scale Flow Model.

It should be noted that for all four of the cases in this sensitivity study, the simulated contaminant migration is advectively dominated; that is, diffusion only plays a minor role. Only in Case #4 is there some small amount of diffusion out of the waste and into the backfill evident in Figure 40. The conclusion that transport is dominated by advective processes relative to diffusion can be confirmed by examination of the Peclet Number for the system. The Peclet Number is a dimensionless variable that expresses the relative importance of advection versus diffusion in solute transport and is defined by the following equation:

$$P_e = \frac{vd}{D_d}$$

where, in this case, v is the groundwater flow velocity within the waste, d is the transport distance through the waste (approximately 8 m), and D_d is the effective molecular diffusion coefficient (assumed to be 1 x 10^{-11} m^2/s). Using the results of Case #4 for the groundwater flow rate in the waste and assuming a flow porosity of 0.15, the simulated velocity of the groundwater in the waste is 0.0298 m/year (9.44 x 10^{-10} m/s). The resulting value of P_e for flow through the waste is 755. Values of greater than 100 for P_e are considered to be advectively dominated. Given the higher simulated groundwater flow rates in the waste for Cases #1, #2, and #3, transport in the waste is also advectively dominated in these cases.

The second set of transport simulations was conducted for the four cases of the drift-scale flow model with a pulse source from the waste. The results of these simulations are shown as the

breakthrough curves of mass release rate at the model boundaries shown in Figure 41. Note that the y-axis of the plots of the breakthrough curves is on a log scale, so the simulated peak release rates for the four cases vary over almost two orders of magnitude. The highest peak release rate is for Case #1, in which there is no diversion of flow around the drift, and the lowest peak release rate is for Case #4, in which there is the greatest diversion of flow around the drift. The time of peak release rate also varies among the four cases, but the time of peak release only varies over a few decades. It should be noted that the total mass released in each of the four cases of the Site #6 drift-scale flow model is the same. The mass release at the model boundaries is spread over a much longer time for the cases in which there is significant diversion of groundwater flow around the drift, such as Case #3 and Case #4. This effect is evident in the longer "tails" of the breakthrough curves for Case #3 and Case #4 shown in Figure 41.

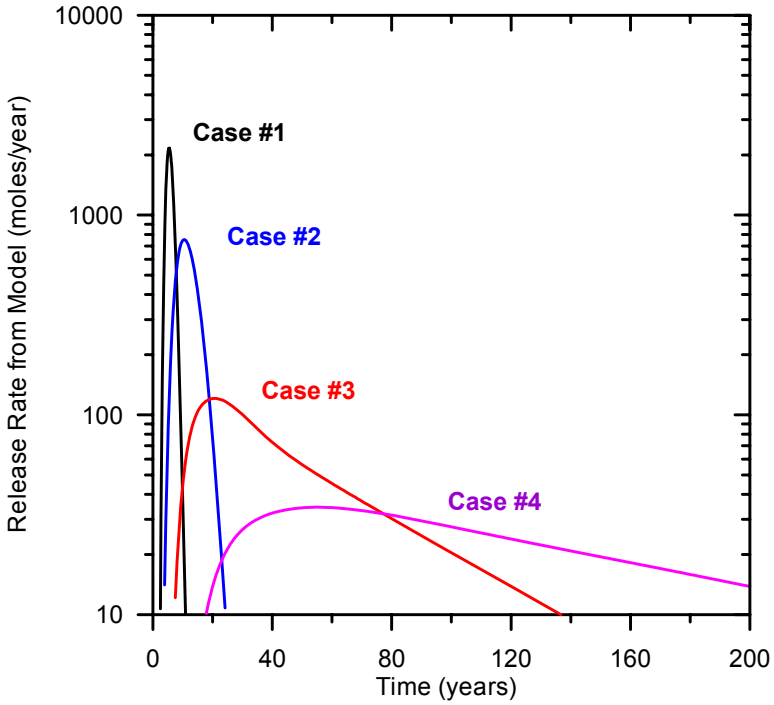

Figure 41. Simulated Breakthrough Curves of Mass Released at the Drift-Scale Model Boundaries for Cases #1 to #4.

Lower permeability of various engineered components of the drift results in diversion of groundwater flow into the host rock surrounding the drift, as demonstrated by the results of Cases #2, #3, and #4. This diversion of flow around the drift results in lower groundwater flow rates through the waste. For Case #3 and Case #4, in which the permeability of the backfill is significantly lower than for other components of drift, the groundwater flow through the waste is primarily by circulation of groundwater up through the floor of the drift and then outward through the floor on the opposite side of the waste zone. So the presence of the bentonite-amended backfill can form an "umbrella" over the waste and can reduce the flow rate through the waste, but does not eliminate groundwater circulation from other components of the system into the waste.

One reasonable strategy for abstracting the results of the flow simulations with the drift-scale flow model for use in modeling radionuclide transport with the BLT-MS software code, and subsequent incorporation in the TSPA, is presented here. The average flow rate in the waste, as tabulated in Table 13, can be specified for the elements containing waste in the BLT-MS site-scale model. The ambient flow vectors in the host rock, as derived from the Site #6 site-scale FEHM flow model, could be applied to the elements between the drifts and in the surrounding host rock in the BLT-MS site-scale model.

The transport simulations with the drift-scale flow model demonstrate the impacts of different distributions of permeability within the engineered system of the drift. The lower the permeability values within the drift, the lower the simulated contaminant concentrations are downstream from the drift. Transport simulations using a pulse source, such as a highly soluble contaminant, show that the lower the permeability values within the drift, the lower the simulated peak release rate downstream from the drift. Lower values of permeability within the drift cause the contaminant release to be spread over a longer period of time.

Another interesting observation with regard to the transport simulations is that there is very limited simulated migration of the contaminants into the bentonite-amended backfill, by either advection or diffusion. This suggests that there would be little added performance of the LLW repository from enhanced sorption of radionuclides onto the bentonite-amended backfill. The transport simulations show that the majority of contaminants leave the drift by flow through the floor of the drift.

Alternative FEHM Basin-Scale Flow Model

An alternative basin-scale groundwater flow model for Site #6 was constructed with the FEHM code that encompasses the entire surface-water drainage basin for the site. This alternative model was constructed to address concerns that the western boundary of the site-scale flow model may not be realistically represented as a no-flow boundary.

The numerical grid for the Site #6 basin-scale flow model was generated as an unstructured triangular finite-element mesh and projected in the vertical direction to produce a three-dimensional grid consisting of triangular prisms, in a manner similar to the site-scale flow model grid. The boundaries of the two-dimensional grid are defined by the topographic boundaries of the surface water drainage basin. Higher grid resolution was specified along the boundaries and in the area of the repository, as shown in Figure 42.

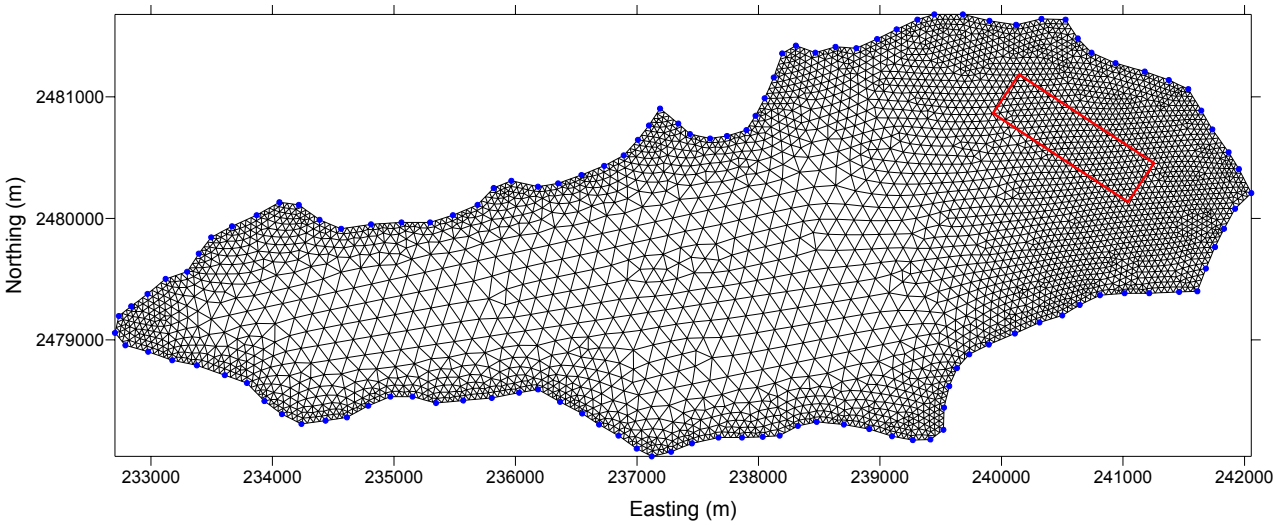

Figure 42. Finite-Element Grid for the FEHM Basin-Scale Flow Model. Repository Outline Is Shown in Red.

The boundary conditions of the basin-scale flow model consist of a constant head boundary at the ocean shoreline, no-flow boundary conditions along the sides and the base of the model, and specified recharge flux on the upper surface of the model. In addition, the streams are represented as head-dependent flux boundaries, in which the flow into or out of the model is controlled by the difference in head in the stream and in the underlying aquifer. The recharge flux is assumed to be 500 mm/year, which corresponds to about 20% of the precipitation at Site #6.

The resulting steady-state groundwater flow solution from the basin-scale flow model is shown with the plot of hydraulic head at sea-level elevation in Figure 43. As in the site-scale flow model the gradient in head indicates that the groundwater flow is generally toward the constant-head boundary of the ocean shoreline on the right. The head contours also show convergent groundwater flow toward the creeks near the repository, where the elevation of the creeks is near or somewhat above sea level. At higher elevations, toward the west side of the basin-scale flow model, the head contours do not indicate flow toward the creeks because the plot shown in Figure 43 is relatively deep beneath the topographic surface. Nearer the topographic surface there is convergent flow and significant groundwater discharge to the creeks simulated in the model.

The alternative basin-scale flow model has results that are generally similar to the site-scale flow model with regard to groundwater flow near the repository at potential Site #6. The direction of groundwater flow and the simulated pattern of discharge are very similar in the two model simulations. However, the higher magnitude of the horizontal gradient in the basin-scale flow model (compare Figure 43 and Figure 28) in the area of the repository indicates that the groundwater flow vectors have a higher magnitude and are oriented more horizontally in the basin-scale flow model.

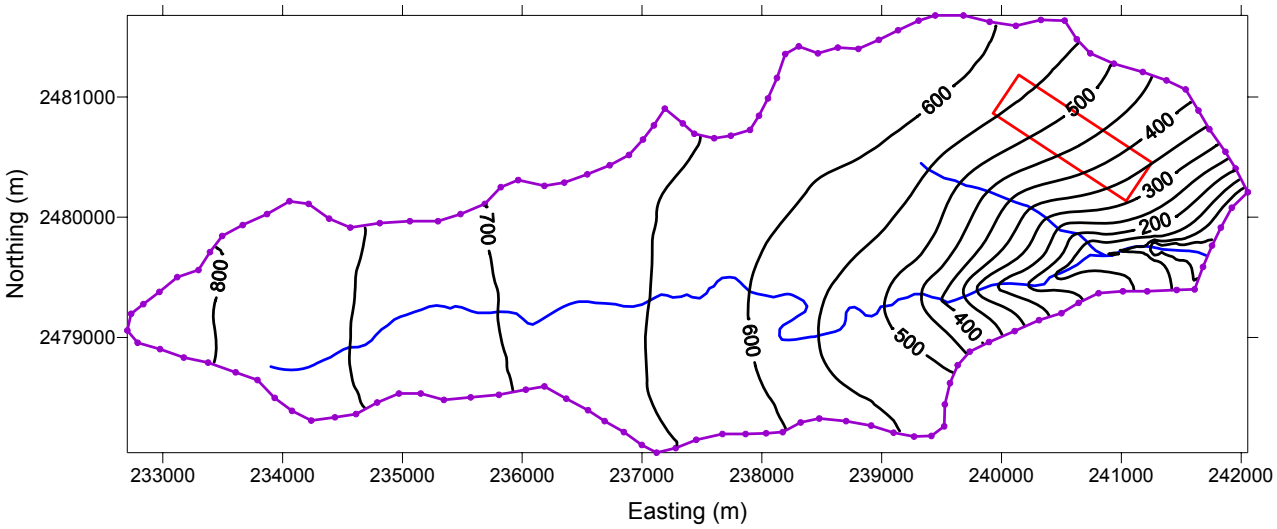

Figure 43. Simulated Hydraulic Head at Sea Level in the Basin-Scale Flow Model for Site #6. Streams Are Shown in Blue and Repository Outline Is Shown in Red.

As in the other flow modeling conducted for potential Site #6, it is important to note that these conclusions are based on a preliminary, uncalibrated basin-scale flow model. Site-specific information that could constrain the flow modeling includes water-level measurements in wells, stream gauging data, and well testing results. Water-level measurements would provide specific targets for the calibration of the flow model and could indicate the magnitudes of vertical hydraulic gradients, if piezometers are completed at different depths. However, water-level measurements alone cannot constrain the groundwater budget through the system. Stream gauging data would help to quantify the interaction between groundwater and the surface water in the basin and constrain the water budget. Hydraulic testing of wells (pump testing or slug testing) would provide information on the hydraulic conductivity of the bedrock.

3.3.4. Radionuclide Release and Transport Model

An evaluation was conducted of available codes potentially suitable for the source-term release and far-field transport of radionuclides from the proposed repositories. Most transport simulators do not contain a robust set of mathematical models to simulate the container degradation and waste-form release mechanisms desired for a performance assessment analysis. These types of codes require the user to assume the radionuclides are released to the host rock and instantaneously mixed with soil-water as a starting concentration in the transport model. The performance of the engineered barrier system would not be explicitly quantified if this type of model were used in the performance assessment analysis.

Two codes developed by the U.S. Nuclear Regulatory Agency (NRC) have the capability to simulate source-term releases as well as far-field transport of radionuclides. These codes are the Disposal Unit Source Term (DUST) code and the Breach, Leach, and Transport – Multiple Species (BLT-MS) code. The DUST code is one-dimensional, whereas the BLT-MS code is

two-dimensional. The INER staff expressed a strong desire for a multi-dimensional analysis. Therefore, the BLT-MS code was selected for the performance assessment analysis.

The BLT-MS code is a FORTRAN code developed in the mid-1990's that has been compiled to run under DOS or a DOS-emulator. SNL did not modify any of the code's functionality relative to the process models incorporated in the code. However, modifications to the input/output constructs of the model were necessary to integrate the code with GoldSim.

BLT-MS has the following functionality:

- Able to simulate the degradation of waste containers in the source term for two types of processes:
    - Localized corrosion, where pitting occurs and the rate of water contact with the waste form is proportional to the extent of corrosion of the container; and
    - Generalized corrosion, where the container fails instantaneously once a breach time is achieved.
- Four types of waste-form release, or leaching, mechanisms, including:
    - Rinse release, where the groundwater comes in contact with the waste and radionuclides are solubilized into the groundwater;
    - Diffusion release, which is the dominant release mechanism for stabilized waste, the code has several analytical models to choose from as well as a numerical solution;
    - Degradation release, where the waste form is depleted by dissolution linearly over a set time-frame; and
    - Solubility-limited release.
- Finite-element based transport solver for the far-field movement of radionuclides, including the following processes:
    - Advection;
    - Dispersion;
    - Sorption;
    - Ingrowth and decay;
    - Sources and sinks; and
    - Boundary conditions, including Neumann, Cauchy, and Dirichlet type conditions.

As mentioned in Section 3.3.1, two conceptual models were used to simulate radionuclide transport for the proposed repository locations: a two-dimensional advective-dispersive transport case, and a one-dimensional matrix-diffusion case. The Breach, Leach, and Transport – Multiple Species (BLT-MS) code was used for the two-dimensional transport and is considered the base case model for radionuclide transport from the two potential sites. GoldSim, a probabilistic simulator with 1-D mass transport capabilities, was used for the alternative radionuclide release model using a 1-D transport solution. The two-dimensional advective-dispersive transport case is discussed first.

The BLT-MS model does not have a flow solver. Darcy flow velocities must be input to the model in order to simulate transport. These data are abstracted from another model, FEHM, and input to BLT-MS (see Section 3.3.3).

BLT-MS was developed during the 1990's. Computers at that time did not have the processing or storage capacity of today's computers. Several iterations during the development of the radionuclide release and transport model domain revealed that the BLT-MS code had some limitations relative to the number of finite-element nodes, the number of waste containers allowed, and the number of time steps. It was determined to accurately simulate the proposed sites, arrays in the code associated with these attributes were increased to accommodate models having up to 30,000 nodes, 5000 waste containers, and 5000 time steps. Dr. Terry Sullivan, of Brookhaven National Laboratory, helped modify the code for the new requirements. Dr. Sullivan was the lead developer of the BLT-MS code when it was first developed for the NRC.

For the one-dimensional matrix-diffusion case, two models were integrated in order to achieve the desired functionality. First, the BLT-MS model was employed to simulate the source-term release. Next, the results of the source-term release model were input to GoldSim, where the internal model capabilities of this code were utilized to construct the matrix-diffusion functionality.

The one-dimensional transport models for both sites were implemented within the GoldSim software using the "pipe" pathway option in GoldSim. The pipe pathway represents a fluid conduit in which advection, dispersion, and sorption of radionuclides can occur and from which diffusion into the immobile groundwater of the rock matrix can occur. The numerical solution of transport through the pipe is solved using the computationally efficient Laplace transform method. The important characteristics of each pipe include the cross sectional area, the volumetric flow rate into the pipe, the length, the properties of any infill medium, and the diffusive characteristics of the rock matrix outside the pipe.

To simulate transport at the near-surface disposal system site and the mined cavern disposal system site sets of pipes were defined to approximate the groundwater flow rates and flow path lengths simulated by the corresponding three-dimensional flow models. For Site #7 three flow pathways were specified, with each flow path consisting of a pipe for unsaturated flow beneath the disposal cell and a pipe for saturated flow, connected in series. One of the cells on the island site was divided into three equal areas and each of these areas functions as a source to one of the pipe pathways. For Site #6 there were 21 pipe pathways defined, with each pipe being connected to one drift as a source. The properties of the pipes used in these one-dimensional transport models are summarized in Table 14 and Table 15. Note that the lengths of the pipes for Site #6 (mined cavern disposal system site) vary from 100 m to 1700 m due to the length of the repository and the approximate orientation of the groundwater flow parallel to this length.

Table 14. Pipes in the One-Dimensional Transport Model for Site #7.

Pipe #	Cross Sectional Area (m^2)	Volumetric Flow Rate (m^3/year)	Length (m)
1 (UZ)	13550.	610.	18.
2 (UZ)	13550.	610.	18.
3 (UZ)	13550.	610.	18.
1 (SZ)	469.	610.	250.
2 (SZ)	469.	610.	190.
3 (SZ)	469.	610.	130.

Table 15. Pipes in the One-Dimensional Transport Model for Site #6.

Pipe #	Cross Sectional Area (m^2)	Volumetric Flow Rate (m^3/year)	Length (m)
1	24965.	22100.	100.
2	24656.	23300.	180.
3	24339.	25000.	260.
4	24016.	26500.	340.
5	23684.	28000.	420.
6	23346.	29500.	500.
7	23001.	31200.	580.
8	22648.	33600.	660.
9	22289.	35200.	740.
10	21923.	36300.	820.
11	21550.	37400.	900.
12	21170.	38400.	980.
13	20785	39400.	1060.
14	20393.	41800.	1140.
15	19994.	44200.	1220.
16	19590.	49500.	1300.
17	19179.	54500.	1380.
18	18763.	56300.	1460.
19	18341.	57900.	1540.
20	17913.	62200.	1620.
21	17480.	66200.	1700.

Material properties such as porosity, dispersivity, and sorption coefficients were assigned within the one-dimensional transport model to match the values used in the corresponding BLT-MS transport models. For the fractured rock units the matrix diffusion coefficient and fracture spacing were also specified. A simplified conceptual model for matrix diffusion is employed in the pipe pathway, in which there are multiple equally spaced parallel fractures. It should be noted that in the fractured medium the pipes are conceptualized to represent only the open

fractures. Consequently, the cross sectional area specified in the GoldSim model is the total cross sectional area (as tabulated in Table 14 and Table 15) multiplied by the fracture porosity and the porosity within the pipe is set to a value of 1.0.

3.3.5. Software Code Integration and System Model

Several codes were integrated in order to facilitate a comprehensive modeling capability for a LLW probabilistic performance assessment. A list of these codes appears in Table 16. Each of these codes in the ensemble, as well as the computer platforms available for use, have strengths and limitations that need to be accounted for in building the integrated model. A summary of these considerations is offered below.

Table 16. List of Software Used for Radionuclide Release and Transport Calculations

Preprocessors	BLTMS_WIN.EXE	
	BLTMS_GRID.EXE	
Total System Model (Radionuclide release, transport and dose calculations)	BLTMS.EXE	See Appendix A for detailed description of the coupled model.
	GOLDSIM.EXE	
	READ_BLTv1.1.002.DLL	
	LAUNCH_BTLMSv1.1.011.DLL	
Postprocessors	BLTMS_UNCERT.EXE	

BLTMSIN-WIN.EXE:

When BLT-MS was originally developed, a DOS-based preprocessor, BLTMSIN.EXE, was also developed in order to facilitate the creation and editing of input files for BLT-MS. This preprocessor is documented in an NRC publication (NRC, 1996a). Being DOS-based and fairly comprehensive in its features, the preprocessor is far from user-friendly. As part of this project, a Windows-based preprocessor was developed to facilitate a more user-friendly package for creating and editing the BLT-MS input files. This code is called BLTMSIN-WIN.EXE. The code has been designated as open-source and is freely available. It can be accessed on a Sandia National Laboratories website at the following URL: http://www.sandia.gov/icp/.

BLTMS_GRID.EXE:

The BLT-MS model employs a rectangular finite-element grid for the transport simulations in the far-field. The BLTMSIN and BLTMSIN-WIN input processors have a rudimentary automatic grid generating option that allows the user to specify either a uniform grid spacing setup or one that has an incrementally increasing grid spacing setup. If the user needs more specificity to create a unique grid layout, the code allows for individual node prescription. This option would be quite burdensome for a user to create if they have a rather large grid size. Therefore, a small FORTRAN routine was written to help facilitate the creation of a non-uniform grid. This software package is called BLTMS_GRID.EXE. The code has been designated as open-source and is freely available. It can be accessed on a Sandia National Laboratories

website at the following URL: http://www.sandia.gov/icp/. The user must create a text input file that has the x-axis and z-axis spacing for each finite element in the model. The BLTMS_GRID code then creates the necessary data to conform to the formatting for the input file to BLT-MS.

GoldSim-BLTMS Coupled Model:

In implementing a probabilistic version of BLT-MS, decisions were made regarding what input constructs to consider to represent uncertainty. In the extreme, each realization of a probabilistic analysis could have a unique finite-element mesh, source term configuration, and parameter uncertainties. The input/output requirements, as well as the computational burden, could get prohibitive if this much flexibility were built into the tool. Therefore, some simplifying assumptions were made in order to make the code integration more practical.

It is quite common in probabilistic analyses that involve the potential to address spatial variability that the physical aspects of the problem are fixed, such as the model boundaries and finite-element mesh configuration. If there is a question about the design of the finite-element mesh and the boundary conditions, then this should be evaluated in terms of potential conceptual model uncertainty and additional model configurations contemplated to address this uncertainty explicitly. Therefore, it was recommended that a fixed, deterministic approach be taken for the design of the finite-element mesh and the specification of boundary node types (i.e., Cauchy, Neumann, or Dirichlet).

In addition to the overall configuration of the finite-element mesh and boundary conditions, it is also advantageous to fix the locations of the source term containers. If the elements containing containers are allowed to vary with each realization of a probabilistic analysis then the dependent specifications for container types, waste form types and breach/leach processes becomes much more intensive in terms of data configuration and formatting. In practice, any given site under consideration will have a proposed engineering design layout of the disposal area, so the physical configuration of the source term could be fixed based on this design. This still allows the user flexibility with the specifications of container types and waste form types for any of the specified containers. Therefore, the physical source-term configuration (e.g., elements containing containers) was assumed to be fixed/deterministic for any given probabilistic analysis, but the characteristics of each of the containers could be uncertain.

In summary, the input parameters that will remain fixed, or deterministic, are:

- Finite-element mesh design parameters/specifications;
- Material property assignments within the finite element mesh (although the characteristics of each material may be uncertain, the element assignments will remain fixed for a given material type);
- Finite element nodes for boundary conditions, including keeping the type of boundary condition fixed for a given node (i.e., Cauchy vs. Neumann vs. Dirichlet);
- Number of isotopic species (because specifying different decay chains for each model realization would be burdensome);
- Number of decay chains and branching fractions;
- Number of container types; and

- Number of waste types.

In general, the parameter sets that can be considered uncertain are in these areas:

- Initial concentrations within the source term;
- Boundary flux/concentration quantities;
- Breaching characteristics for any given container type;
- Leaching characteristics for any given waste type;
- Transport characteristics of the host rock/soil; and
- Darcy flux and moisture content distributions within the host rock/soil.

Figure 44 outlines the flow of information during a simulation using the coupled BLTMS-GoldSim model. This model was used for the probabilistic analysis discussed in Sections 4.1 and 5.1. GoldSim is a probabilistic simulation software code that has been used for Monte Carlo radionuclide transport models (GoldSim Technology Group, 2002 and 2003). Coupling BLTMS to GoldSim allows the BLT-MS code to take advantage of GoldSim's probabilistic features including Latin Hyper-cube Sampling (LHS). Therefore, a method was developed that takes advantage of GoldSim's ability to link to external codes. Two methods can be employed to connect GoldSim to an external code; an external DLL element or an external pathway element (elements in GoldSim are pre-programmed functions, (GoldSim Technology Group, 2003)). External Pathway Elements provide a mechanism by which external program modules for contaminant transport (e.g., analytical, finite element or finite difference solute transport models) can be directly integrated into GoldSim. These modules (referred to as External pathway functions) require the transport code, in this case BLTMS.EXE, to be compiled as a DLL (Dynamic Link Libraries) and linked directly into GoldSim at run time. To maintain a valid pedigree and reduce the number of changes to BLTMS.EXE, this option was not used. The second option, External Elements (DLL), are generic modules (codes) linked to GoldSim as DLLs (Dynamic Link Libraries) at run time. Two generic "wrapper" (or "shell") codes were created and compiled as DLLs. These codes contain the logic for launching the executable and reading the output back into GoldSim. The concept is simple, as can be seen on the flow chart in Figure 44. When executing a probabilistic simulation, GoldSim is launched, reads a BLT-MS input file, and writes a new BLT-MS input file replacing uncertain parameter values with the sampled value contained in the GoldSim model file using the READ_BLT.DLL. GoldSim then launches a BLT-MS simulation using the LAUNCH_BLTMS.DLL. The output from the BLT-MS simulations is read back into the GoldSim model and used for the 1-D transport simulation and dose calculations. The model is exercised over the total number of realizations selected.

Specific details on the functionality of the coupled BLTMS-GoldSim model are described in a report entitled GoldSim-BLTMS Model Users Guide. In addition the source codes have been designated as open-source and are freely available. The users guide and source codes can be accessed on a Sandia National Laboratories website at the following URL: http://www.sandia.gov/icp/.

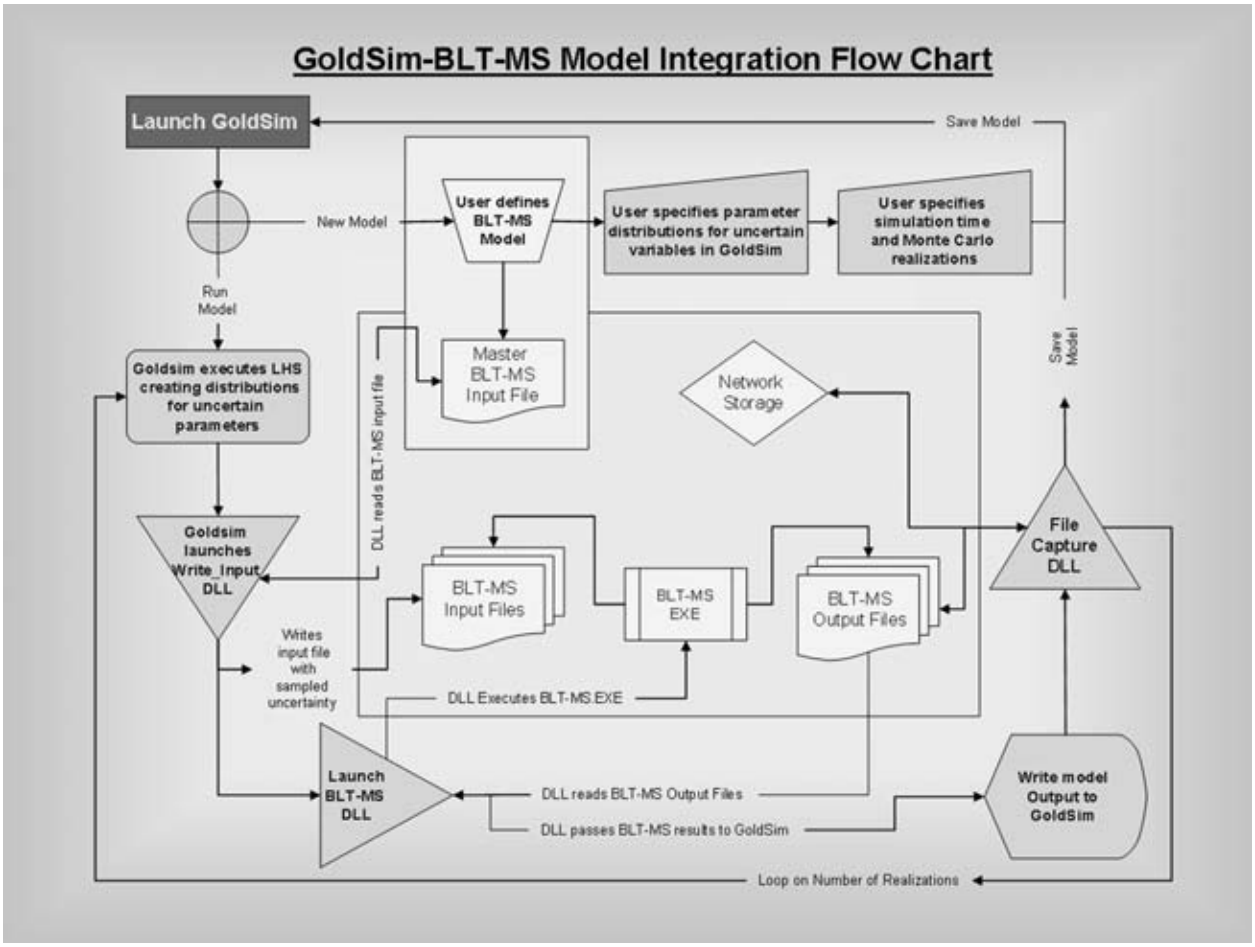

Figure 44. Flow Chart for GoldSim/BLTMS Integration Model

BLTPLOT_UNCERT.EXE

When BLT-MS was first developed in the 1990's, a post-processor was also developed to visualize the results. This code was called BLTPLOT. BLTPLOT was compiled with a Microsoft FORTRAN compiler and employed DOS-based screen graphics (not Windows-based graphics). The functionality was good for its time, but does not meet today's standards. The problem with employing this code for post-processing is that the output format of the BLT-MS code has changed since BLTPLOT was developed, such that the code can no longer read BLT-MS output properly in order to visualize results. The Microsoft FORTRAN compiler is no longer supported by Microsoft, and no copies were located at Sandia, so there was no reasonable way to recompile the code for use with today's computers. However, there is still a need to visualize results. Therefore, a simple FORTRAN code was written to post-process BLT-MS model results for 2-dimensional concentration data. This code is named BLTPLOT_UNCERT.EXE. The code has been designated as open-source and is freely available. It can be accessed on a Sandia National Laboratories website at the following URL: http://www.sandia.gov/icp/. The BLTPLOT_UNCERT code can extract information on the concentration distribution for a single model run or it can take the output from a Monte

Carlo/LHS uncertainty analysis and produce an average concentration distribution from the suite of results. The code requires several output files from a completed BLT-MS model run. The code queries the results files and then asks the user to specify which radionuclide and what time step they would like to save the data. The output from the BLTPLOT_UNCERT is a file containing x, z, and concentration paired data for all the finite-element nodes in the model. This data can then be plotted with 2-D plotting software, such as SURFER or TECPLOT.

3.3.6. Radiological Dose Calculations

A performance assessment methodology not only requires the ability to simulate the potential source-term release and far-field transport of the radionuclides of concern, but must also consider the potential exposure pathways of the radionuclides to a near-by resident population and the accompanying dose that these individuals might incur. A comprehensive dose assessment would likely include exposure from the following: drinking, or ingestion, of potentially contaminated water; dermal adsorption from showering; food uptake from irrigating crops with potentially contaminated water; milk ingestion from exposed dairy animals; and fish consumption from contaminated streams or the ocean. This is not necessarily a comprehensive list, and other exposure routes might be assessed as well. For the purpose of demonstrating a performance assessment methodology, the radiological dose assessment was simplified to only a drinking water ingestion pathway.

The implementation of the dose assessment strategy in the models was done with the following considerations. The 2-D advective-dispersive model and the 1-D matrix-diffusion model were constructed to allow the concentrations of radionuclides to be output at a distance of 100 meters down-gradient of the edge of the repository to approximate the groundwater concentrations for a hypothetical drinking-water well, based on regulatory guidelines. The dose assessment was performed utilizing guidelines from ICRP Publication-72, "Age-dependent Doses to Members of the Public from Intake of Radionuclides: Part 5 Compilation of Ingestion and Inhalation Dose Coefficients, Annals of the ICRP. The ICRP dose coefficients have been adopted in the International Basic Safety Standards (IAEA, 1996) and in the Euratom Directive (EC, 1996).

The dose model was constructed based upon ICRP-72 dose coefficients for ingestion (Table 17). The drinking water pathway was used as the exposure pathway in this model. The primary radionuclides in the groundwater are represented by average concentrations at the well nodes. The average concentration is calculated to give a 'vertical slice' of the finite element grid, e.g. representing a well intersecting the saturated zone 100 m down gradient of the proposed repository.

The annual dose from ingestion of radionuclides in drinking water is expressed as:

$$Dose = EFD^{RN}_{ICRP72}(Sv/Bq) \times C^{RN}_{Water}(Bq/L) \times ACR(L/yr)\text{, where:}$$

EFD = effective dose conversion factor from ICRP-72 for a specific radionuclide species

C = average concentration of a radionuclide species in the well pathway

ACR = annual water consumption rate (2 L/day).

The annual consumption rate of 2 liters/day or 730 L/yr was used as specified in 10 CFR 63.312(d).

Table 17. Dose Conversion Factors

Radionuclide	ICRP-72 DCF (Sv/Bq)
Ni-63	1.5×10^{-10}
Cs-137	1.3×10^{-8}
C-14	5.8×10^{-10}
Co-60	3.4×10^{-9}
Sr-90	2.8×10^{-8}
Tc-99	6.4×10^{-10}
I-129	1.1×10^{-7}
H-3	1.8×10^{-11}
Pu-240	2.5×10^{-7}
Pu-239	2.5×10^{-7}

4. PRELIMINARY ASSESSMENT OF NEAR-SURFACE DISPOSAL SYSTEM DESIGN CONCEPT

4.1 Base Case Analysis

The near-surface disposal system design proposed for consideration on an island west of Taiwan is a fairly conventional design for low-level radioactive waste disposal facilities (see Figure 4). In this particular case, however, the water table is fairly shallow and allows potential contact with the groundwater system almost immediately upon release of any radionuclides from the disposal cells.

4.1.1 Radionuclide Release and Transport Conceptual Model

For the near-surface disposal system design there are three separate disposal areas on the island. The waste inventory was assumed to be split evenly among the three disposal areas. For the purpose of modeling the performance of the system, just one of these disposal areas was considered. The basis for this modeling assumption rests on the island morphology and FEHM flow modeling results. As discussed in Section 3.3.1 for the island site, horizontal gradients in head indicate that groundwater flows from the central part of the island towards the ocean shoreline. Therefore, based on flow modeling and repository layout, only one-third of the inventory is considered for this preliminary performance assessment.

The base case analysis for the near-surface disposal system design was constructed in such a manner as to approximate the design concepts as closely as possible. The following attributes of the source term were taken into consideration in constructing the numerical model for the site:

- Shallow trench burial on a small island with up to about 40 m elevation gain from sea level.
- Disposal cell design has the following attributes:
    - Waste disposed in 55-gallon galvanized drums in disposal cells.
    - Each disposal cell is nominally 7.6 m wide by 7.6 m long by 7.5 m high. The base and side wall is 1m thick.
    - Each disposal cell can accommodate 1,008 drums, with 12 drums wide by 12 drums long and 7 layers high.
    - Total number of disposal cells in the repository will be 1,014.
    - The capacity of the repository will be 1,022,112 drums.
    - Once a disposal cell is filled, grout is placed between all drums.
    - Two concrete caps, 60 cm and 40 cm thick, are placed on top of a disposal cell after it is filled.
    - An earthen cap will be placed over the disposal cells, above the concrete caps, to control infiltration and runoff.

Other considerations for this site include:

- Local meteorological data are available.
- Underlying geology is mainly fractured basalt with some sandstone/mudstone interbeds generally 1 to 2 m thick, but up to 10 m thick.

- Hydrogeologic and geochemical data are not available at this time.
- Typhoons will impact the island (although their impacts are not evaluated explicitly).
- Sea level may rise as much as 200 cm in the next 300 years.
- Seismic activity is believed to be minimal.
- Volcanic activity is believed to be minimal.

As mentioned above, the BLT-MS model was used to model the source term, both the failure of the waste canisters as well as the leaching of the radionuclides from the waste forms after breach has occurred. The source term elements in BLT-MS were constructed to have the same basic dimensions of the disposal cells listed above. At least two elements were needed in any given disposal cell to adequately approximate the release mechanisms within the model. The source term was modeled with a total of 480 waste container elements. A set of elements was also assigned to the top, bottom, and sides of the disposal cell area to represent the concrete encasement of the disposal cells. The model was constructed to have the ability to represent the material properties within the disposal cell area to be different from that of the host rock in order to simulate the effects of the grout backfill and concrete lining on the transport process.

The overall model setup has the following attributes. The model boundaries were selected as follows. The upstream end of the disposal area was established as the left side of the model. The right side of the model was coincident with the approximate area where the fresh-water/salt-water interface is likely to occur at the point where the island meets the ocean. The top boundary is the water table. The bottom boundary is that surface that likely represents the lowest flow path of any groundwater passing through the disposal area. As shown in the previous section, groundwater flow is generally from left-to-right in the model domain (e.g. from the island center to the ocean shore). For the transport solution in the model, the right side boundary of the model was assigned a Dirichlet zero constant concentration condition. All other model boundaries preclude mass transfer out of the model domain. The dimensions of the model are 100 meters high by 400 meters wide. There are 31 finite-element nodes in the vertical, z, direction and 175 nodes in the horizontal, x, direction. The total number of finite-element nodes in the model is 5425. The total number of finite elements in the model is 5220. The flow velocities required in the model were abstracted from the FEHM modeling results onto the existing finite-element grid. Flow velocities within the source-term area, as well as the landfill cover, were set to very low values, in a strictly downward vertical vector, corresponding to the percolation flux through the cover.

The waste inventory in the source term was derived from information provided by INER along with a number of assumptions where information or data did not exist. Section 3.3.1 above discussed the assumptions and approach to developing estimates of the waste inventory. Table 7 provided a synopsis of the activity for each radionuclide associated with each waste type for the radionuclides selected for analysis.

INER has chosen to evaluate a design in which all the waste will be encapsulated in concrete and grout. Concrete and grout generally have about a 300 year failure time or greater. Localized corrosion of the waste drums would likely be occurring during this time, but releases would not occur due to the concrete/grout encapsulation. Therefore, generalized corrosion was invoked as the release mechanism with a failure time of 300 years.

4.1.2 Base Case Analyses:

The first conceptual model of the site involves a very conservative assumption about the leaching process that occurs once the drums have failed. The assumption is that all the waste is subject to rinse release. Rinse release allows the radionuclides to freely mix with the incoming infiltration water. There is little credit given for source term controls in this conceptual model. The rationale behind invoking this conceptual model is that if the performance of the system is in compliance with the standard, then the site is likely suitable because the engineered barrier system would just add to the performance.

The computational model was set up with little site-specific data relative to transport properties. Values were taken mainly from the literature (e.g., NRC, 1996a). Porosity was assumed to be 0.014 throughout the far-field model domain. Table 18 shows the input values for key transport properties for each of the radionuclides of concern.

Table 18. Key Input Parameters for Transport Processes

Radionuclide	Sorption coefficients [cm^3/g]	Solubility Limit [g/cm^3]	Half-Life [years]	Diffusion Coefficient [cm^2/s]
Ni-63	100.	$6.3x10^{-4}$	80.0	$1.0x10^{-8}$
Cs-137	500.	1.0	30.17	$2.8x10^{-12}$
C-14	0.01	1.0	5480.	$1.0x10^{-8}$
Co-60	10.	$6.0x10^{-4}$	5.21	$1.0x10^{-8}$
Sr-90	8.	1.0	27.4	$4.0x10^{-11}$
Tc-99	0.001	1.0	$2.11x10^{5}$	$1.0x10^{-8}$
I-129	0.001	1.0	$1.73x10^{7}$	$1.0x10^{-8}$
H-3	0.001	1.0	12.3	$1.0x10^{-8}$
Pu-240	100.	$2.4x10^{-14}$	6580.	$1.0x10^{-8}$
Pu-239	100.	$2.4x10^{-14}$	$2.44x10^{4}$	$1.0x10^{-8}$

Figure 45 shows concentration versus time for each of the radionuclides in the analysis over a 10,000 year time frame. Sensitivity exists regarding the publishing of actual dose estimates from the modeling at such an early stage in the development of the performance assessment methodology. That is especially true given the general lack of site data for each site under consideration and the uncertainty that is created in the modeling results. Therefore, dose values are presented as normalized quantities. The maximum total dose estimate from the rinse release case was used as a divisor for all dose estimates to put all the output on a relative scale without having to publish a dose estimate that can be compared to the standard. Therefore, in the presentation of the rinse model case results the maximum total normalized dose will be a value of 1.0, and all other dose estimates will be a fraction of that. Figure 46 shows normalized dose versus time for the same radionuclides as shown in Figure 45, along with the total normalized dose (a summation of all the dose estimates from each of the radionuclides). The normalized dose is calculated for a drinking water exposure scenario. Several conclusions can be drawn from these results. First, several of the radionuclides have decayed significantly over the first several thousand years. These radionuclides include Cs-137, Co-60, Sr-90, and H-3. They do not contribute any appreciable dose to the total. Ni-63 is persistent in the system for slightly

longer duration, up to about 7000 years, but is still not a significant contributor to dose. The three radionuclides that are essentially non-sorbing, C-14, I-129, and Tc-99, are the main contributors to dose. The plutonium isotopes, Pu-239 and Pu-240, become more dominant at later times. These radionuclides are controlled by solubility release mechanisms.

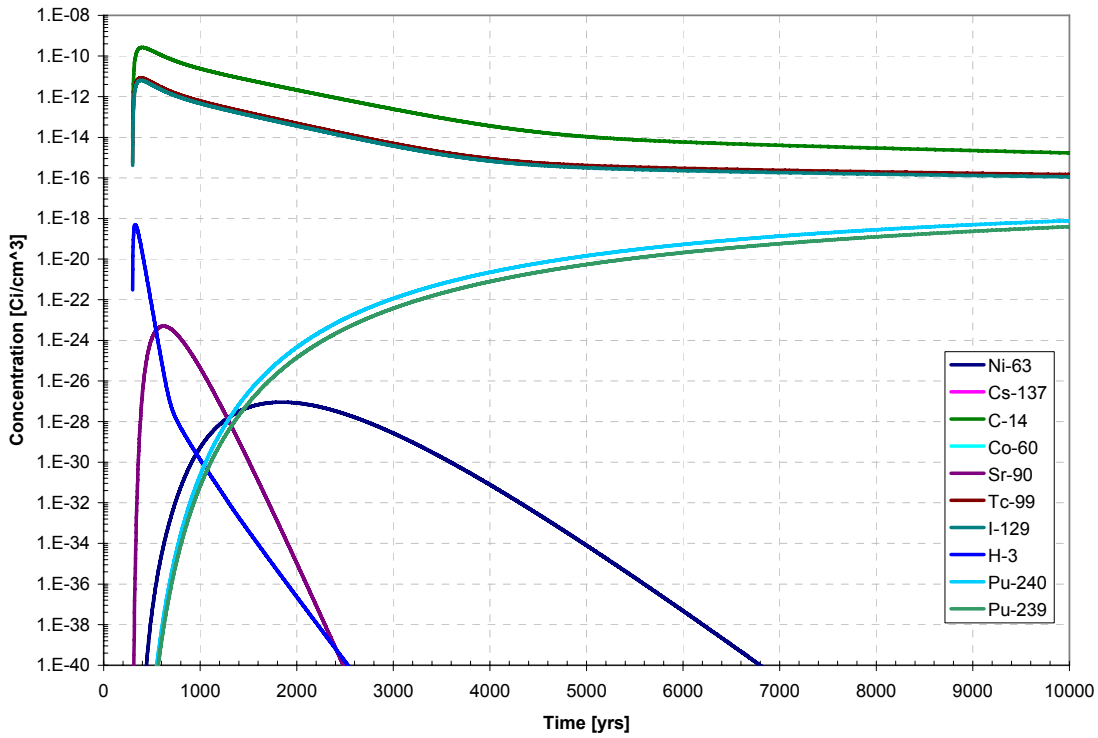

Figure 45 – Concentration Versus Time for the Near-Surface Disposal Site With a Rinse Release Conceptual Model

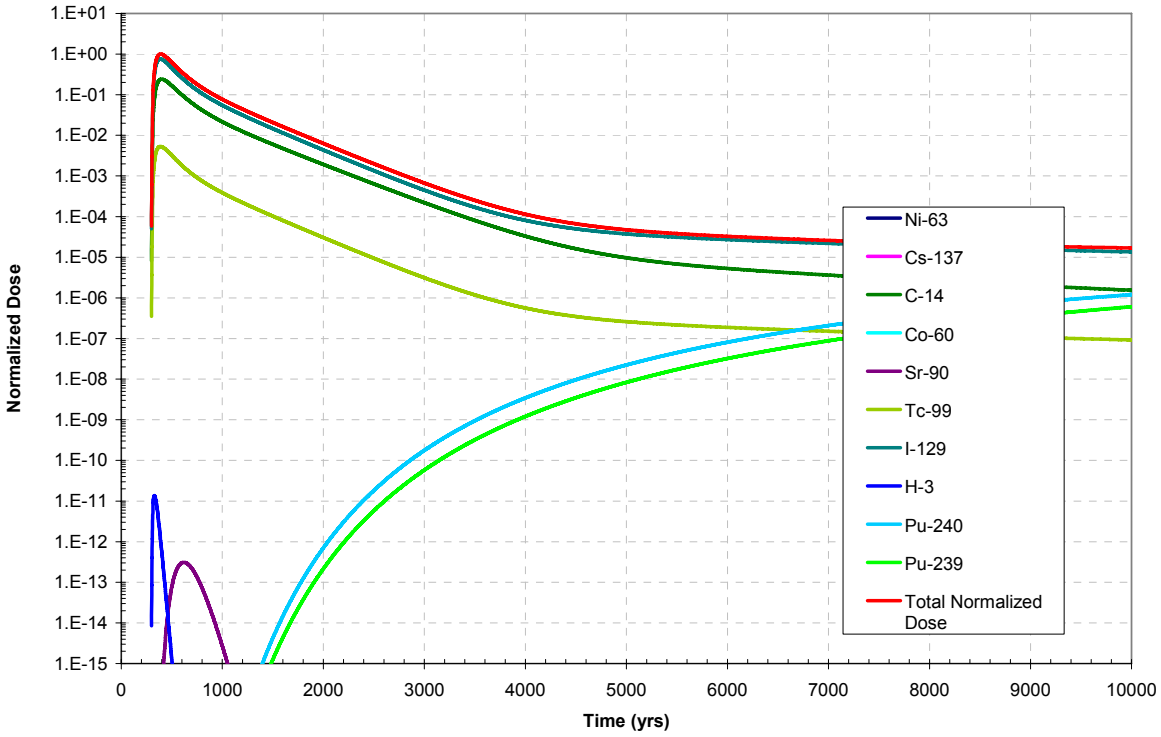

Figure 46 – Dose Versus Time for the Near-Surface Disposal Site With a Rinse Release Conceptual Model

The next conceptual model modified the leaching mechanisms for the various waste types that were prescribed in Table 7. For this conceptual model, the operational waste was split between a non-solidified waste fraction with a 50% rinse and 50% diffusion release specification and a solidified waste fraction with diffusion release, then the decommissioning waste was split between a non-metal waste fraction with rinse and diffusion release and a metal waste fraction with a dissolution release. These waste type designations are still preliminary and likely to change as INER further evaluates the sites.

Figure 47 shows concentration versus time for each of the radionuclides in the analysis over a 10,000 year time frame. Figure 48 shows normalized dose versus time for the same radionuclides, along with the total normalized dose. Several conclusions can be drawn from these results. The peak dose is lower by about half for this conceptual model compared to the rinse release only model. So there is improvement in performance with more realistic source-term assumptions.

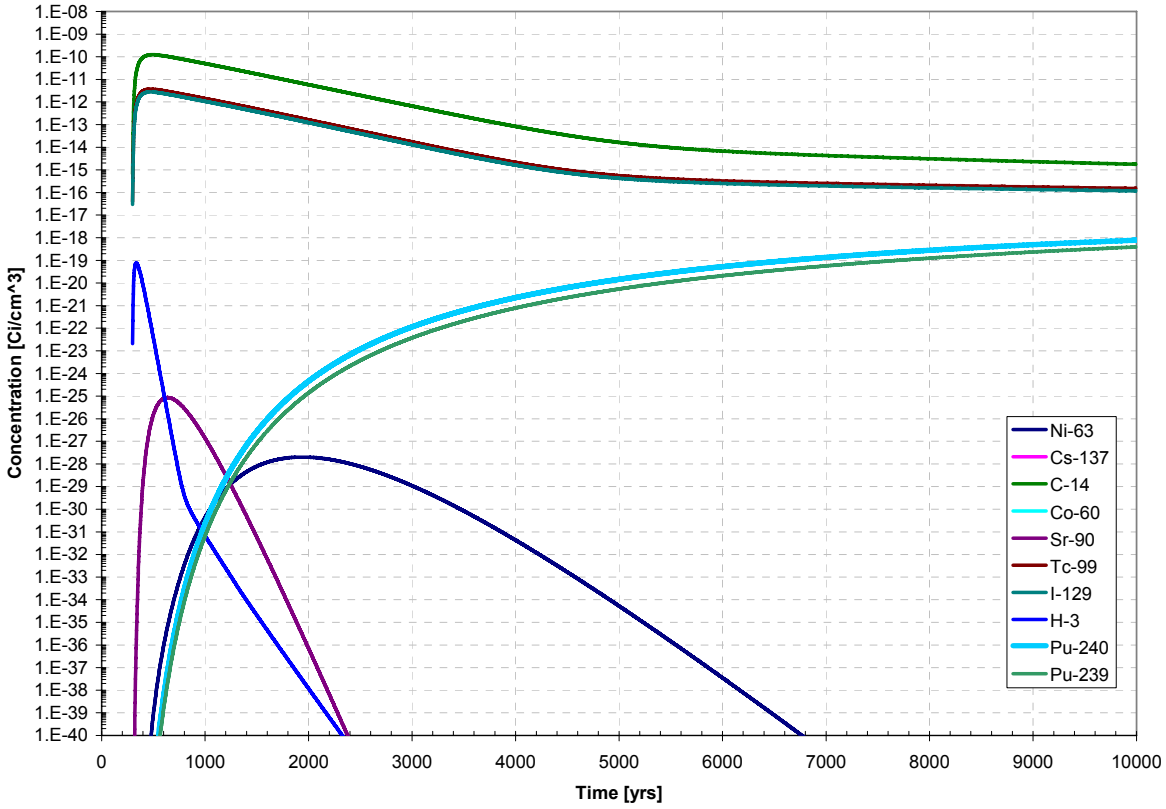

Figure 47 - Concentration Versus Time for the Near-Surface Disposal Site for the Modified Conceptual Model Using More Realistic Release Mechanisms

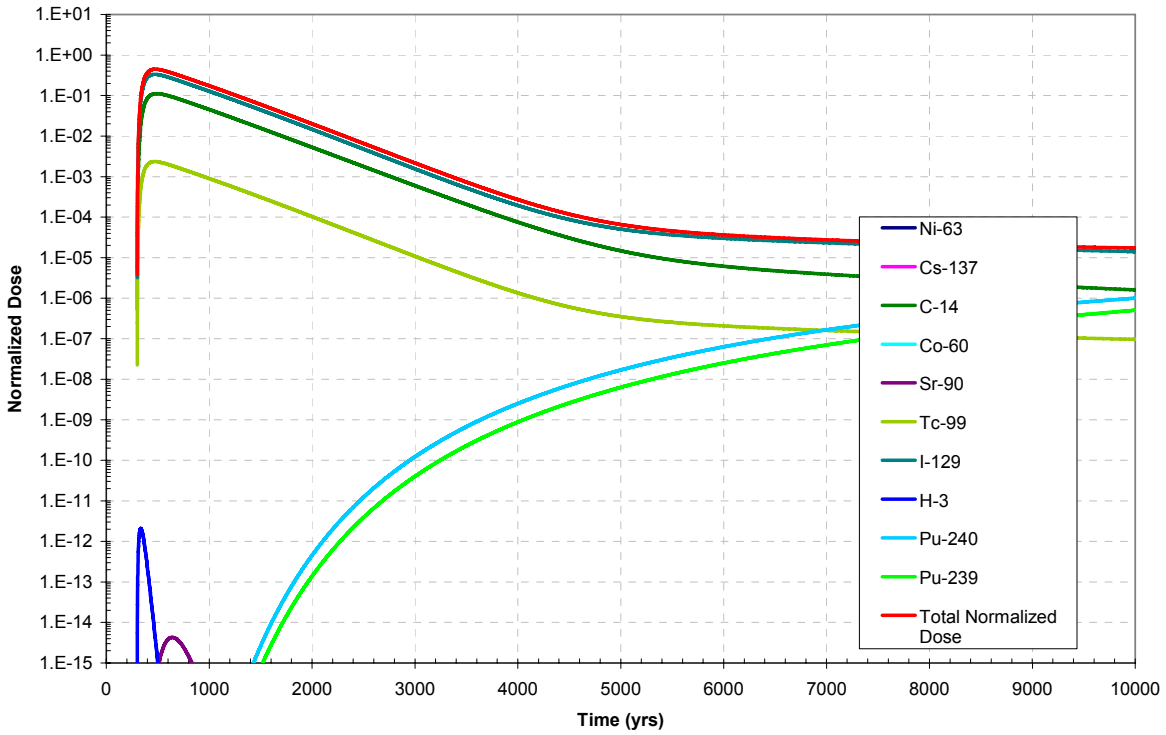

Figure 48 - Dose Versus Time for the Near-Surface Disposal Site for the Modified Conceptual Model Using More Realistic Release Mechanisms

The next modification to the conceptual model attempts to account for the effects of the concrete and grout surrounding the waste drums. The concrete/grout has a different porosity and molecular diffusion coefficient than the surrounding host rock. Diffusion of the radionuclides through the concrete/grout should impede the release to a degree. This conceptual model is designated as the baseline case model in that it incorporates the best estimates of the waste release mechanisms as well as a representation of the engineered barrier system performance.

Figure 49 shows concentration versus time for each of the radionuclides in the analysis over a 10,000 year time frame. Figure 50 shows normalized dose versus time for the same radionuclides, along with the total normalized dose. The behavior of the radionuclide release and transport is virtually identical to that of the previous conceptual model. It was thought that accounting for the diffusion release through the concrete/grout would impede the release of the radionuclides somewhat to the far field. It may be that the release mechanisms from the waste form are likely the limiting factor. The peak dose is lower by about half for this conceptual model compared to the rinse release only model.

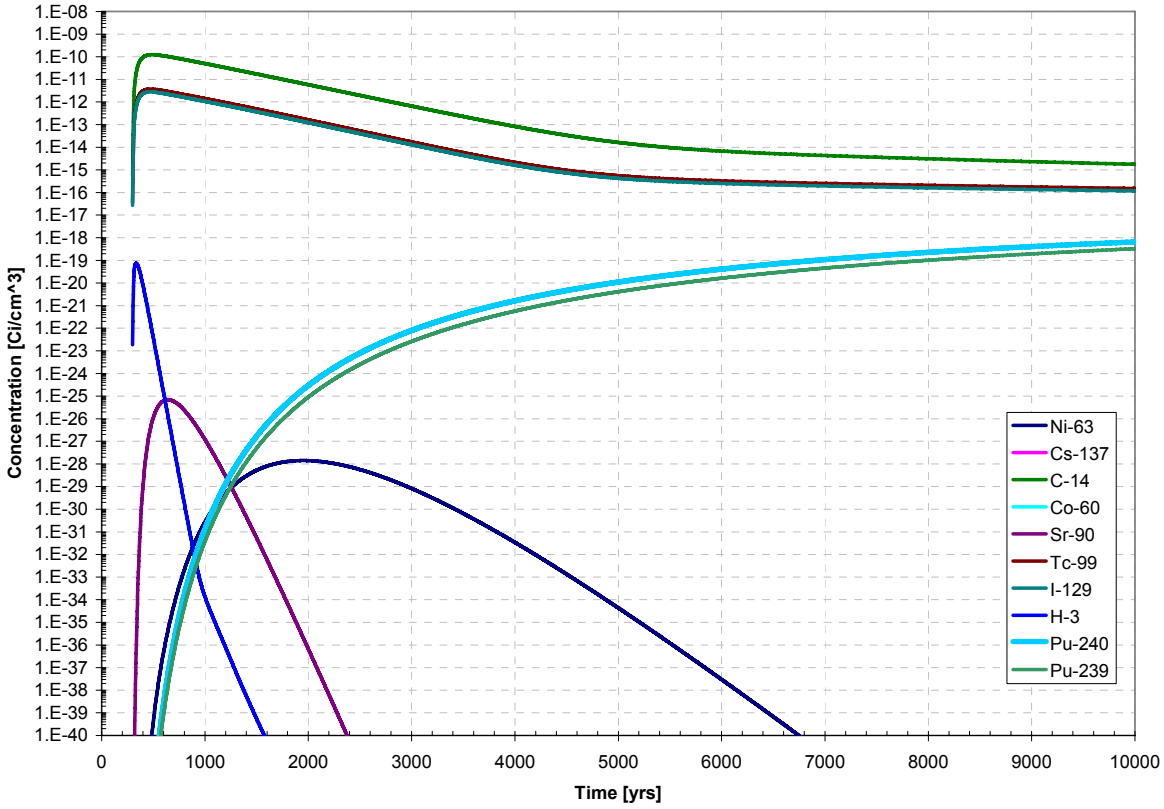

Figure 49 - Concentration Versus Time for the Near-Surface Disposal Site for the Baseline Conceptual Model

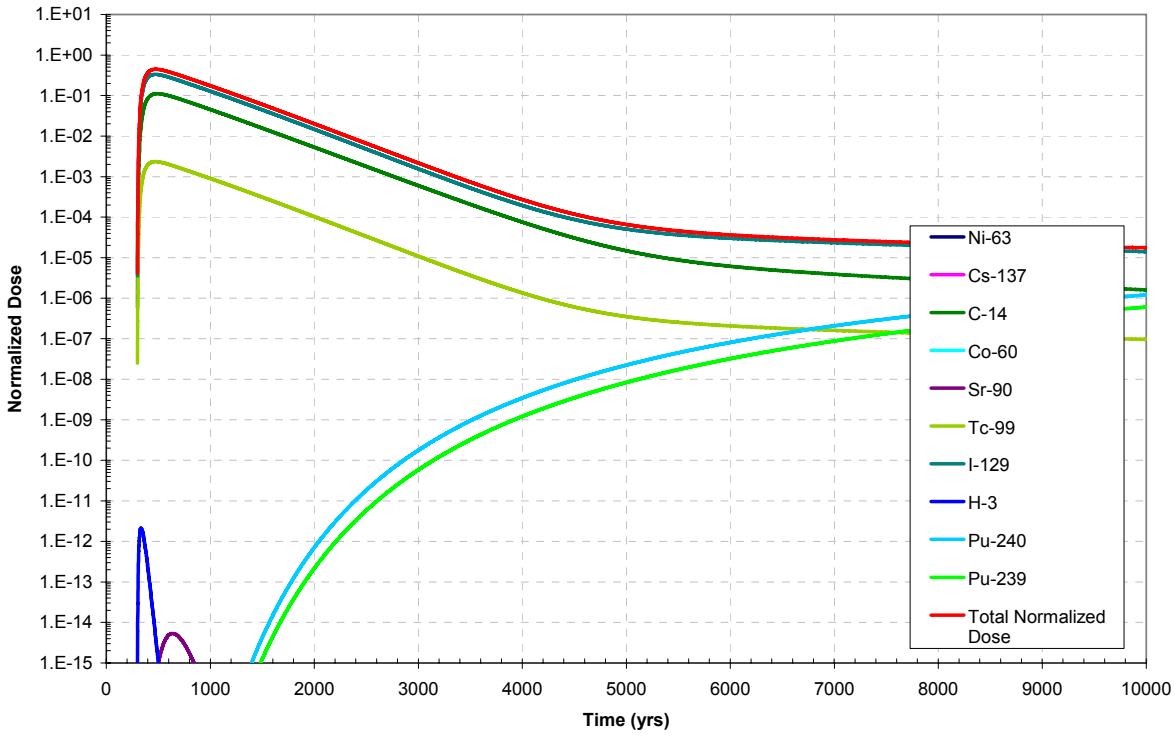

Figure 50 - Dose Versus Time for the Near-Surface Disposal Site for the Baseline Conceptual Model

After concluding that the waste form release mechanisms appear to be a limiting factor, the INER staff considered the possibility that they might prescribe that all waste disposed in the facility would be solidified. This translates into a conceptual model where all the waste is subject to a diffusion release mechanism. The next conceptual model evaluated invoked the assumption that all the waste was subject to diffusion release.

Figure 51 shows concentration versus time for each of the radionuclides in the analysis over a 10,000 year time frame. Figure 52 shows normalized dose versus time for the same radionuclides, along with the total normalized dose. The behavior of the radionuclide release and transport is virtually identical to that of the previous conceptual model. It was thought that accounting for the diffusion release from all the waste forms would impede the release of the radionuclides somewhat to the far field. The peak dose is lower by about half for this conceptual model compared to the rinse release only model.

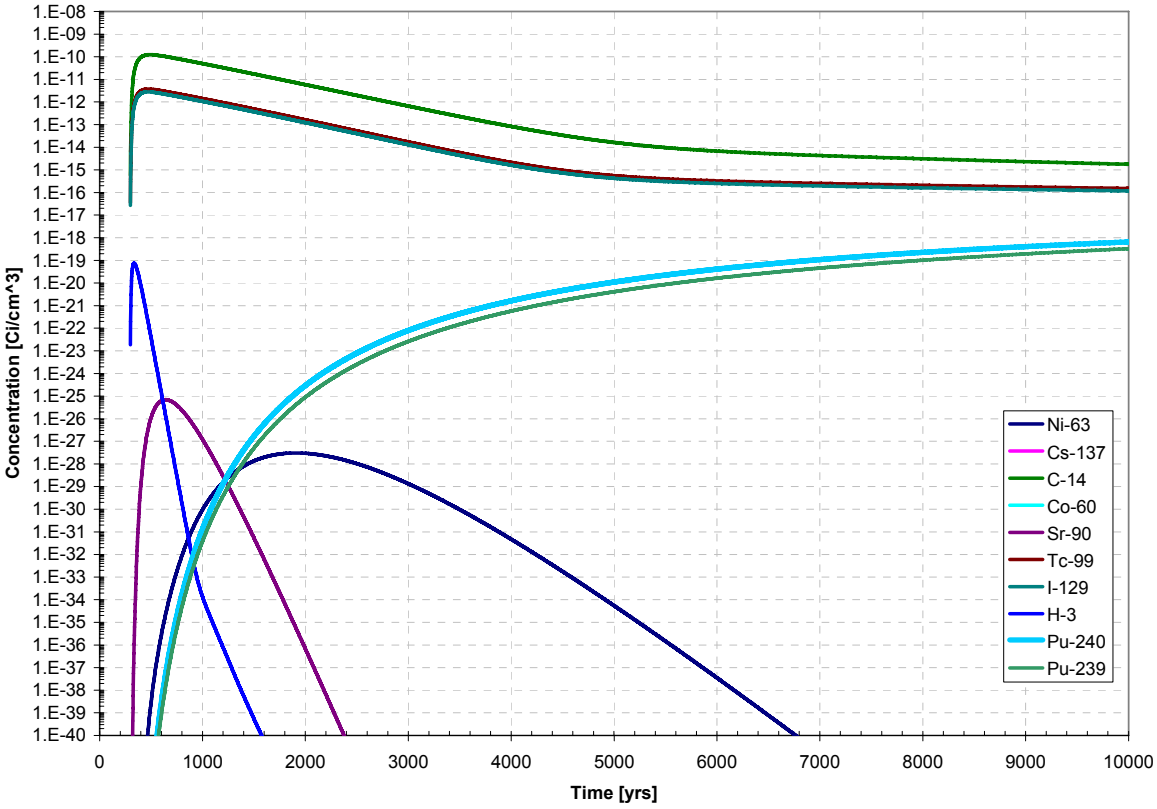

Figure 51 - Concentration Versus Time for the Near-Surface Disposal Site for the Modified Conceptual Model With Only Diffusion Release

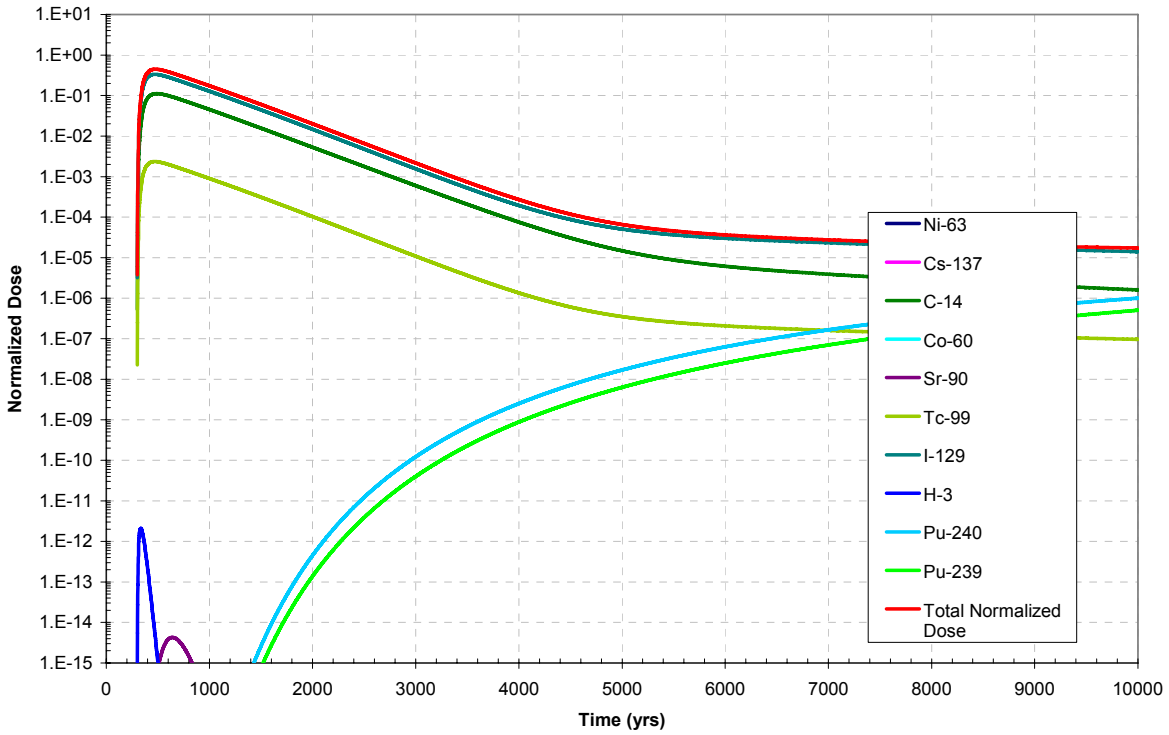

Figure 52 - Dose Versus Time for the Near-Surface Disposal Site for the Modified Conceptual Model With Only Diffusion Release

Several conceptual model variations have been presented. It was pointed out that the behavior of the radionuclide release and transport was quite similar for the latter conceptual models, those that were not a rinse only release. Figure 53 shows a comparison of the total normalized dose estimates with time for each of these conceptual models. It is quite evident that the behavior is indeed similar for all but the rinse release model.

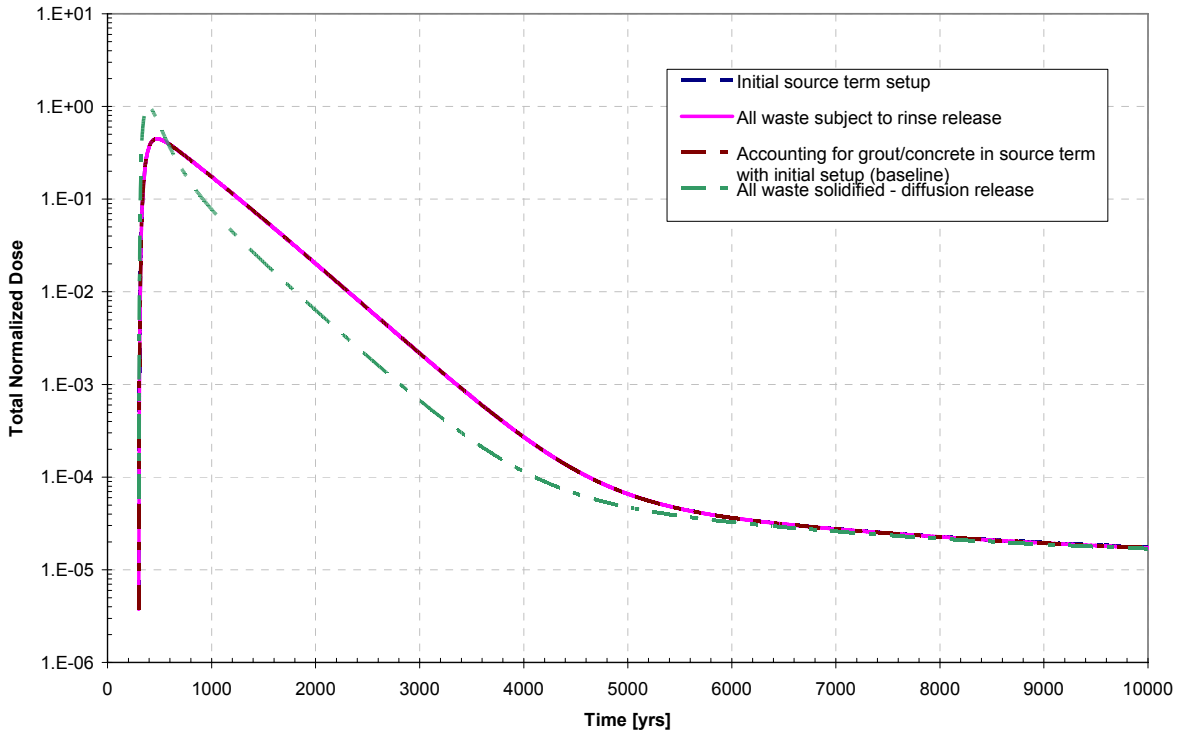

Figure 53 – Dose Versus Time for the Near-Surface Disposal Site for Four Alternative Conceptual Models

As mentioned above, the BLTPLOT_UNCERT code was written to extract 2-dimensional concentration distribution data from the model output. Figure 54 shows a time-history of the Pu-240 concentration for the baseline conceptual model. The output times are 320, 1000, 5000, and 9000 years. The concentration contours are labeled in log space for units of Ci/cm^3. These plots show that the Pu-240 is building in concentration with time and moving from left to right across the model domain, as would be expected given the flow regime.

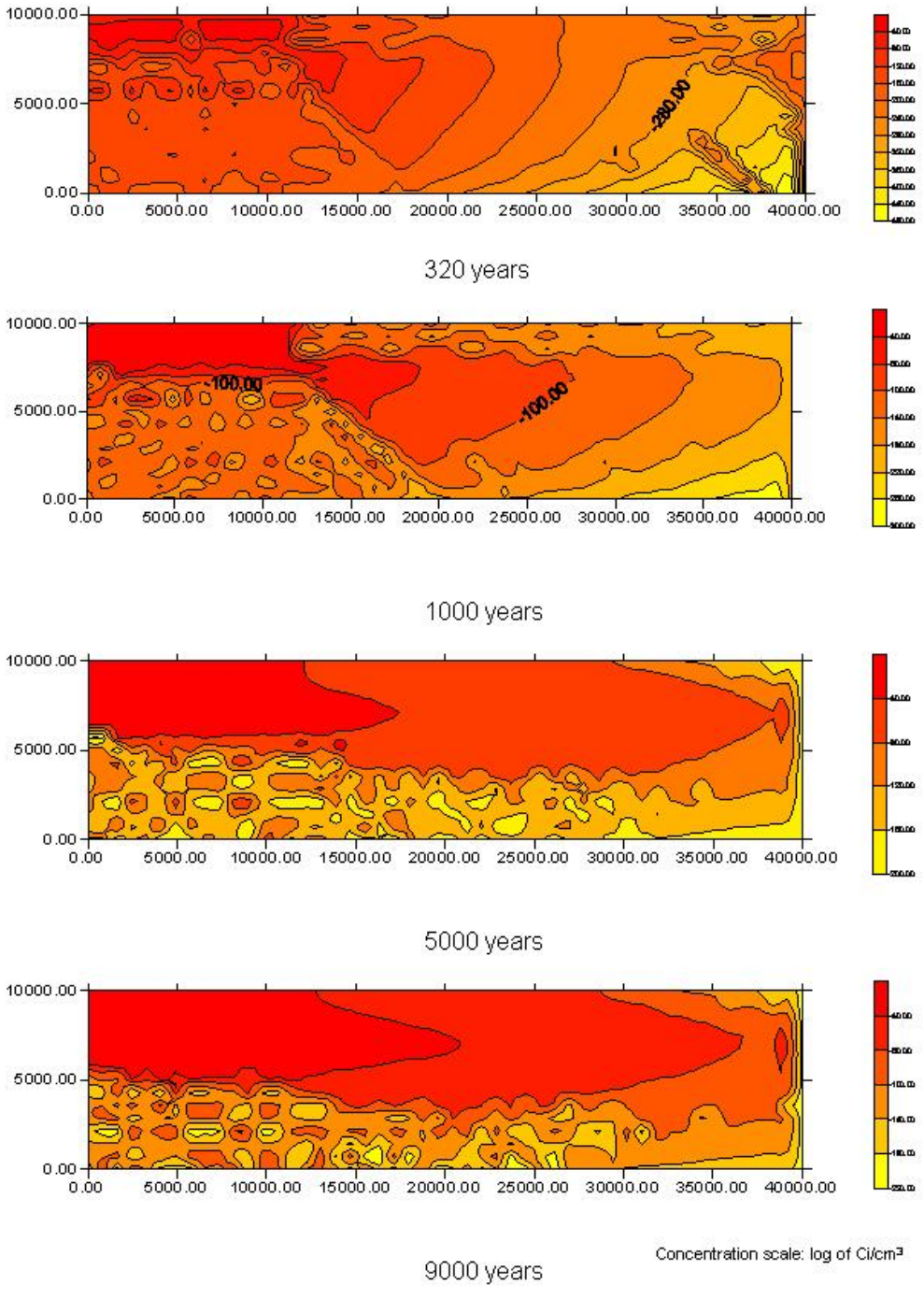

Figure 54 – 2-D Concentration Versus Time for Pu-240 With the Baseline Conceptual Model for the Near-Surface Disposal Site.

4.1.3 Probabilistic Analysis

Uncertainties will inevitably exist in projections of the geologic and environmental conditions surrounding the disposal site 1,000 or 10,000 years into the future. Assessment of the disposal site performance over this period must take these uncertainties into account. Uncertainty is usually expressed in two categories, aleatory and epistemic. Aleatory uncertainty arises from quantities that stem from variability in populations, from which random samples are taken. The basic idea underlying the concept of aleatory uncertainty is that a range of possible values exists, all having a certain probability of occurring. An example of aleatory uncertainty considered is that of early failed containers. The second category is referred to here as epistemic uncertainty. Epistemic uncertainty arises from a lack of knowledge about a quantity that is believed to have a fixed (or deterministic) value. Thus, the quantity is not random in the sense used above. Rather, there is a lack of knowledge about what its value should be due to limited data and knowledge. Epistemic uncertainties arise due to, among others, incomplete data, measurement errors, and estimates based upon expert judgment. Unlike aleatory uncertainty, epistemic uncertainty is potentially reducible with additional data and knowledge. A particular epistemic quantity can be a parameter for a probability distribution (e.g., diffusion coefficients for release of radionuclides from the waste form).

The baseline conceptual model presented above was used to perform an uncertainty analysis. To demonstrate the probabilistic capabilities of the BLTMS-GoldSim coupled model, an analysis is presented that considers only two parameters as uncertain. Table 19 lists the uncertain parameters and the range of values used.

Table 19. Uncertain Parameter Ranges for Probabilistic Analysis

Parameter	Range			Description
GRATE (cm/s)	Triangular Distribution			BLT-MS Data Set 20: Container general corrosion rate (NRC, 1989)
	Most Likely	Min	Max	
	1.48×10^{-11}	1.0×10^{-11}	2.0×10^{-11}	
DEFF (cm^2/s)	ISO	Uniform Distribution		BLT-MS Data Set 21: Waste for effective diffusion coefficient (NRC, 1989)
		Min	Max	
	Ni-63	1×10^{-9}	1×10^{-7}	
	Cs-137	2.8×10^{-13}	2.8×10^{-11}	
	C-14	1×10^{-9}	1×10^{-7}	
	Co-60	1×10^{-9}	1×10^{-7}	
	Sr-90	4×10^{-12}	4×10^{-10}	
	Tc-99	1×10^{-9}	1×10^{-7}	
	I-129	1×10^{-9}	1×10^{-7}	
	H-3	1×10^{-9}	1×10^{-7}	
	Pu-240	1×10^{-9}	1×10^{-7}	
	Pu-239	1×10^{-9}	1×10^{-7}	

For LLW disposal waste container performance is an important factor controlling the release of radionuclides for transport to the accessible environment. The GRATE parameter in BLT-MS is

invoked to calculate the general corrosion rate for a waste container. Given a waste container thickness of 0.14 cm for the base case model and using the distribution in Table 19, the waste package container failure times were varied between 220 years to 300 years for the probabilistic analysis for Site #7. The DEFF parameter in BLT-MS is the effective diffusion coefficient used to calculate the release of radionuclides from the waste form for a diffusion controlled release model. The effective diffusion coefficient is radionuclide specific; Table 19 lists the distributions used for each of the radionuclides considered in this analysis. The probabilistic case was run using the coupled GoldSim-BLTMS model. The analysis was run for 100 realizations for 1,000 years. A Latin Hyper-Cube Sampling (LHS) was used in a Monte Carlo analysis to select the input values for the uncertain distributions.

Figure 55 shows the base case total normalized dose release versus the probabilistic mean total normalized dose for the near surface disposal site. Compared to the base case, the mean dose curve from the probabilistic case shows an earlier initial release which reflects the earliest waste container failure at approximately 220 years. The base case deterministic model has a corrosion rate equal to 1.48×10^{-11} cm/s which results in a waste container failure at about 300 years. The effect of the uncertainty can be seen in higher mean normalized doses in the probabilistic case between 200 years and 600 years. Figure 55 shows the spread of releases in the 2-D transport normalized dose results due to the variable failure times in the probabilistic case. The effect of uncertain diffusion of radionuclides from the waste form can be seen on Figure 56. In Figure 57 the probabilistic case was reduced to show the effect of the waste form diffusion coefficient. Six realizations were used to calculate a mean total normalized dose for comparison to the base case results. The realizations were selected that had a general corrosion rate which resulted in a waste container failure between 296 years and 302 years to be consistent with the base case analysis. The mean for these six realizations shows a higher peak normalized dose due to higher sampled diffusion rates from the waste form for I-129. The base case diffusion coefficient for I-129 was 1.0×10^{-8}, whereas the sampled values over the six representative realizations varied between approximately 5.0×10^{-8} to 7.0×10^{-8}, five to seven times higher that the base case values. The combined effects of earlier release due to the uncertainty in the general corrosion rates and the higher peak normalized dose results due to the realizations with high diffusion coefficients are reflected in the mean normalized dose rate for the probabilistic analysis.

The example simplified probabilistic study shows the importance of considering the aleatory and epistemic uncertainty represented in the geologic disposal system. The combined effects in this example yielded a higher normalized dose on average, than that of the expected case as represented by the deterministic base case results. Given the high number of assumptions in the design and site properties for the near surface disposal site, the uncertainty study displays the importance of an iterative approach that couples design and feedback to the safety assessment. A probabilistic safety assessment can be used to refine the data for parameters that have an impact on the repository performance (e.g. reduce epistemic uncertainty) and identify the important design features (e.g. aleatory uncertainty).

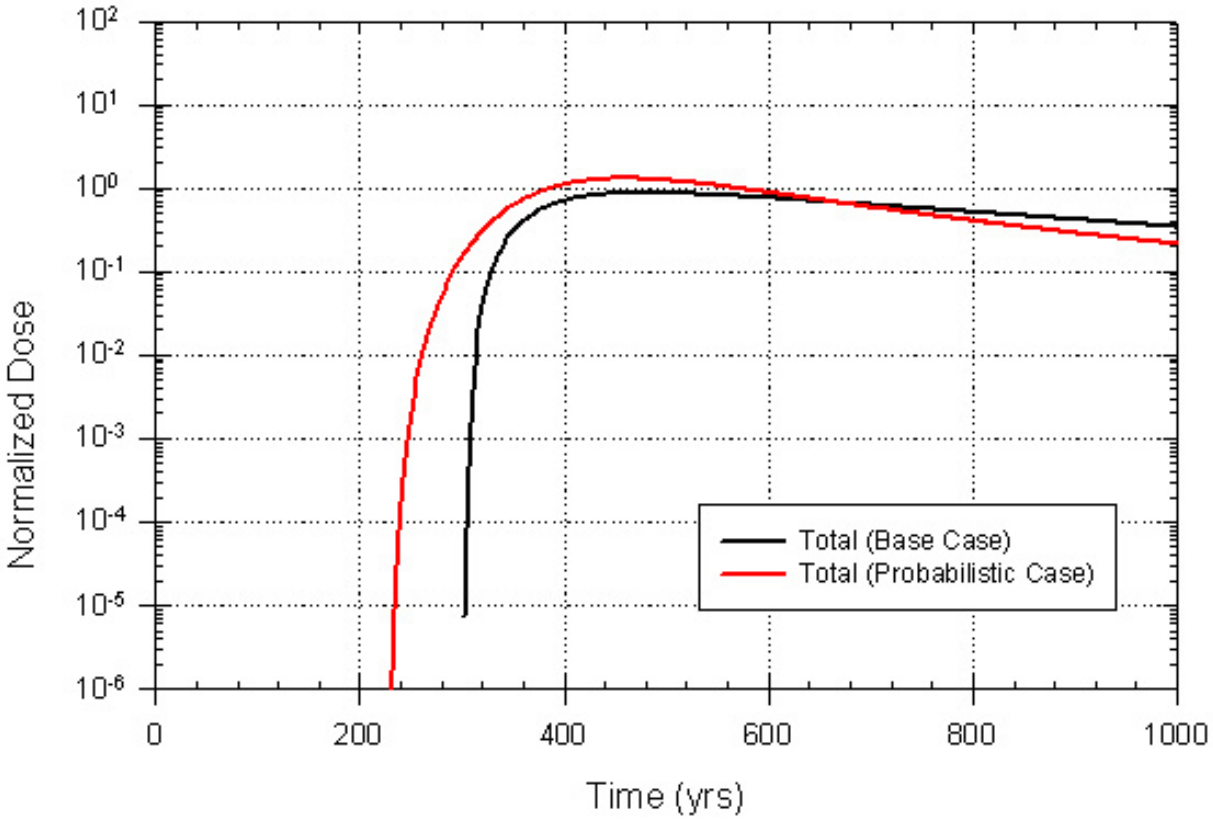

Figure 55: Near surface disposal site BLT-MS base case total dose vs. BLT-MS probabilistic case mean total dose

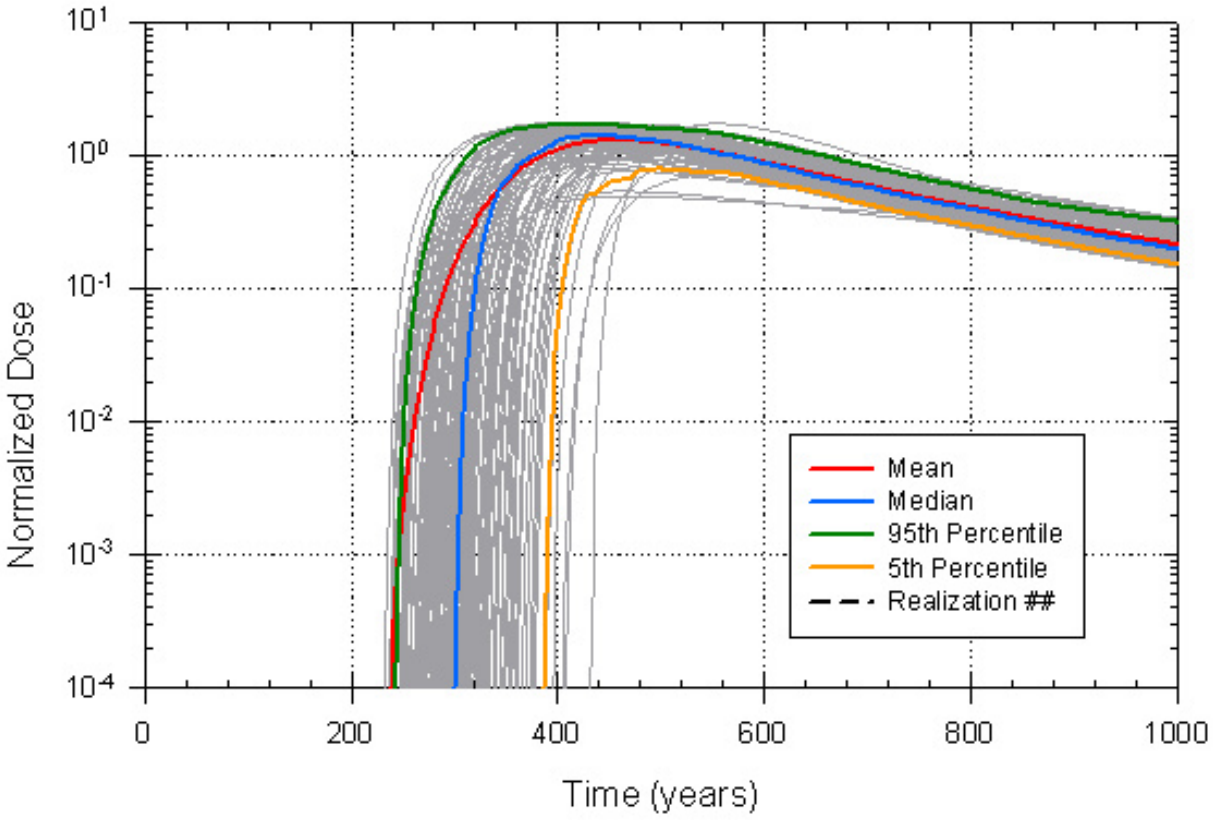

Figure 56: Near surface disposal site 2-D BLT-MS Model Probabilistic Results

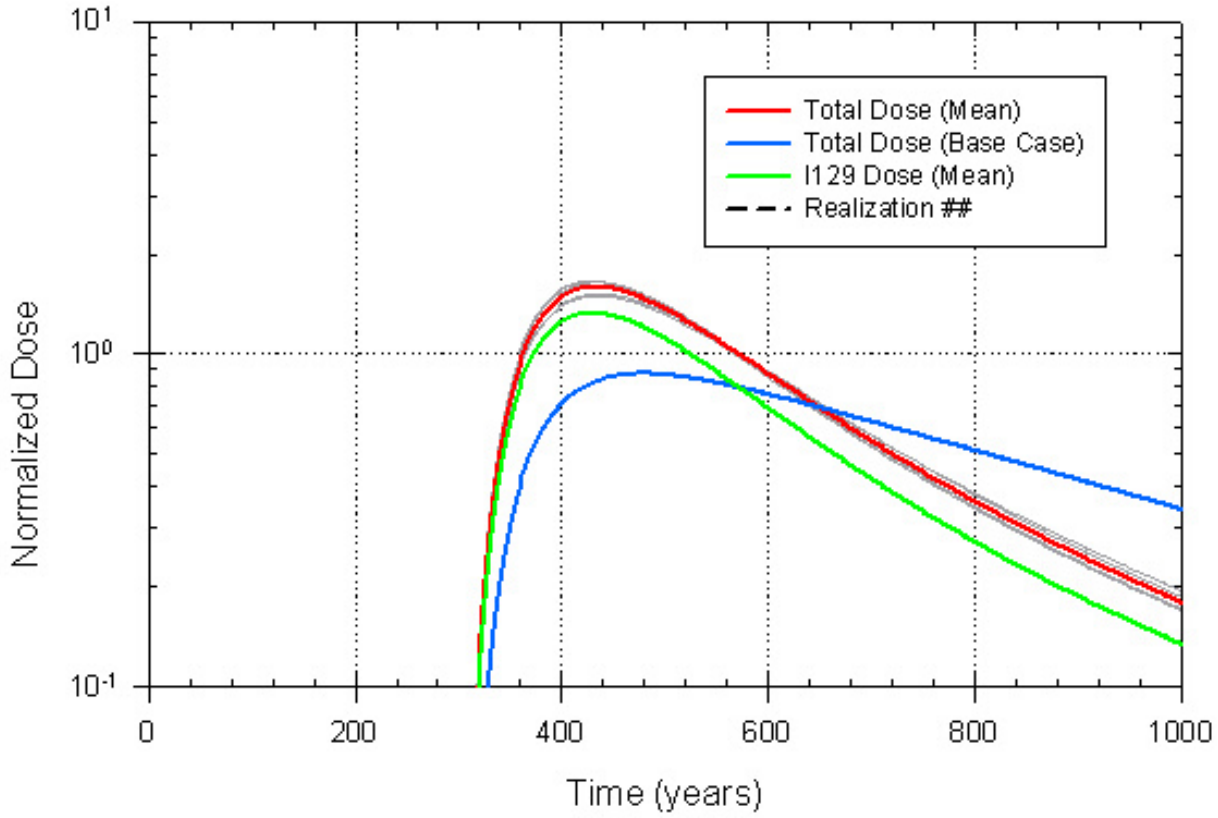

Figure 57: Near surface disposal site mean total dose for select realizations from probabilistic analysis vs. base case total dose, showing the effect of increased waste form diffusion rates.

4.2. Alternative Case Analyses

In addition to the baseline conceptual model presented in Section 4.1, a one-dimensional matrix-diffusion model was constructed as an alternative conceptual model of transport through the fractured basalt (see Section 3.3.4). For the near-surface disposal site the 1-D transport model implemented in GoldSim consists of three pathways from different locations within the disposal cell, with a vertical pipe segment representing flow in the unsaturated zone beneath the disposal cell and a horizontal pipe segment for flow in the saturated zone for each pathway. The goal of the 1-D transport model is to approximate the groundwater flow rates and geometry of flow pathways in the 2-D BLT-MS model as closely as possible. However, the approximations inherent in the 1-D transport model construction and the lack of transverse dispersion in the 1-D transport model result in differences with the 2-D BLT-MS transport model.

Simulation results from the 1-D transport model are compared to the 2-D BLT-MS transport model with regard to total normalized dose in Figure 58. The 1-D transport model results

indicate a higher peak normalized dose value and a slightly earlier time for peak normalized dose relative to the 2-D BLT-MS transport model. At later times the simulated normalized dose from the 1-D transport model is lower than from the 2-D BLT-MS transport model. The lower peak dose from the 2-D BLT-MS transport model is probably due to the greater numerical and transverse dispersion in the 2-D finite-element solution method used by BLT-MS. Such dispersion spreads radionuclide mass throughout the cross section of the groundwater flow system leading to dilution of simulated radionuclide concentrations, relative to the 1-D transport model in which transport is confined within the defined flow pathways. At later times, the radionuclide mass in the 2-D BLT-MS transport model that has dispersed into areas of slower flow continues to be flushed from the flow system, leading to higher simulated normalized doses, relative to the 1-D transport model.

The differences in simulated normalized dose from the 1-D transport model compared to the 2-D BLT-MS transport model are also affected by matrix diffusion in the 1-D transport model. However, the overall differences are dominated by the effects of dimensionality and numerical dispersion. This is particularly true for this system in which only the unsaturated vertical portion of the pathway (18 m) in the natural system is treated as a fractured medium.

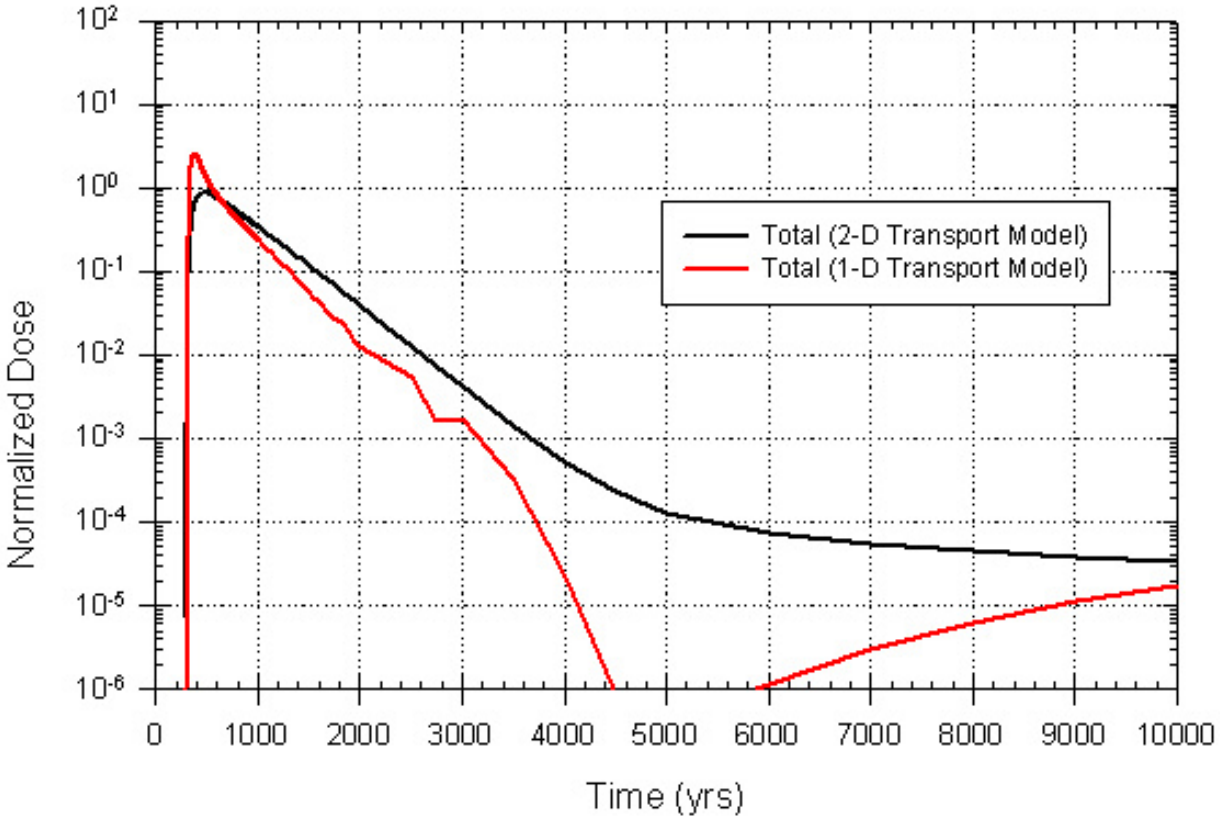

Figure 58. Dose Versus Time for the Near-Surface Disposal Site from the 2-D BLT-MS Transport Model and the 1-D Transport Model

The contributions to simulated total normalized dose in the 1-D transport model from individual radionuclides are shown in Figure 59. This plot shows that ^{129}I and ^{14}C are the greatest contributors to normalized dose during approximately the first 4500 years following closure of the LLW repository. The contributions to normalized dose from ^{239}Pu and ^{240}Pu, which are strongly sorbing species, dominate the simulated total normalized dose at later times; however, the normalized dose rate at later times is several orders of magnitude lower than the peak normalized dose.

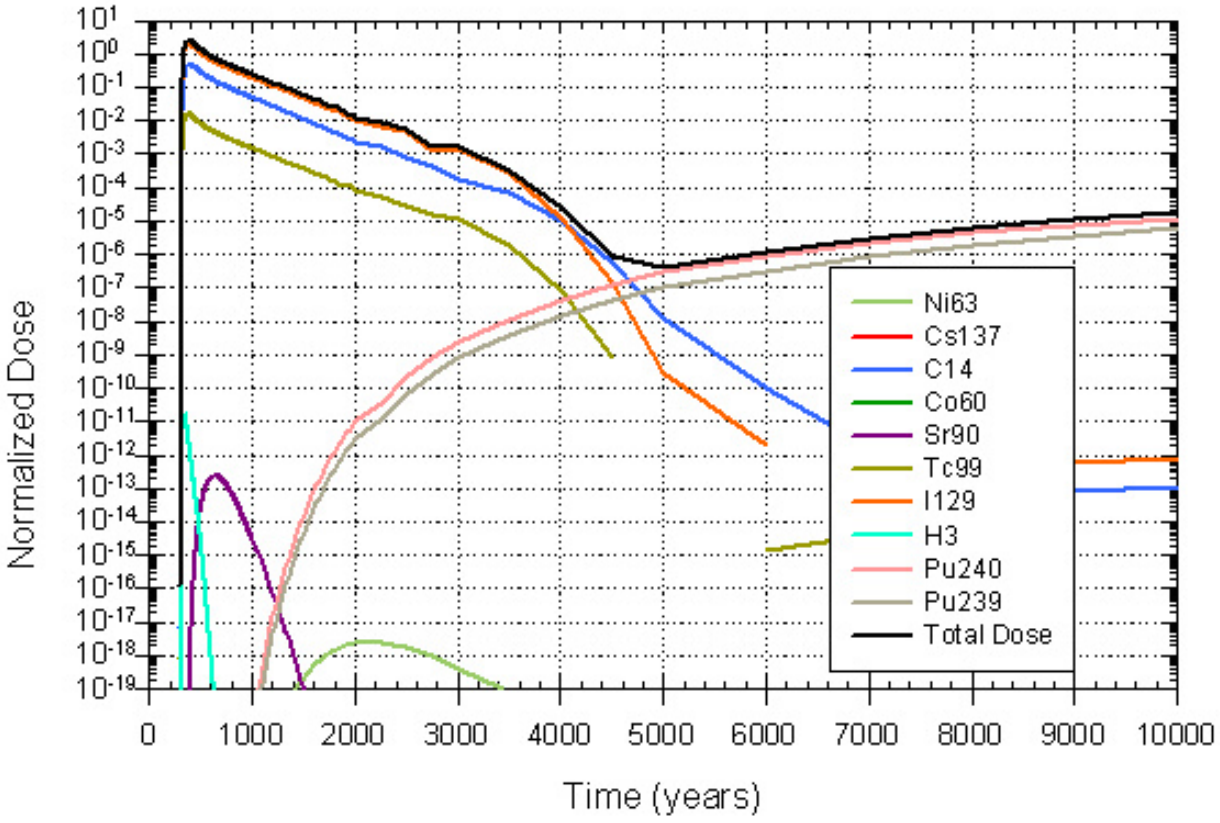

Figure 59. Dose Versus Time for the Near-Surface Disposal Site from the 1-D Transport Model and Showing the Contributions from Individual Radionuclides

5. PRELIMINARY ASSESSMENT OF MINED CAVERN DISPOSAL SYSTEM DESIGN CONCEPT

5.1 Base Case Analysis

The mined cavern disposal system design proposed for consideration in the southeast coastal area of Taiwan is a fairly ambitious design for low-level radioactive waste disposal facilities (see Figure 5). In this particular case, the system would be emplaced in a saturated, fractured bedrock which allows potential contact with the groundwater system almost immediately upon release of any radionuclides from the disposal cells.

5.1.1 Radionuclide Release and Transport Conceptual Model

For the mined cavern disposal system design there are a series of disposal tunnels that must be considered in the design layout. The waste inventory was assumed to be split evenly amongst all of the disposal tunnels.

The base case analysis for the mined cavern disposal system design was constructed in such a manner as to approximate the design concepts as closely as possible. The following attributes of the source term were taken into consideration in constructing the numerical model for the site:

- Cavern excavation and burial in the southeast portion of Taiwan in the side of a mountain.
- Disposal cell design has the following attributes:
    - Waste disposed in 55-gallon galvanized drums in disposal tunnels.
    - Each disposal tunnel is nominally circular on the sidewalls and roof but flat on the floor for emplacement of the waste. The height is 11.6 m. Each disposal tunnel is 400 m long. The ends of the tunnel are connected to two access tunnels for transporting the waste into the disposal tunnels. The disposal tunnels are spaced 63 m apart. At the center of each disposal tunnel, a concrete vault is built. The vault can divide into 10 disposal cells with 0.4 m thick inner walls and 0.6 m thick outer walls. The length of a vault is approximately 355.8 m. The spacing between the vault and the access tunnels, on either end of the disposal tunnel, is designed for transportation, monitoring, and maintenance of the vault. Each disposal cell is nominally 7.6 m wide by 8.3 m high by 35.1 m long.
    - Each disposal cell can accommodate 4,704 drums, with 12 drums wide by 56 drums long and 7 layers high. With 10 disposal cells in each disposal tunnel there will be 47,040 drums per disposal tunnel.
    - Total number of disposal tunnels in the repository will be 21, thereby accommodating 210 disposal cells with 987,840 drums.
    - Once a row of drums is emplaced in a disposal cell, grout is placed between all drums.
    - A concrete cap will be placed on top of each disposal cell after it is filled.
    - After the vault has been filled, a suitable host rock/clay mixture will be used for tunnel backfilling.

Other considerations include:

- Local meteorological data are available.
- The host rock geology that the repository would potentially be constructed in is mainly argillite/slate with subordinate meta-sandstone. The thickness of meta-sandstone layers at the potential site area ranges from 2-15 cm.
- Hydrogeologic and geochemical data are not available at this time.
- Typhoons will impact the island and may need to be considered in future analyses.
- Sea level may rise as much as 200 cm in the next 300 years, but is not considered explicitly in this analysis.
- Seismic activity may need to be assessed in the performance assessment in future analyses.
- Volcanic activity is believed to be minimal.

As mentioned above, the BLT-MS model was used to model the source term, both the failure of the waste canisters as well as the leaching of the radionuclides from the waste forms after breach has occurred. The source term elements in BLT-MS were intended to have the same basic dimensions of the disposal cells listed above. At least two elements were needed in any given disposal cell to adequately approximate the release mechanisms within the model.

The model domain for the mined cavern site is considerably larger than that of the near-surface disposal design for the island site. Two conceptualizations of the mined cavern site were developed in order to facilitate the objectives. One conceptualization attempted to honor as much of the specificity of the tunnel design as possible, resulting in a relatively large finite-element grid that is computationally burdensome. The second conceptualization was more coarse in its representation of the source term, but would be easier to implement in a probabilistic framework because it is less computationally burdensome. A comparison of the two conceptual models would allow conclusions to be drawn as to the representativeness of each model.

For the more detailed model, the source term was modeled with a total of 672 waste container elements. A set of elements was also assigned to the top, bottom, and sides of the disposal cell areas to represent the concrete encasement of the disposal cells within each of the 21 disposal tunnels. The model was constructed to have the ability to represent the material properties within the disposal cell areas to be different from that of the host rock in order to simulate the effects of the grout backfill and concrete lining on the transport process.

The overall model setup has the following attributes. The model boundaries were selected as follows. The upstream end of the disposal area was established as the left side of the model. The right side of the model was coincident with the approximate area where the fresh-water/salt-water interface is likely to occur at the point where the coast meets the ocean. The top boundary is a plane surface several meters above the disposal horizon. The bottom boundary is that surface that likely represents the lowest flow path of any groundwater passing through the disposal area. As shown in Section 3.3.3, groundwater flow is generally from left-to-right in the model domain. For the transport solution in the model, the right side boundary of the model was assigned a Dirichlet zero constant concentration condition. All other model boundaries preclude mass transfer out of the model domain. The dimensions of the model are 600 meters high by

1740 meters wide. There are 68 finite-element nodes in the vertical, z, direction and 441 nodes in the horizontal, x, direction. The total number of finite-element nodes in the model is 29988. The total number of finite elements in the model is 29480. The flow velocities required in the model were abstracted from the FEHM modeling results onto the existing finite-element grid. Flow velocities within the source-term area, were set to very low values, in a strictly downward vertical vector, corresponding to the percolation flux through the disposal area.

The waste inventory in the source term was derived from information provided by INER along with a number of assumptions where information or data did not exist. Section 3.3.1 above discussed the assumptions and approach to developing estimates of the waste inventory. Table 7 provided a synopsis of the activity for each radionuclide associated with each waste type for the radionuclides selected for analysis.

INER has decided that all the waste will be encapsulated in concrete and grout. Concrete and grout generally have about a 300 year failure time or greater. Localized corrosion of the waste drums would likely be occurring during this time, but releases would not occur due to the concrete/grout encapsulation. Therefore, generalized corrosion was invoked as the release mechanism with a failure time of 300 years.

The detailed conceptual model has the following waste form attributes. The operational waste was split between a non-solidified waste fraction with a 50% rinse and 50% diffusion release specification and a solidified waste fraction with diffusion release, the decommissioning waste then was split between a solidified non-metal waste fraction with rinse and diffusion release and a metal waste fraction with a dissolution release. These waste type designations are still preliminary and likely to change as INER further evaluates the sites.

In addition, the model was set up to account for the effects of the concrete and grout surrounding the waste drums. The concrete/grout has a different porosity and molecular diffusion coefficient than the surrounding host rock. Diffusion of the radionuclides through the concrete/grout should impede the release to a degree. Key parameters controlling transport are shown in Table 18. This conceptual model is designated as the baseline case model in that it incorporates the best estimates of the waste release mechanisms as well as a representation of the engineered barrier system performance.

5.1.2 Base Case Analyses:

Figure 60 shows concentration versus time for each of the radionuclides in the analysis over a 1,000 year time frame. Figure 61 shows normalized dose versus time for the same radionuclides, along with the total normalized dose (a summation of all the dose estimates from each of the radionuclides). The normalized dose was calculated by dividing all the simulated dose estimates by the peak dose from the near-surface disposal rinse release model, which is the maximum dose simulated for any of the deterministic cases and therefore a benchmark for normalized comparisons. The normalized dose is calculated for a drinking water exposure scenario. Several conclusions can be drawn from these results. First, several of the radionuclides have decayed significantly over the first several hundred years. These radionuclides include Cs-137, Co-60, Sr-90, and H-3. They do not contribute any appreciable dose to the total. Ni-63 is persistent in

the system for slightly longer duration, but is still not a significant contributor to dose. The three radionuclides that are essentially non-sorbing, C-14, I-129, and Tc-99, are the main contributors to dose. The plutonium isotopes, Pu-239 and Pu-240, become more dominant at later times. The plutonium isotopes are controlled by solubility release mechanisms. It should be noted that the normalized dose estimates are nearly two orders of magnitude lower than those of the baseline model for the near-surface disposal design. It appears from these preliminary results that the mined-cavern disposal concept has better performance potential than the near-surface disposal concept.

As mentioned previously, this detailed version of the baseline conceptual model is computationally burdensome. It would take more than a week to perform a probabilistic analysis with this configuration, which is not practical. Therefore, a more simplified version of this conceptual model was constructed.

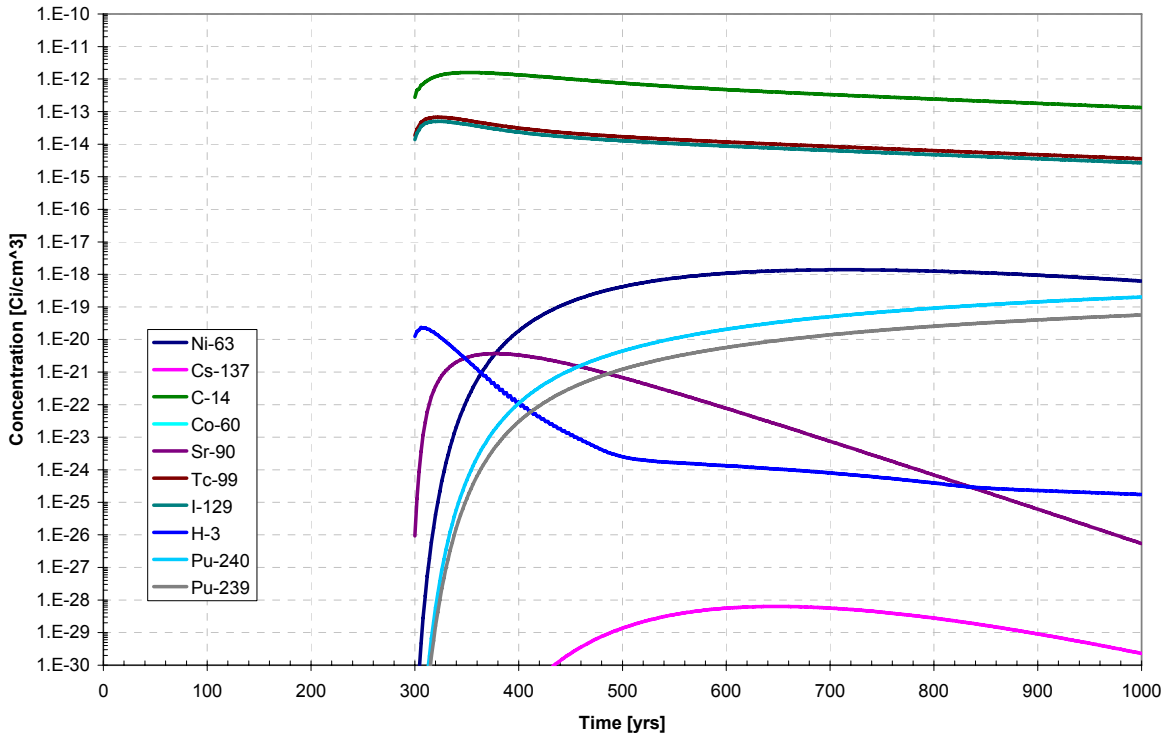

Figure 60 – Concentration Versus Time for the Detailed Mined Cavern Site Model for the Baseline Conceptual Model

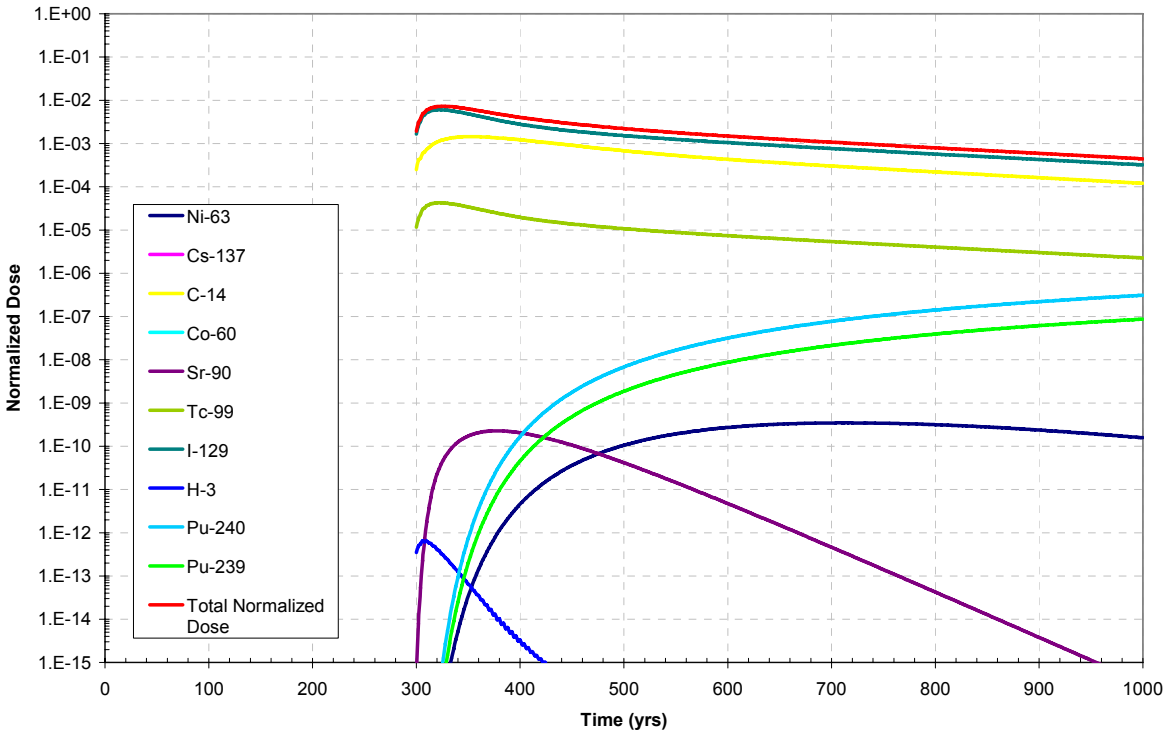

Figure 61 – Dose Versus Time for the Detailed Mined Cavern Site Model for the Baseline Conceptual Model

The smaller, simplified version of the baseline conceptual model has the following attributes. The model boundaries were basically the same as those of the larger baseline model. The dimensions of the model are 640 meters high by 2200 meters wide. There are 41 finite-element nodes in the vertical, z, direction and 258 nodes in the horizontal, x, direction. The total number of finite-element nodes in the model is 10578. The total number of finite elements in the model is 10280. Therefore, this version of the baseline conceptual model has a little over a third of the nodes that the detailed model has. The flow velocities required in the model were abstracted from the FEHM modeling results onto the existing finite-element grid. Flow velocities within the source-term area, were set to very low values, in a strictly downward vertical vector, corresponding to the percolation flux through the disposal area. This smaller version of the baseline conceptual model did not have nodes surrounding the waste container nodes that represent the concrete encapsulation, as did the detailed model. Concrete/grout media were considered though for all the elements representing the source term. There are 252 container elements in the smaller, simplified model.

Figure 62 shows concentration versus time for each of the radionuclides in the analysis over a 1,000 year time frame. Figure 63 shows normalized dose versus time for the same radionuclides, along with the total normalized dose. Several conclusions can be drawn from these results. The temporal behavior of the radionuclides is quite similar comparing the detailed versus smaller

simplified model results. There are some differences, but they are not appreciable. One obvious difference in the results relates to the tritium, H-3, behavior. The simplified model has the concentration distribution oscillating after about 500 years. There appears to be some sensitivity of the model to the groundwater flow rate, the time step size, and the half-life of tritium. Tritium does not contribute any appreciable dose to the total performance of the site, so it is not an issue. Future work may address this issue.

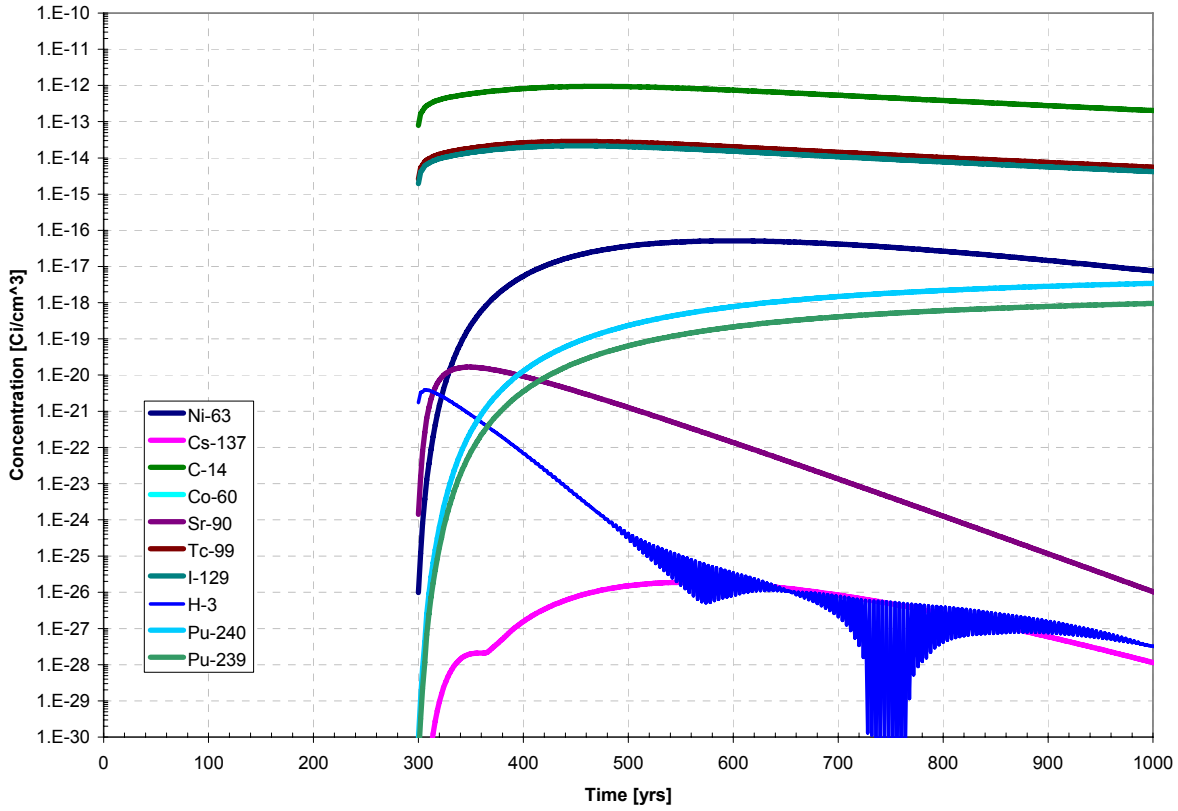

Figure 62 – Concentration Versus Time for the Simplified Mined Cavern Site Model for the Baseline Conceptual Model

Another conceptual model of the site involves a very conservative assumption about the leaching process that occurs once the drums have failed. The assumption is that all the waste is subject to rinse release. Rinse release allows the radionuclides to freely mix with the incoming infiltration water. There is little credit given for source term controls in this conceptual model. The rationale behind invoking this conceptual model is that if the performance of the system is in compliance with the standard, then the site is likely suitable because the engineered barrier system would just add to the performance.

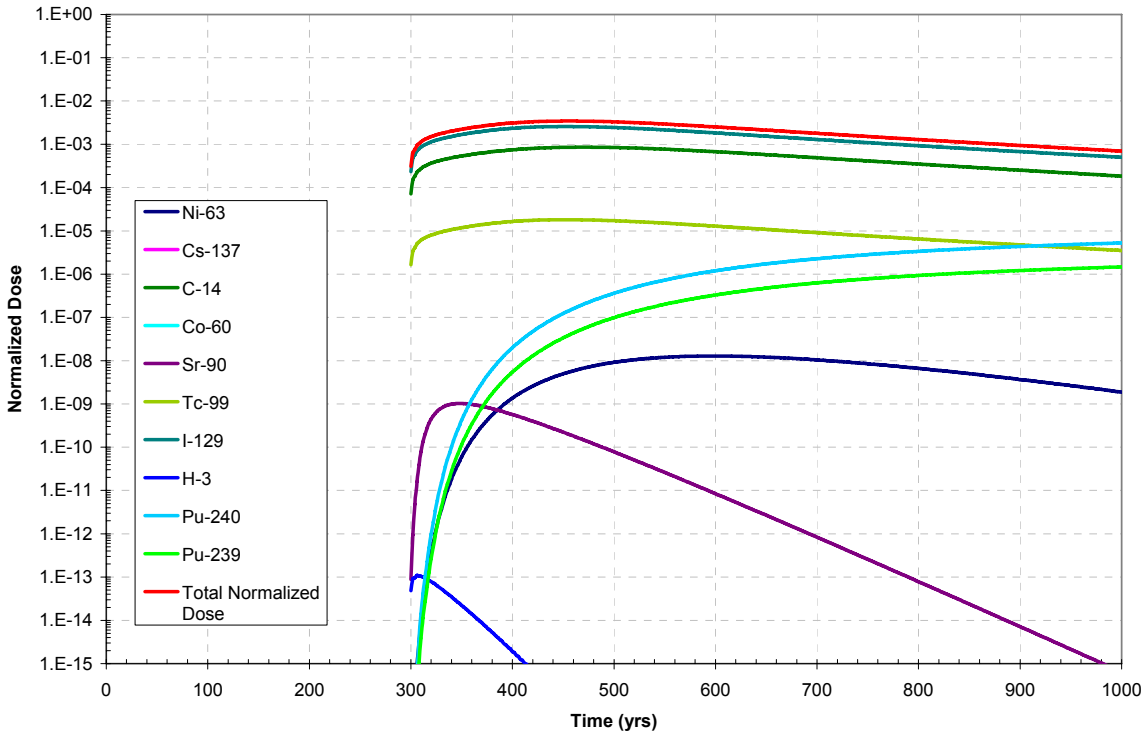

Figure 63 – Dose Versus Time for the Simplified Mined Cavern Site Model for the Baseline Conceptual Model

To better understand the comparison of the detailed versus simplified baseline conceptual models, a plot of total normalized dose versus time was constructed and shown in Figure 64. The behavior of the two models is slightly different, but not appreciable. The maximum normalized dose for the detailed model is about a factor of two difference compared to the simplified model. The detailed model appears to release the radionuclides to the far-field more quickly right after container failure than the simplified model. The simplified model is predicting slightly higher normalized dose estimates than the detailed model after about 400 years. The simplified model exhibits more of a diffusion-dominated result compared to the detailed model. The differences in model behavior are not appreciable, and the simplified model appears to adequately represent the system for further analyses. As mentioned above, the detailed model is too computationally burdensome to be used in the probabilistic analysis but the simplified model should work just fine.

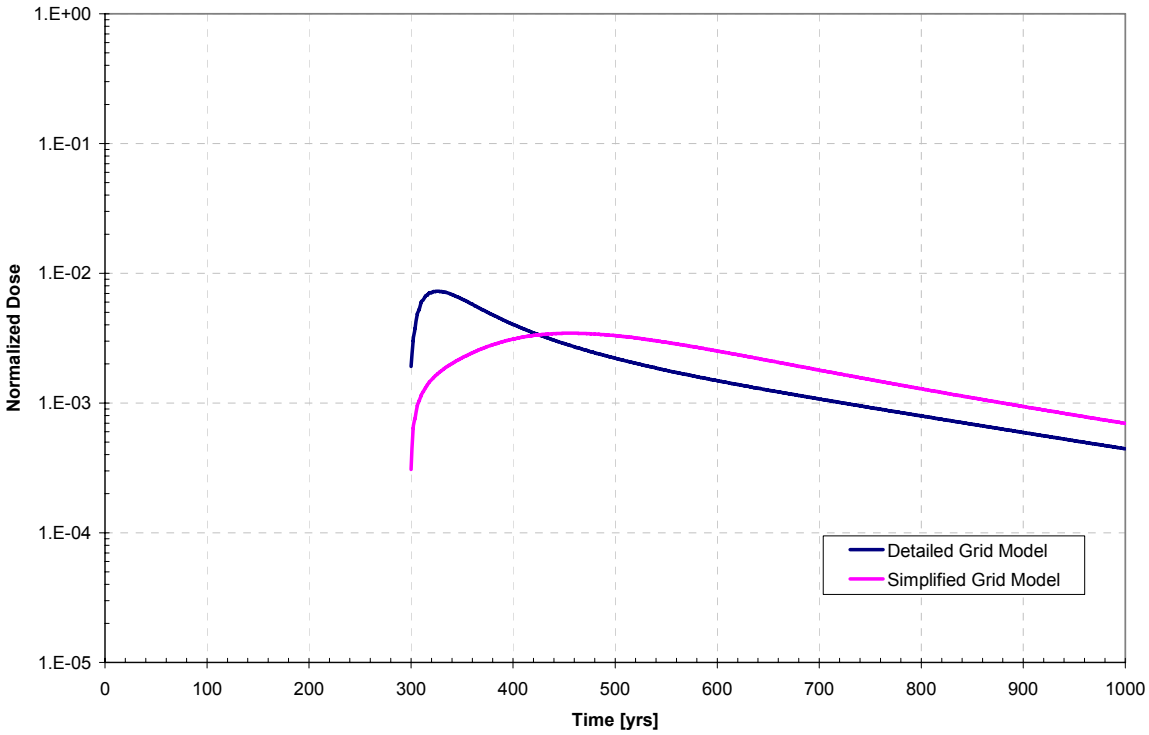

Figure 64 – Comparison of Total Dose Versus Time for Detailed and Simplified Baseline Conceptual Models for the Mined Cavern Site Model

Another conceptual model of the site involves a very conservative assumption about the leaching process that occurs once the waste containers have failed. The assumption is that all the waste is subject to rinse release. Rinse release allows the radionuclides to freely mix with the incoming infiltration water. There is little credit given for source term controls in this conceptual model. The rationale behind invoking this conceptual model is that if the performance of the system is in compliance with the standard, then the site is likely suitable because the engineered barrier system would just add to the performance.

Figure 65 shows concentration versus time for each of the radionuclides in the analysis over a 10,000 year time frame. Figure 66 shows normalized dose versus time for the same radionuclides, along with the total dose. Several conclusions can be drawn from these results. The main radionuclides of concern in this conceptual model are I-129, Tc-99, and C-14 within the first few hundred years followed by the two plutonium isotopes at later times. The mobile radionuclides appear to be flushing through the system more quickly in this conceptualization compared to the baseline conceptual model, due to the leaching and transport process being dominated by advection. Other radionuclides do not contribute significantly to dose. The tritium, H-3, results show some instability, likely due to the size of the time step, the half-life of the isotope, and the groundwater flow velocity. It should be noted that this normalized dose assessment only includes a drinking water scenario and to be more thorough should include other exposure pathways (e.g., eating food contaminated with the groundwater, dermal contact, etc.).

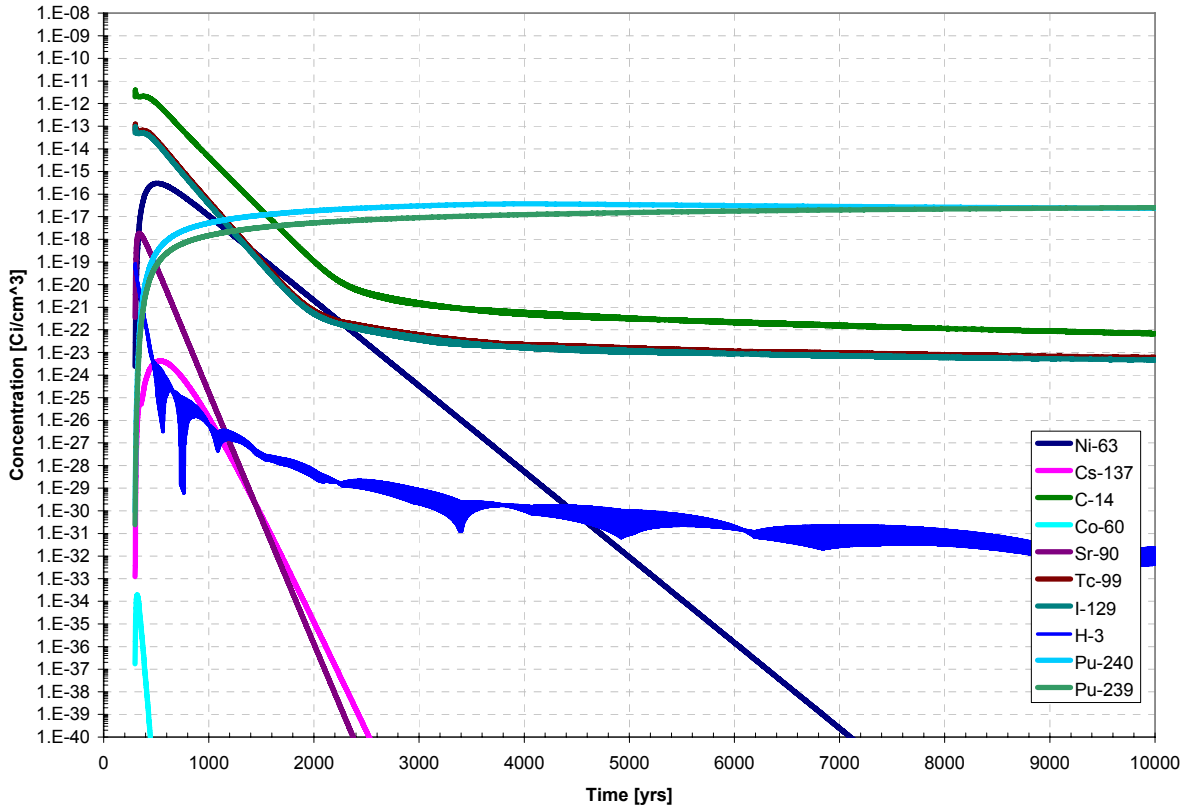

Figure 65 – Concentration Versus Time for a Simplified Mined Cavern Site Model With Rinse Only Waste-Form Release

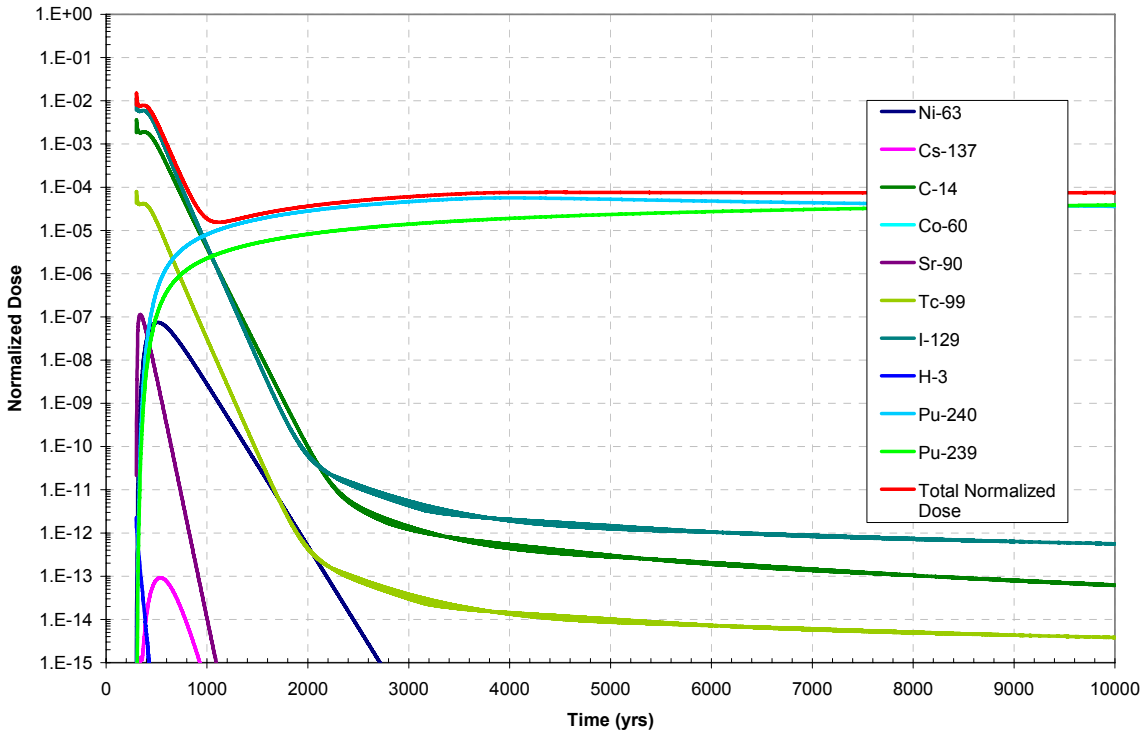

Figure 66 - Dose Versus Time for a Simplified Mined Cavern Site Model With Rinse Only Waste-Form Release

Another variation of the simplified conceptual model for the mined cavern site involves partitioning the waste types according to the following groupings: the operational waste was split between a non-solidified waste fraction with a 50% rinse and 50% diffusion release specification and a solidified waste fraction with diffusion release, then the decommissioning waste was split between a non-metal waste fraction with rinse and diffusion release and a metal waste fraction with a dissolution release.

Figure 67 shows concentration versus time for each of the radionuclides in the analysis over a 10,000 year time frame. Figure 68 shows normalized dose versus time for the same radionuclides, along with the total dose. Several conclusions can be drawn from these results. This conceptualization has some diffusion release, dissolution release, and accounts for concrete encapsulation, but appears to have similar performance to the rinse-only release model. That being the case, the rinse release portions of the model must be dominant over the other processes.

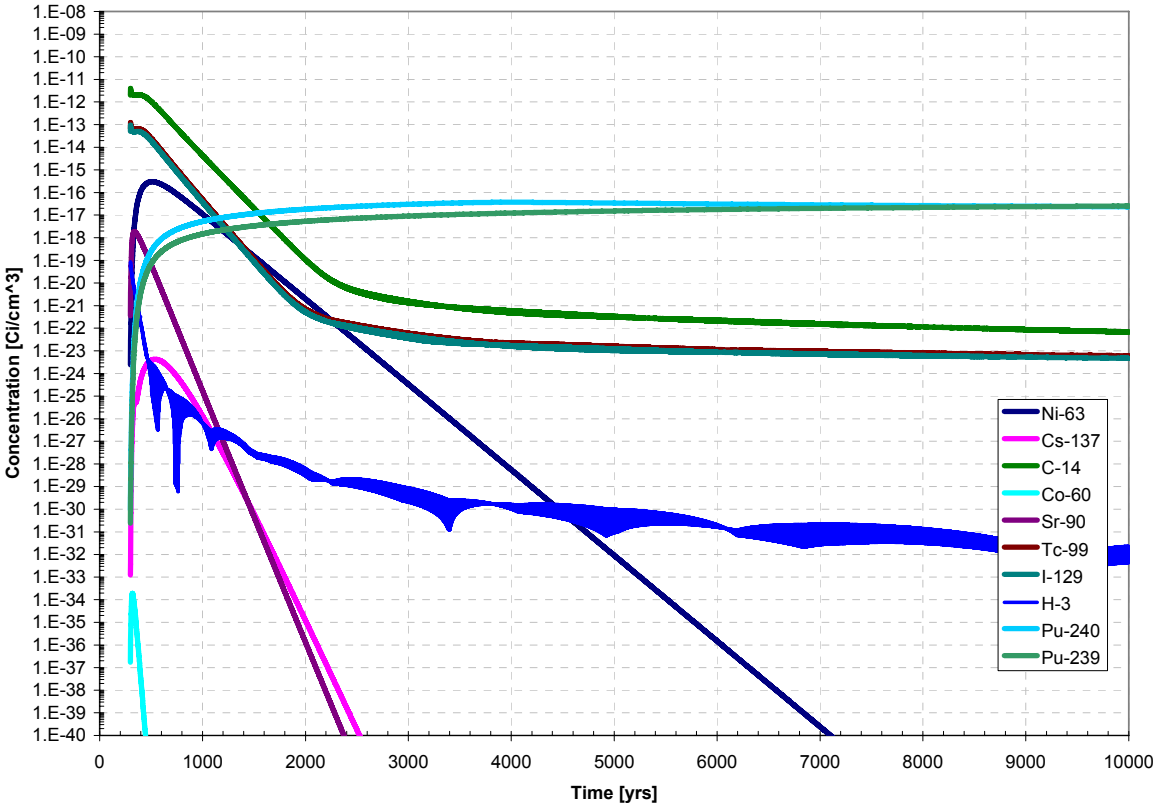

Figure 67 – Concentration Versus Time for a Simplified Mined Cavern Site Model With Multiple Waste Type Designations

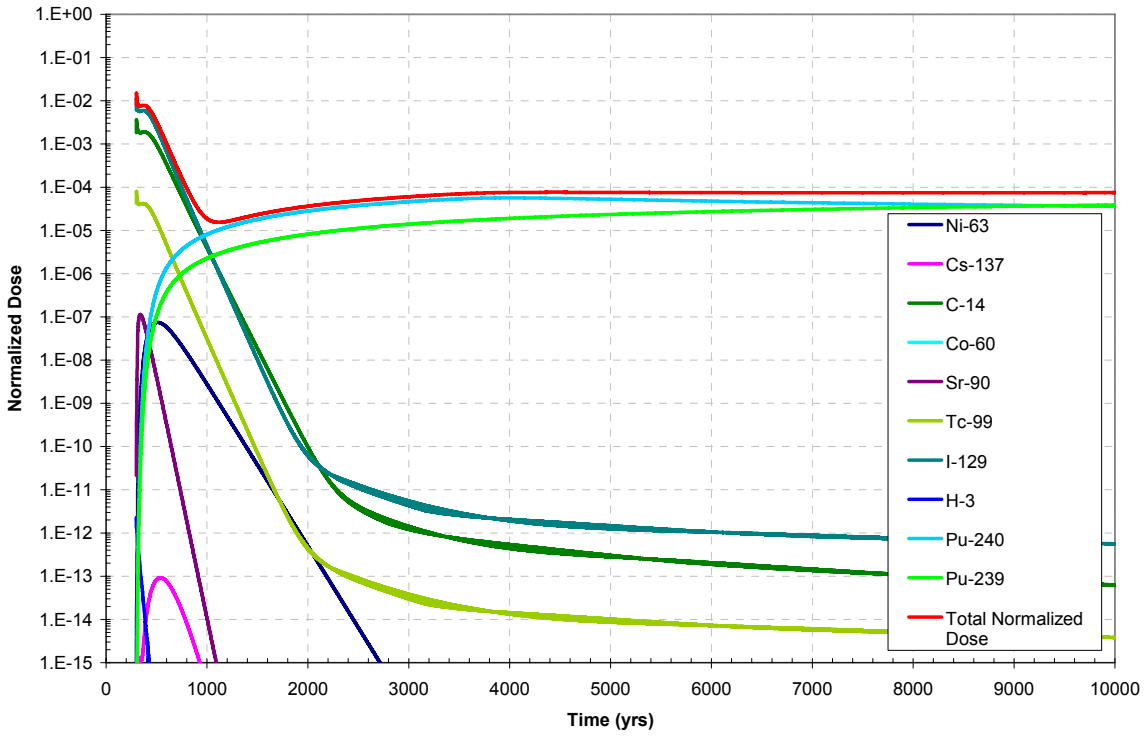

Figure 68 – Dose Versus Time for a Simplified Mined Cavern Site Model With Multiple Waste Type Designations

Yet another variation of this conceptual model assumes that all the waste is solidified (e.g., grout added to the waste in the disposal drums) and subject to a diffusion release. Figure 69 shows concentration versus time for each of the radionuclides in the analysis over a 10,000 year time frame. Figure 70 shows normalized dose versus time for the same radionuclides, along with the total normalized dose. Several conclusions can be drawn from these results. In this conceptualization, the mobile radionuclides, I-129, Tc-99, and C-14, are dispersed through the system over a longer time frame than in most of the other conceptual models, with the exception of the baseline conceptual model. One could conclude that the absence of a rinse release mechanism decreases the influence of advection on the transport of the radionuclides.

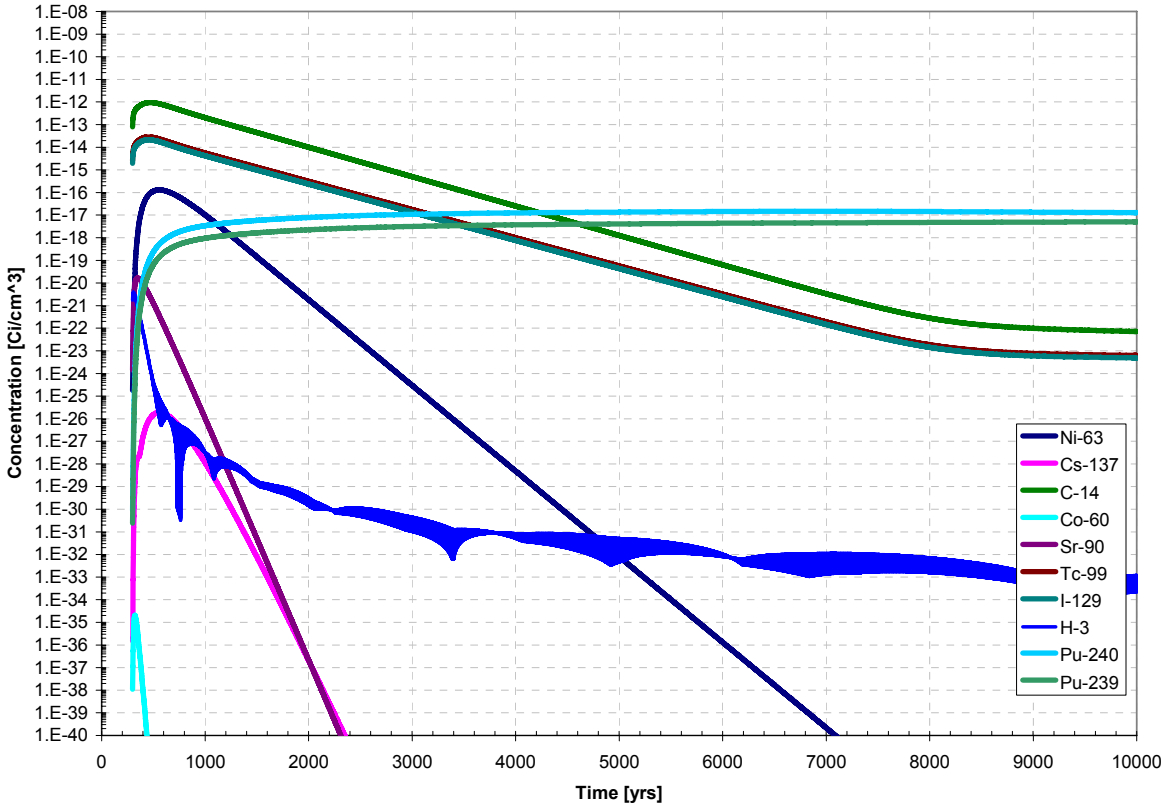

Figure 69 - Concentration Versus Time for a Simplified Mined Cavern Site Model With Diffusion Release Only

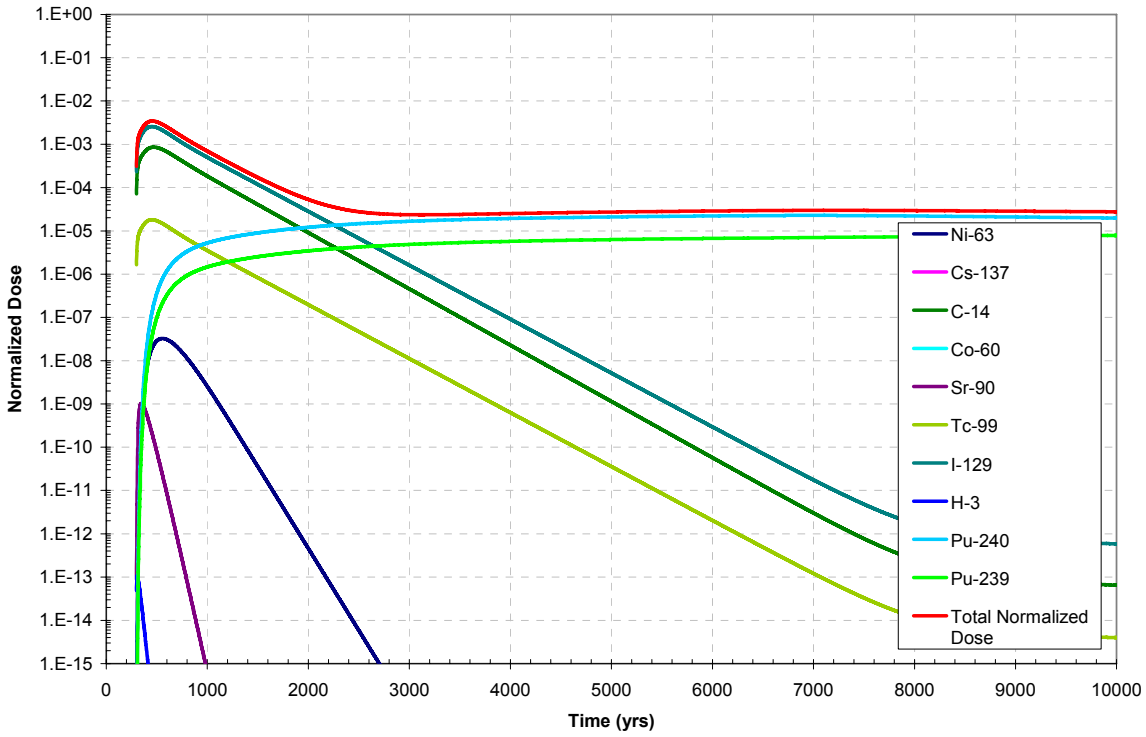

Figure 70 - Dose Vs. Time for a Simplified Mined Cavern Site Model With Diffusion Release Only

It is helpful to plot the total dose estimates for each of these conceptual model variations to compare results. Figure 71 provides a plot of the results of each conceptual model variation for the simplified mined cavern site model. It appears that the conceptual models that invoke either all rinse or even partial rinse release mechanisms exhibit very similar behavior. The conceptual model that has some dissolution release of metal waste in addition to diffusion release has essentially the same response as just diffusion release. Therefore, it may be important to solidify most of the waste, but may not need to do so for the metal waste from decommissioning.

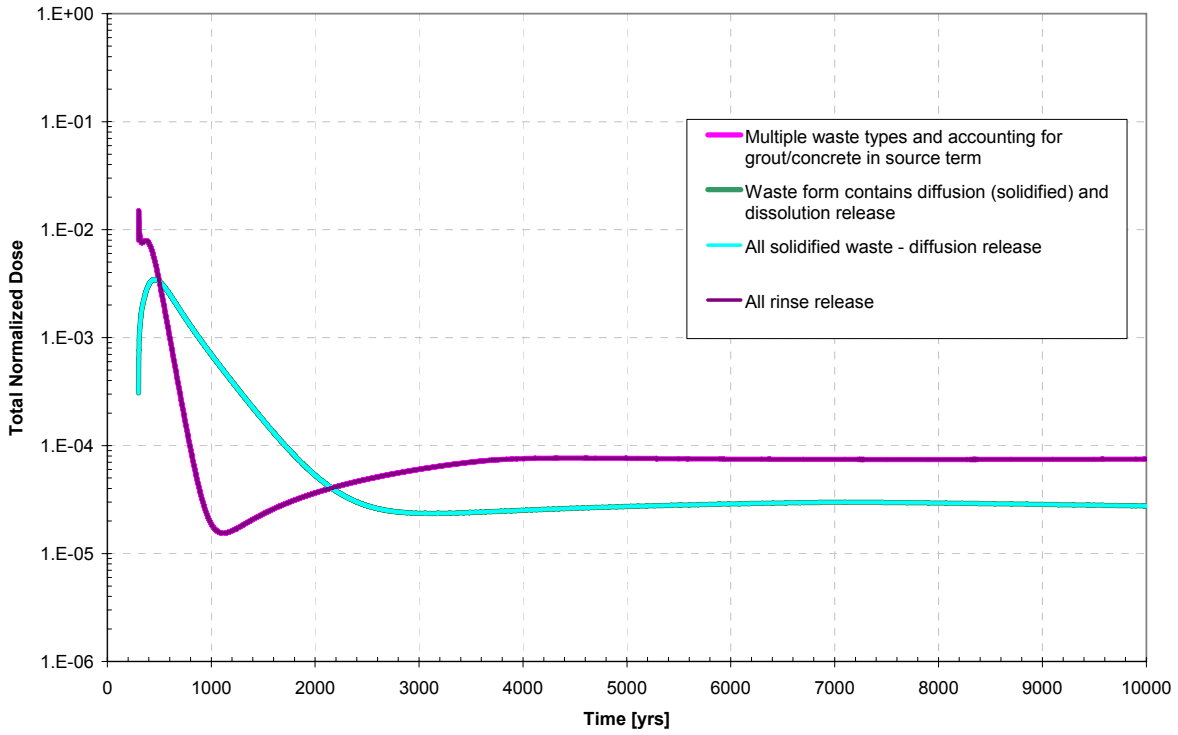

Figure 71 – Comparison of Different Conceptual Model Configurations for the Simplified Mined Cavern Model

As mentioned above, the BLTPLOT_UNCERT code was written to extract two-dimensional concentration distribution data from the model output. Figure 72 shows a time-history of the Pu-240 concentration for the baseline conceptual model. The output times are 320, 1000, 5000, and 9000 years. The concentration contours are labeled in log space for units of Ci/cm^3. These plots show that the Pu-240 is building in concentration with time and moving from left to right across the model domain, as would be expected given the flow regime.

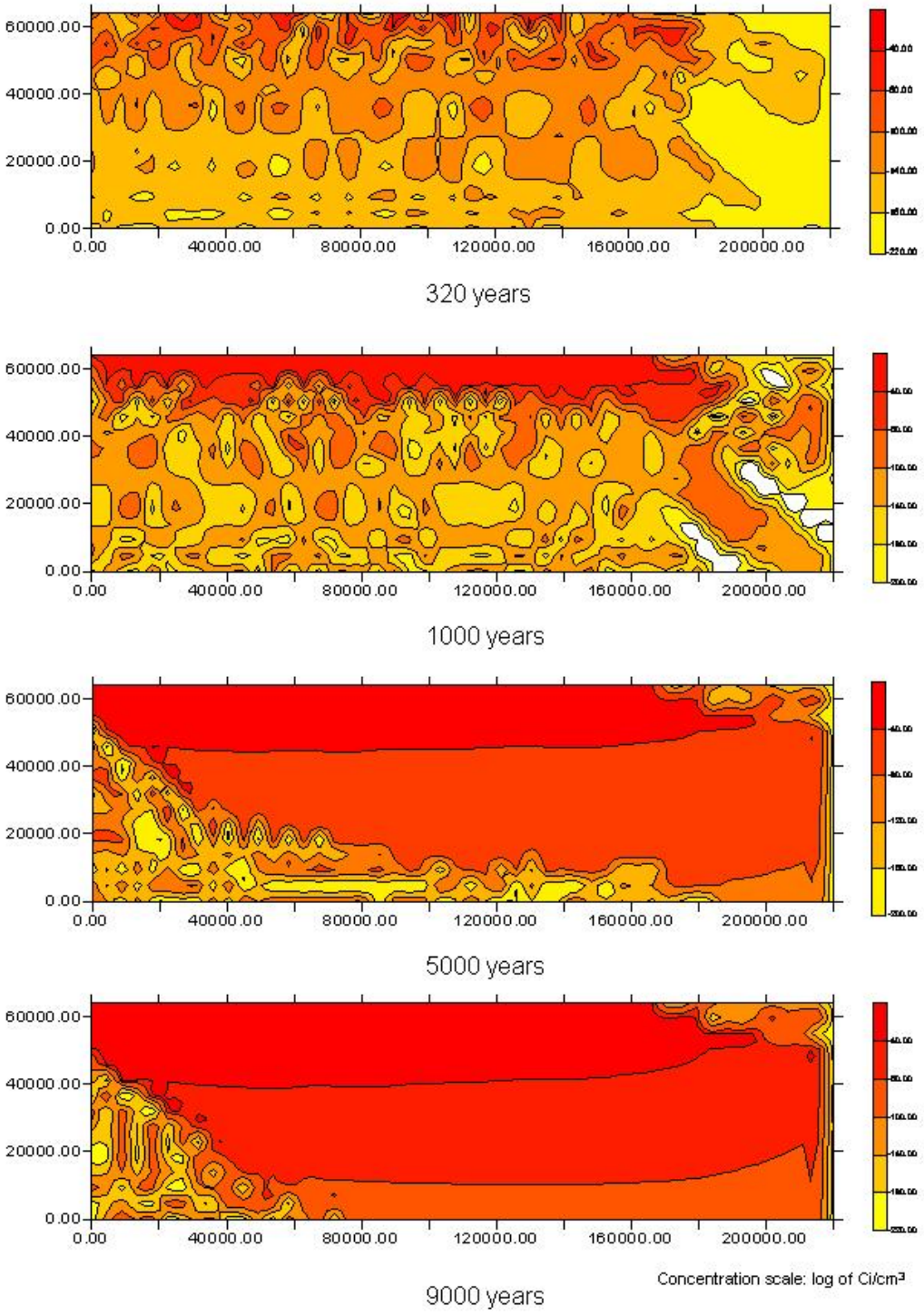

Figure 72 – 2-D Concentration Versus Time for Pu-240 With the Baseline Conceptual Model for the Mined Cavern Disposal Site.

5.1.3 Probabilistic Analysis

Uncertainties will inevitably exist in projections of the geologic and environmental conditions surrounding the disposal site 1,000 or 10,000 years into the future. Assessment of the disposal site performance over this period must take these uncertainties into account. Uncertainty is usually expressed in two categories, aleatory and epistemic. Aleatory uncertainty arises from quantities that stem from variability in populations, from which random samples are taken. The basic idea underlying the concept of aleatory uncertainty is that a range of possible values exists, all having a certain probability of occurring. An example of aleatory uncertainty considered is that of early failed containers. The second category is referred to here as epistemic uncertainty. Epistemic uncertainty arises from a lack of knowledge about a quantity that is believed to have a fixed (or deterministic) value. Thus, the quantity is not random in the sense used above. Rather, there is a lack of knowledge about what its value should be due to limited data and knowledge. Epistemic uncertainties arise due to, among others, incomplete data, measurement errors, and estimates based upon expert judgment. Unlike aleatory uncertainty, epistemic uncertainty is potentially reducible with additional data and knowledge. A particular epistemic quantity can be a parameter for a probability distribution (e.g., diffusion coefficients for release of radionuclides from the waste form).

The baseline conceptual model presented above was used to perform an uncertainty analysis. To demonstrate the probabilistic capabilities of the BLTMS-GoldSim coupled model, an analysis is presented that considers only two parameters as uncertain. Table 20 lists the uncertain parameters and the range of values used.

Table 20. Uncertain Parameter Ranges for Probabilistic Analysis

Parameter	Range			Description
GRATE (cm/s)	Triangular Distribution			BLT-MS Data Set 20: Container general corrosion rate (NRC, 1989)
	Most Likely	Min	Max	
	1.48×10^{-11}	1.0×10^{-11}	2.0×10^{-11}	
DEFF (cm^2/s)	ISO	Uniform Distribution		BLT-MS Data Set 21: Waste for effective diffusion coefficient (NRC, 1989)
		Min	Max	
	Ni-63	1×10^{-9}	1×10^{-7}	
	Cs-137	2.8×10^{-13}	2.8×10^{-11}	
	C-14	1×10^{-9}	1×10^{-7}	
	Co-60	1×10^{-9}	1×10^{-7}	
	Sr-90	4×10^{-12}	4×10^{-10}	
	Tc-99	1×10^{-9}	1×10^{-7}	
	I-129	1×10^{-9}	1×10^{-7}	
	H-3	1×10^{-9}	1×10^{-7}	
	Pu-240	1×10^{-9}	1×10^{-7}	
	Pu-239	1×10^{-9}	1×10^{-7}	

For LLW disposal waste container performance is an important factor controlling the release of radionuclides for transport to the accessible environment. The GRATE parameter in BLT-MS is invoked to calculate the general corrosion rate for a waste container. Given a waste container thickness of 0.14 cm for the base case model and using the distribution in Table 20, the waste package container failure times were varied between 220 years to 300 years for the probabilistic analysis for Site #6. The DEFF parameter in BLT-MS is the effective diffusion coefficient used to calculate the release of radionuclides from the waste form for a diffusion controlled release model. The effective diffusion coefficient is radionuclide specific; Table 20 lists the distributions used for each of the radionuclides considered in this analysis. The probabilistic case was run using the coupled GoldSim-BLTMS model. The analysis was run for 100 realizations for 1,000 years. A Latin Hyper-Cube Sampling (LHS) was used in a Monte Carlo analysis to select parameter values for each realization from the stated distributions.

Figure 73 shows the base case total normalized dose release versus the probabilistic mean total normalized dose for the mined cavern disposal site. Compared to the base case, the mean normalized dose curve from the probabilistic case shows an earlier initial release which reflects the earliest waste container failure at approximately 220 years. The base case deterministic model has a corrosion rate equal to 1.48×10^{-11} cm/s which results in a waste container failure at about 300 years. The effect of the uncertainty can be seen in higher mean normalized doses in the probabilistic case between 200 years and 600 years. Figure 74 shows the spread of releases in the 2-D transport dose results due to the variable failure times in the probabilistic case. The effect of uncertain diffusion of radionuclides from the waste form can be seen on Figure 75, where the probabilistic case was reduced to show the effect of the waste form diffusion coefficient. Six realizations were used to calculate a mean total normalized dose for comparison to the base case results. The realizations were selected that had a general corrosion rate which resulted in a waste container failure between 296 years and 302 years to be consistent with the base case analysis. The mean for these six realizations shows a higher peak normalized dose due to higher sampled diffusion rates from the waste form for I-129. The base case diffusion coefficient for I-129 was 1.0×10^{-8}, whereas the sampled values over the six representative realizations varied between approximately 5.0×10^{-8} to 7.0×10^{-8}, five to seven times higher that the base case values. The combined effects of earlier release due to the uncertainty in the general corrosion rates and the higher peak dose results due to the realizations with high diffusion coefficients are reflected in the mean normalized dose rate for the probabilistic analysis.

The example simplified probabilistic study shows the importance of considering the aleatory and epistemic uncertainty represented in the geologic disposal system. The combined effects in this example yielded a higher dose on average, than that of the expected case as represented by the deterministic base case results. Given the high number of assumptions in the design and site properties for the mined cavern disposal site, the uncertainty study displays the importance of an iterative approach that couples design and feedback to the safety assessment. A probabilistic safety assessment can be used to refine the data for parameters that have an impact on the repository performance (e.g. reduce epistemic uncertainty) and identify the important design features (e.g. aleatory uncertainty).

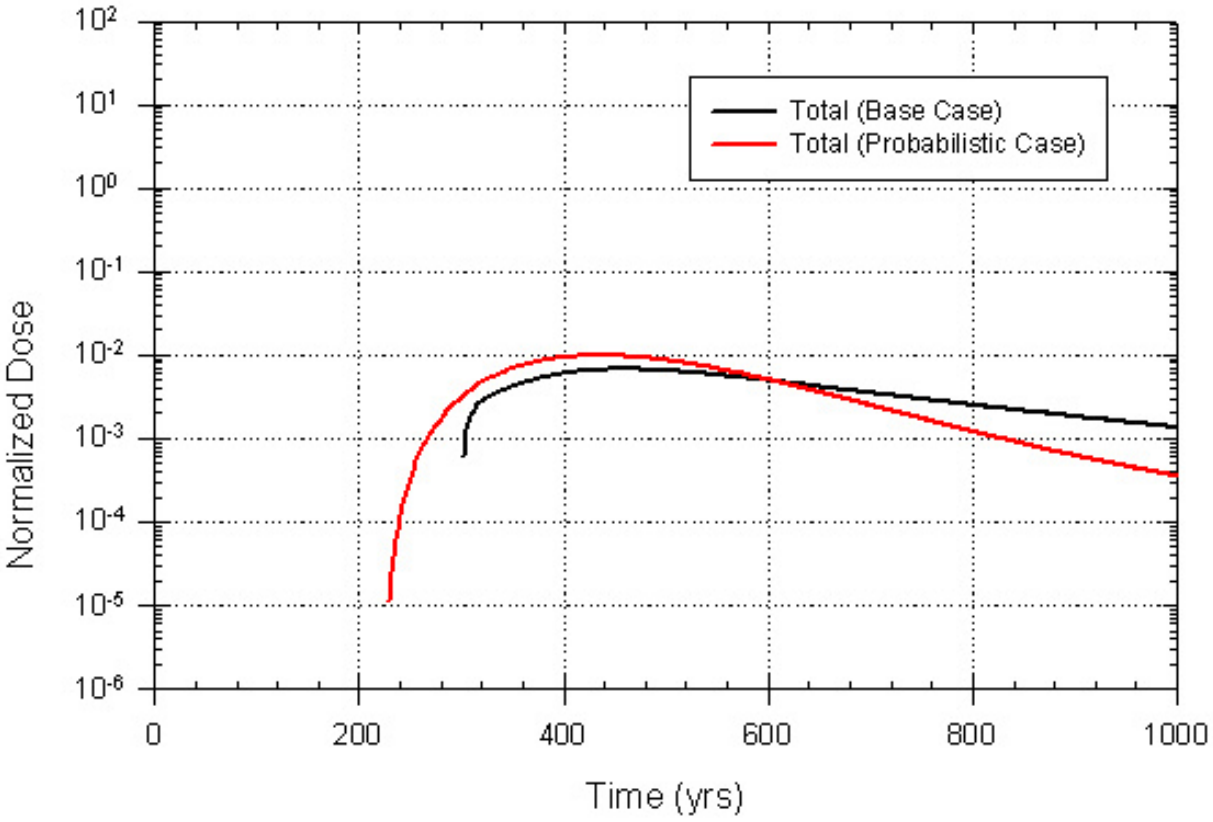

Figure 73: Mined cavern disposal site BLT-MS base case total dose vs. BLT-MS probabilistic case mean total dose

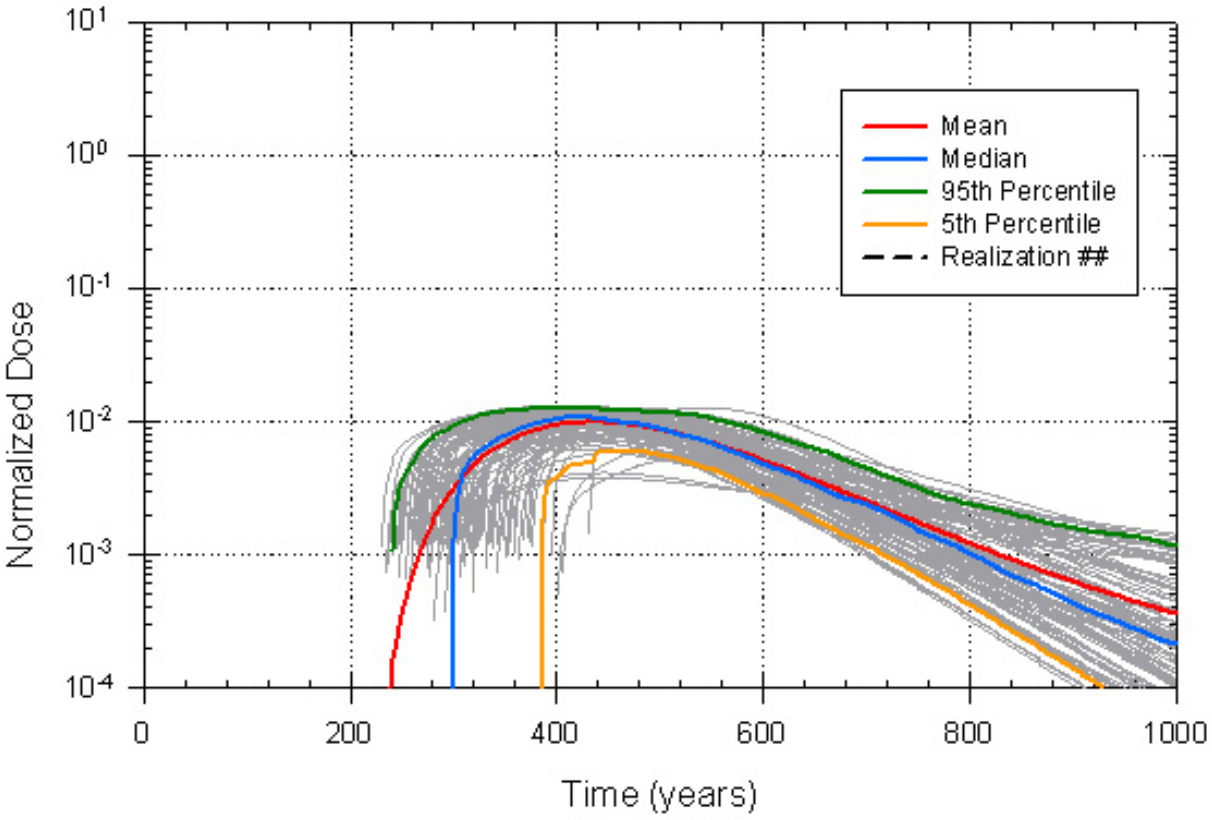

Figure 74: Mined cavern disposal site 2-D BLT-MS Model Probabilistic Results

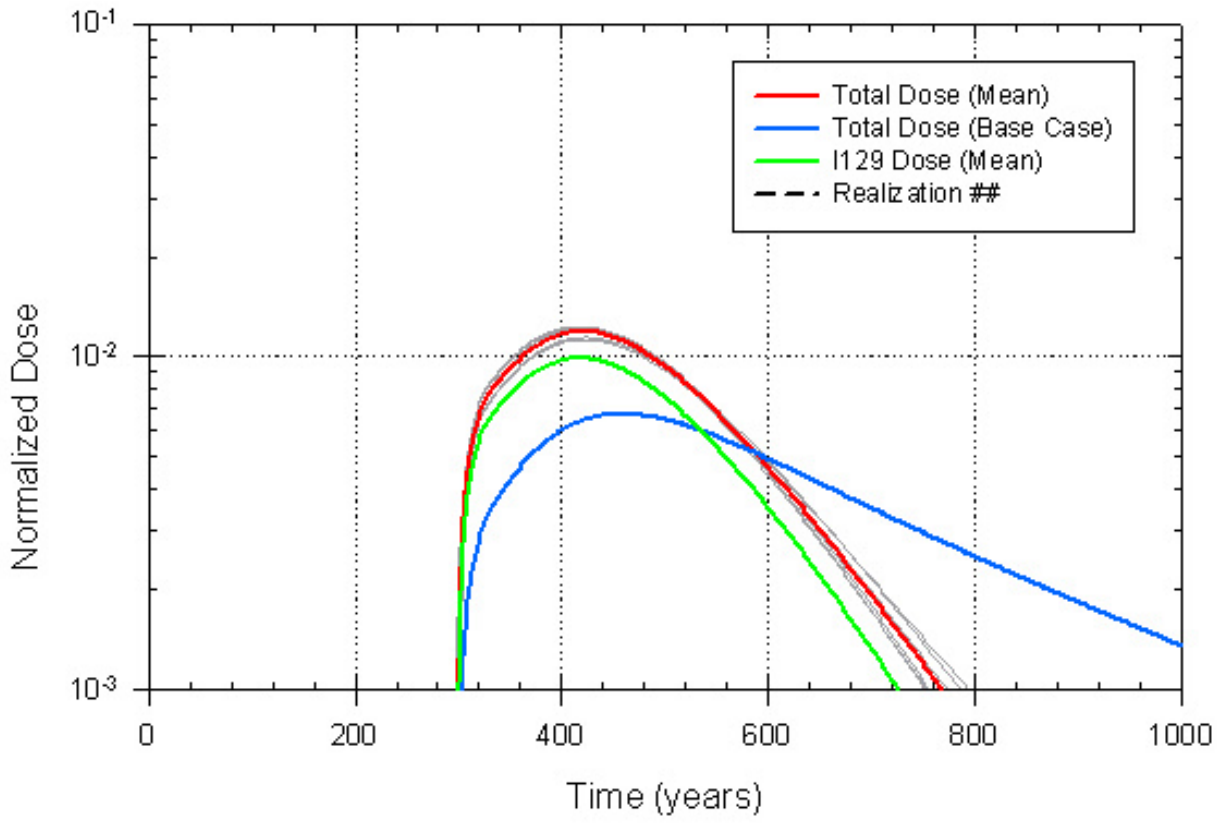

Figure 75: Mined cavern disposal site mean total dose for select realizations from probabilistic analysis vs. base case total dose, showing the effect of increased waste form diffusion rates.

5.2. Alternative Case Analyses

In addition to the baseline conceptual model presented in Section 5.1, a one-dimensional matrix-diffusion model was constructed as an alternative conceptual model of transport through the fractured bedrock (see Section 3.3.4). For the mined cavern disposal site the 1-D transport model implemented in GoldSim consists of 21 pathways, each originating from one of the disposal drifts in the LLW repository. The goal of the 1-D transport model is to approximate the groundwater flow rates and geometry of flow pathways in the 2-D BLT-MS model as closely as possible. However, the approximations inherent in the 1-D transport model construction and the lack of transverse dispersion in the 1-D transport model result in differences with the 2-D BLT-MS transport model.

Simulation results from the 1-D transport model are compared to the 2-D BLT-MS transport model with regard to total normalized dose in Figure 76. The 1-D transport model results indicate a higher peak normalized dose value (by a factor of approximately 2) and a slightly higher normalized dose rate out to times of about 2500 years, relative to the 2-D BLT-MS

transport model. At later times, the 1-D transport model simulates normalized dose rates that are about 5 to 6 times higher than the 2-D BLT-MS transport model. As in the model for the near surface disposal site, the lower normalized dose rates from the 2-D BLT-MS transport model are probably due to the greater numerical and transverse dispersion in the 2-D finite-element solution method used by BLT-MS. Such dispersion spreads radionuclide mass throughout the cross section of the groundwater flow system (see Figure 72) leading to dilution of simulated radionuclide concentrations, relative to the 1-D transport model in which transport is confined within the defined flow pathways. Overall, the simulated values of total normalized dose rate from the 1-D transport model and the 2-D BLT-MS transport model are quite similar, given the differences in which these models are constructed and implemented in the analysis. Similarities in the results from the two models lend confidence to these independently implemented representations of radionuclide transport in the natural system.

The differences in simulated normalized dose from the 1-D transport model compared to the 2-D BLT-MS transport model are also affected by matrix diffusion in the 1-D transport model. However, the overall differences are dominated by the effects of dimensionality and numerical dispersion.

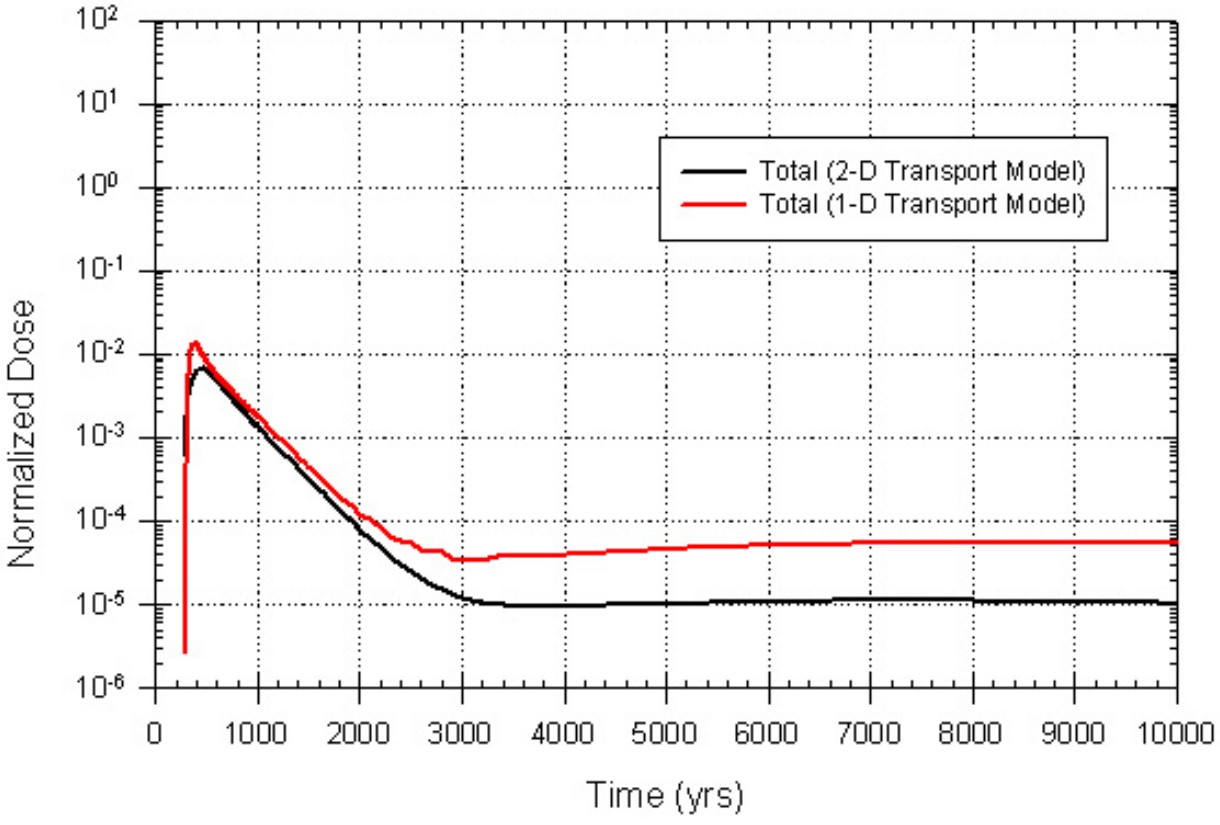

Figure 76. Dose Versus Time for the Mined Cavern Disposal Site from the 2-D BLT-MS Transport Model and the 1-D Transport Model

The contributions to simulated total normalized dose in the 1-D transport model from individual radionuclides are shown in Figure 77. This plot shows that ^{129}I and ^{14}C are the greatest contributors to normalized dose during approximately the first 2500 years following closure of the LLW repository. The contributions to dose from ^{239}Pu and ^{240}Pu, which are strongly sorbing species, dominate the simulated total normalized dose at later times; however, the normalized dose rate at later times is greater than two orders of magnitude lower than the peak normalized dose.

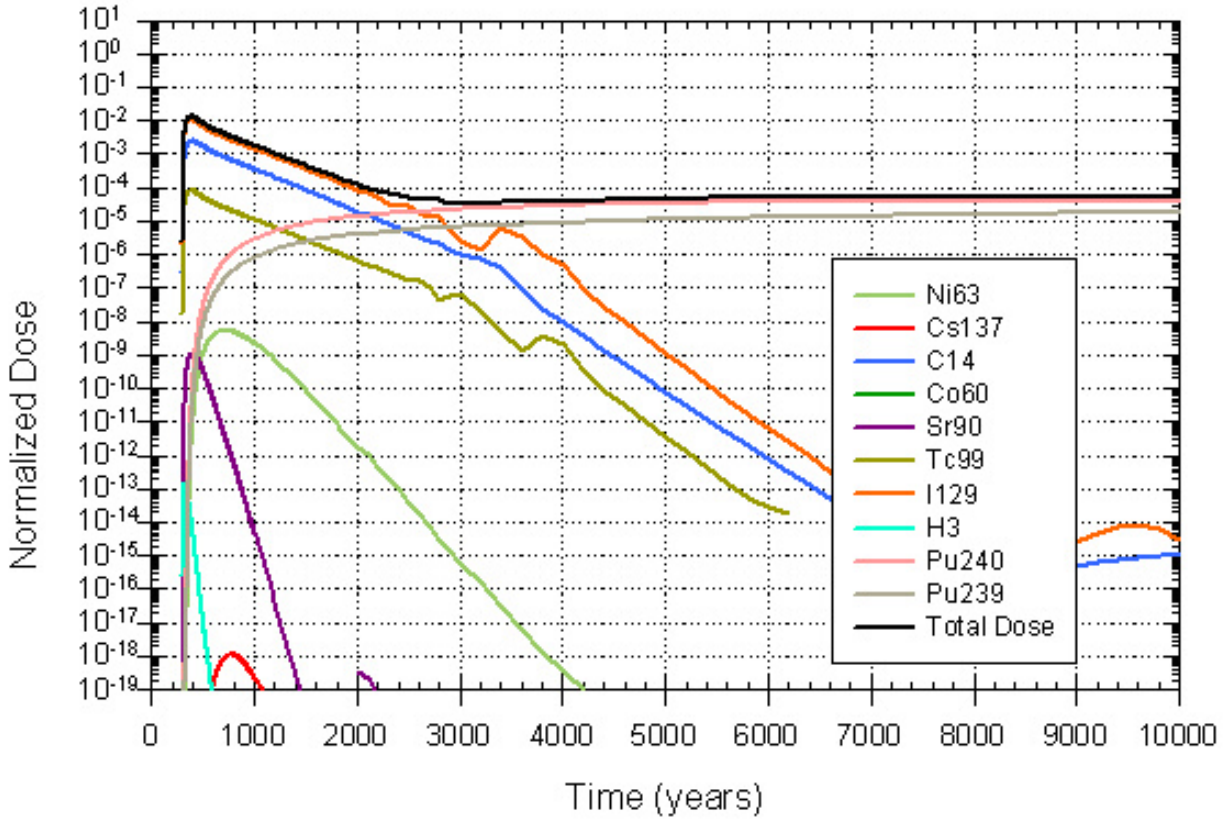

Figure 77. Dose Versus Time for the Mined Cavern Disposal Site from the 1-D Transport Model and Showing the Contributions from Individual Radionuclides

This page intentionally blank.

6. SUMMARY AND COMPARATIVE DISCUSSION OF RESULTS

Sandia National Laboratories has developed preliminary performance assessment analyses for the disposal of LLW at potential sites in Taiwan in collaboration with the Institute of Nuclear Energy Research. This work was the result of a relationship in which Sandia and INER have been exchanging technical information on geologic repository systems since 1998. Phase I of this technology transfer project has the following main objectives: (1) regulatory analysis of LLW final disposal, (2) development of LLW performance assessment capabilities using NRC-sponsored codes and other computational tools, and (3) conducting performance assessments for two potential LLW final disposal sites using available site and initial conceptual design information.

Taiwan has accumulated LLW from a variety of sources, primarily from commercial nuclear power generation. These wastes are currently in storage at the Lanyu Island Storage Site and on-site at nuclear power plants. In addition to LLW that is currently in storage, substantial quantities of LLW will be generated from continued reactor operations and from the ultimate decommissioning of the existing nuclear power plants. Taiwan has not yet selected a site for the final disposal of LLW, but four potential sites have been identified by the Taiwan Power Company. Two representative sites were chosen from these potential locations for preliminary assessment in this study:

- Site #7 is located on a small island and uses a near-surface (shallow land burial) design with an engineered cover to limit infiltration.

- Site #6 is along the southeastern coast in mountainous terrain and uses a mined cavern design in which the tunnel system is 500 to 800 m below the surface.

The performance assessment methodology was used as the framework for quantitatively assessing the safety at these representative disposal sites. This is a process that consists of establishing quantitative performance objectives, evaluation of available data to formulate conceptual models, development of mathematical models, and evaluation of uncertainty in model parameters and results. This is an iterative process in which additional data collection and model improvements are informed by sensitivity analyses of performance assessment model results.

The performance objectives for LLW disposal are the quantitative metrics against which regulatory compliance can be determined. Taiwan's regulations on the licensing of LLW disposal facilities generally are based on U.S. Nuclear Regulatory Commission regulations, but potentially significant differences were examined. The regulation in Taiwan for protection of the general public specifies a maximum effective equivalent dose of 0.25 mSv/year from all exposure pathways. Taiwan's regulations require protection of an inadvertent human intruder through general requirements, but U.S. regulations more explicitly protect such an intruder though the waste classification system. The regulations in Taiwan do not appear to address the long-term stability of the disposal system by requiring minimization of void space in the waste packages and in the disposal facility, as do U.S. regulations. Based on experience in the U.S., the point of compliance is assumed to be 100 m beyond the edge of the disposal cell and dose

standards are evaluated out to 10,000 years in the future. Future exposure scenarios are based on current technologies and human activities and FEPs are only included if they have a probability of occurrence of > 0.0001/year. Uncertainty in system behavior may be addressed by conducting a single, conservatively bounding estimate of system performance or by performing a full, unbiased probabilistic analysis.

The waste inventory for LLW disposal is estimated to be a total of $2.54 \times 10^{+4}$ Ci contained in about 966,000 fifty-gallon drums, as reported by INER. Some questions remain about whether the estimated inventory includes all sources of waste, such as some activated metal components from reactor decommissioning and typical medical and industrial sources. Inclusion of these waste sources could result in significantly higher total activity in the inventory. The number of waste drums may have been overestimated, given updated U.S. estimates of nuclear power plant decommissioning wastes.

The performance assessment model is constructed for the purpose of evaluating the potential performance of a LLW disposal site and system against regulatory requirements. The probabilistic performance assessment model is constructed from several component models with the GoldSim software code functioning as the primary framework for the analyses. The BLT-MS code is directly coupled with GoldSim and is used to simulate container degradation, leaching of the radionuclide inventory from the LLW, and transport of radionuclides in groundwater to a hypothetical well at the point of compliance. An alternative model for radionuclide transport in groundwater, which includes matrix diffusion, is implemented within GoldSim. The FEHM software code is used to model the groundwater flow near the repository locations and the resulting flow fields are abstracted to provide flow vectors for input to the BLT-MS software. The HELP software code is used to model infiltration through the engineered cover for the near-surface LLW disposal system.

Modeling of infiltration with the HELP code indicates percolation of about 45 mm/year through the base fictitious cover design for the near-surface disposal system. The simulated percolation flux is reduced to about 3 mm/year if an HDPE geomembrane is added to the design below the drainage layer. A Monte Carlo analysis of uncertainty in infiltration through the cover conducted by sampling the HELP model parameters showed significant uncertainty in performance of the base case cover design, with uncertainty in the saturated hydraulic conductivity of the compacted clay layer being an important contributor to uncertainty in percolation flux.

The uncalibrated groundwater flow model for the island at Site #7 was constructed using the FEHM code with available information, but relied on unconfirmed assumptions about the flow system. It provides a plausible representation of groundwater flow for use in the preliminary performance assessment analyses and can be updated if site-specific data become available. An alternative flow model in which the sedimentary layer was assumed to have the same permeability as the basalt was also constructed. Groundwater flow vectors along a profile section through one of the disposal cells were extracted for input to the BLT-MS model of radionuclide transport and for the alternative 1-D transport model implemented in GoldSim.

Similarly, an uncalibrated site-scale groundwater flow model for Site #6 was constructed with the FEHM software, using limited available data from the site. It provides a plausible representation of groundwater flow for use in the preliminary performance assessment analyses and can be updated if site-specific data become available. Results from this preliminary model indicate significant groundwater discharge to the streams that were included as head-dependent flux boundaries in the model. Transport simulations show that about 60% of contaminants from the base-case repository design would be discharged to JJL Creek and JJL0101 Creek, with the remainder of the contaminants being discharged to the ocean. Groundwater flow vectors along a profile section through the repository were extracted for input to the BLT-MS model of radionuclide transport and for the alternative 1-D transport model implemented in GoldSim. A 2-D drift-scale flow model was also constructed with FEHM to evaluate the degree of flow diversion around the backfilled drift and LLW. Results indicate that the groundwater flow rate through the LLW could be more than two orders of magnitude lower than in the host rock, if the engineered materials within the drift have sufficiently low permeability.

The BLT-MS software was used to develop models that included detailed processes of waste container corrosion, leaching of radionuclides from various waste form types, and transport by groundwater through the geosphere to the receptor. These models were developed for both the near-surface disposal system and for the mined cavern disposal system, with model domains and grids that conformed to the engineering designs and simulated groundwater flow systems at each site.

Integration of the BLT-MS software into the performance assessment model in the GoldSim code was accomplished by linking BLT-MS as an external DLL element to GoldSim. Implementation of this linkage required the development of a "wrapper" code that reads a BLT-MS template input file, inserts the uncertain parameter values generated by GoldSim for that particular Monte Carlo realization, and writes a new BLT-MS input file. GoldSim then launches the BLT-MS code, which uses the new BLT-MS input file. Following execution of BLT-MS, the output is read back into the GoldSim performance assessment model. In addition, software codes used as a pre-processor, a grid generator, and a post-processor for the BLT-MS code were developed or updated from preexisting codes.

Results of the Example Calculations and Comparison of Disposal Systems

Several conceptual models for the source term were considered for the near-surface disposal site (Site #7). These conceptual models ranged from a conservative rinse model in which all radionuclides are available for dissolution and transport to a conceptual model in which radionuclides are in a solidified waste form and releases are diffusion limited. The conservative rinse model resulted in higher simulated peak radionuclide concentrations than the diffusion-limited release models. In all cases, the simulated peak concentrations occurred soon after waste container failure began and was dominated by highly soluble, non-sorbing radionuclides, particularly ^{129}I and ^{14}C. At later times, thousands of years into the future, plutonium isotopes dominate the dose estimates. They are delayed mainly due to solubility limited release mechanisms.

A probabilistic analysis for the near-surface disposal system incorporated uncertainty in the general corrosion rate for the containers and the diffusion coefficients. The peak of the mean simulated dose from the probabilistic analysis was higher than for the base case. The results of the performance assessment model with the alternative 1-D transport model indicate somewhat earlier peak dose relative to the base case BLT-MS transport model. Differences in simulated peak dose between the 1-D transport model and the BLT-MS transport model are attributable, at least in part, to the absence of transverse dispersion in the 1-D transport model.

Several options of model complexity and grid resolution were examined with regard to computational efficiency for the mined cavern disposal site (Site #6). Simulated peak dose from these various options were a couple of orders of magnitude lower than the near-surface disposal site.. Simulated peak dose was dominated by ^{129}I and ^{14}C in the options considered, with peak dose occurring soon after container failure began in most of the options. Like the near-surface disposal concept site, plutonium isotopes dominate the dose estimates at later times.

A probabilistic analysis for the mined cavern disposal system incorporated uncertainty in the general corrosion rate for the containers and the diffusion coefficients. The peak of the mean simulated dose from the probabilistic analysis was somewhat higher than for the base case. The results of the performance assessment model with the alternative 1-D transport model indicate somewhat earlier peak dose relative to the base case BLT-MS transport model, with a peak value higher by a factor of about 2.

The most striking result from these preliminary assessments of the near-surface disposal system and the mined cavern disposal system is the difference in simulated peak dose for the two sites. The values of peak simulated dose from the performance assessment modeling of the near-surface disposal system are nearly two orders of magnitude greater than the mined cavern disposal system. This is significant when also considering that the source term modeled in the near-surface disposal system was only one-third that of the mined cavern configuration due to the fact that only one of the three disposal cells was considered for the near-surface disposal site. These differences in the performance assessment analyses at the two sites are primarily due to differences in the volume of groundwater in which the radionuclides are dissolved for calculating their concentrations. Site #7 is located on an island with limited volumetric groundwater flow rates through an aquifer that is probably relatively thin. Precipitation of about 1 m/year at Site #7 is significantly less than the average of about 2.6 m/year at Site #6, resulting in less recharge to the groundwater flow system. There are differences in the BLT-MS model setup for Site #7 and Site #6 that lead to greater numerical dispersion and associated dilution for the mined cavern disposal site, but these differences in model domain size largely reflect probable differences in the physical groundwater flow system. It is possible that some of the difference in performance assessment model results for the two sites can be accounted for by the preliminary nature of the underlying groundwater flow models. However, the physical layout of the repository designs and the nature of the groundwater flow systems at the two sites support the model results that indicate much larger groundwater volumetric flow rates intersecting the LLW at Site #6, relative to Site #7. Nonetheless, caution should be used in drawing conclusions regarding the relative suitability of these two disposal systems at these two sites based on the preliminary performance assessment analyses presented in this report.

7. RECOMMENDATIONS FOR FUTURE WORK

The overall goal of Phase I of this project was to provide INER with a working framework for performance assessment of LLW final disposal. This goal was generally accomplished and staff at INER made significant advances in their abilities to understand, utilize, and adapt this framework. However, the performance assessment models that resulted from this program are not suitable for use in a defensible regulatory analysis and are of limited reliability for use as site-selection tools. Refinements to these models, many of them related to the acquisition of site-specific data, are required to make the models useful.

Significant questions exist regarding the total inventory that would be included in a single LLW disposal system for all of Taiwan. Additional work should be devoted to considering all potential sources of LLW. Most of this work should be conducted by knowledgeable personnel in Taiwan, but additional guidance could be provided by SNL staff. Technologies continue to be developed for the decommissioning of nuclear power plants and estimates of the inventory and volume of such LLW should be updated to reflect current understanding. In addition, the screening of radionuclides for inclusion in the performance assessment should be reevaluated in future work. No formal process was used to select the radionuclides for inclusion in the preliminary performance assessment model.

The validity and defensibility of these performance assessment models should be greatly enhanced by incorporating site-specific data on geology, hydrology, and chemistry if and when they become available. Incorporation of site-specific data would be a high priority for future work. Performance assessment models and the supporting groundwater flow modeling could be refined and updated with new, more specific information. The assessment of uncertainty distributions for parameters in the preliminary performance assessment models was limited in scope and should be improved through consideration of site-specific data and additional literature survey. In addition, the performance assessment models and the insights acquired during their development could be very useful in guiding site characterization activities. Technical interactions with the groups in Taiwan engaged in site characterization could be extremely fruitful with regard to optimization of data collection and to assure that the most useful types of data are collected.

The site-scale groundwater flow model for the near-surface disposal site represents the flow system as a confined aquifer in which the upper boundary of the aquifer is the topographic surface. This simplified representation of the flow system is adequate if the water table is relatively shallow across the island, but site characterization data are likely to show that this is not the case. Future work could include a refinement of the FEHM flow model that would explicitly simulate the position of the water table and downward percolation of infiltration through the overlying unsaturated zone.

The preliminary performance assessment models consider only the drinking water ingestion pathway in the calculation of dose from radionuclide concentrations in groundwater. Future work should include the development of a more complete biosphere model that incorporates other likely exposure pathways, such as food consumption from contaminated crops, meat, and

seafood. Ideally, this biosphere model would utilize information on local agricultural and fishing practices, patterns of food consumption, and lifestyle. In addition, the release scenario for the island site should be evaluated further in future work because other plausible locations for the receptor may result in higher simulated dose in the performance assessment model.

Future work should reconsider the way in which the BLT-MS software is used in the performance assessment model. One possible strategy is to use BLT-MS to model the LLW engineered system only. This would allow a much higher resolution grid to be implemented for waste containers and the surrounding engineered disposal system, which could more accurately simulate the releases of radionuclides to the host rock and site groundwater flow system. The transport of radonuclides in the natural system to the potential receptor could be simulated within GoldSim or using another software code. Results from the preliminary performance assessment model documented in this report revealed some of the numerical limitations of using the BLT-MS code to simultaneously model radionuclide releases at the relatively small scale of individual disposal cells or drifts and at the much larger scale of transport to the receptor. It would also be worthwhile to evaluate alternatives to GoldSim as the supporting software for the LLW performance assessment model. Less complex and more economical software may be adequate for the performance assessment analyses. More robust sensitivity analyses should be performed in future iterations of this work to understand the importance of paramaters contributing to uncertainty. Statistical analyses of the uncertainty results for stability should also be undertaken (i.e., how many realizations are required to capture the uncertainty appropriately). Additional effort should be devoted to methods for visualizing process model results.

8. REFERENCES

10 CFR 63 — U.S. Code for Federal Regulations. Energy: Disposal of High-Level Radioactive Wastes in a Geologic Repository at Yucca Mountain, Nevada.

DOE, 1994 — Wood, D.E., R.U. Curl, D.R. Armstrong, J.R. Cook, M.R. Dolenc, D.C. Kocher, K.W. Owens, E.P. Regnier, G.W. Roles, R.R. Seitz, and M.I. Wood, *Performance Assessment Task Team Progress Report*, DOE/LLW-157 Revision 1, Idaho National Engineering Laboratory, Idaho Falls Idaho, Prepared for the U.S. Department of Energy, 1994.

DOE, 1995 — *Integrated data base report 1994 - U.S. spent nuclear fuel and radioactive waste inventories, projections and characteristics*, DOE/RW-0006, Rev. 11, U.S. Department of Energy, Washington, DC, 1995.

EC, 1996 — *Council Directive 96/29/EURATOM of 13 May 1996, Laying Down the Basic Safety Standards for the Protection of the Health of Workers and the General Public Against the Dangers Arising from Ionizing Radiation.*

EPA, 1994 — Schroeder, P.R., T.S. Dozier, P.A. Zappi, B.M. McEnroe, J.W. Sjostrom, and R.L. Peyton, *The Hydrologic Evaluation of Landfill Performance (HELP) Model: Engineering Documentation for Version 3*, EPA/600/R-94/168b, U.S. Environmental Protection Agency Office of Research and Development, Washington, DC, September 1994.

GoldSim Technology Group, 2002 — GoldSim Contaminant Transport Module, User's Guide. Version 1.30. Redmond, Washington: Golder Associates.

GoldSim Technology Group, 2003 — GoldSim Technology Group. 2003. User's Guide, GoldSim Contaminant Transport Module. Version 2.21. Redmond, Washington: Golder Associates. TIC: 255171.

IAEA, 1996 — *International Basic Safety Standards for Protection against Ionising Radiation and for the Safety of Radioactive Sources.* Jointly sponsored by FAO, IAEA, ILO, OECD/NEA, PAHO, WHO, IAEA Safety Series No. 115. International Atomic Energy Agency, Vienna.

IAEA, 1999 — *Research Reactor Data Base (RRDB)*, International Atomic Energy Agency, Vienna, Austria, 1999. Available at: http://www.iaea.org/worldatom/rrdb

IAEA, 2003 *Safety Assessment Methodologies for Near Surface Disposal Facilities, Results of a co-ordinated research project, Volume I: Review and enhancement of safety assessment approaches and tools*, International Atomic Energy Agency (IAEA), Vienna, Austria, draft TECDOC, June 2003.

ICRP, 1996 *Age-dependent Doses to Members of the Public from Intake of Radionuclides: Part 5 Compilation of Ingestion and Inhalation Dose Coefficients*, Annals of the International Commission on Radiological Protection (ICRP), Publication 72, volume 26, No. 1, 1998.

ICRP, 1998 *Radiation Protection Recommendations as Applied to the Disposal of Long-lived Solid Radioactive Waste*, Annals of the International Commission on Radiological Protection (ICRP), Publication 81, volume 28, No. 4, 1998.

INER, 2003a *Regulations on Final Disposal of Low Level Waste and Safety Management of the Facilities, Enforced by Letter Hui-Wu-Tzu No. 0920023657*, September, 10, 2003.

INER, 2003b *Safety Standards for Protection against Ionizing Radiation, Promulgated on January 30, 2003 by the Atomic Energy Council Per its decree No. Huei-Fu-Tsu-0920002499*.

INER, 2005a *Inventory of Low Level Radioactive Waste in Taiwan*, LLW-ICP-I-INER-DOC-004, Institute of Nuclear Energy Research (INER), Taiwan, ROC, March 2005

INER, 2005b *Supplementary Data for LLW-ICP Project,* LLW-ICP-I-INER-DOC-007, Institute of Nuclear Energy Research (INER), Taiwan, ROC, March, 2005

INER, 2005c *Description of Near Surface Disposal Concept of Low-Level Radioactive Waste Repository in Taiwan*,LLW-ICP-I-INER-DOC-005, Institute of Nuclear Energy Research (INER), Taiwan, ROC, March, 2005

NAS, 1995 *Technical Bases for Yucca Mountain Standards*, National Academy of Sciences, National Academy Press, Washington, DC, 1995.

NRC, 1978 *Technology, Safety, and Costs of Decommissioning a Reference Pressurized Water Reactor Power Station*, NUREG/CR-0130, R.I. Smith, G.J. Konzek, W.E. Kennedy, Jr., U.S. Nuclear Regulatory Commission, Washington, DC, 1978.

NRC, 1980 *Technology, Safety, and Costs of Decommissioning a Reference Boiling Water Reactor Power Station*, NUREG/CR-0672, H.D. Oak, G.M. Holter, W.E. Kennedy, Jr., and G.J. Konzek, U.S. Nuclear Regulatory Commission, Washington, DC, 1980.

NRC, 1981b — *Draft Environment Impact Statement on 10 CFR Part 61 "Licensing Requirements for and Disposal of Radioactive Waste"*, NUREG-0782, U.S. Nuclear Regulatory Commission, Office of Nuclear Material Safety and Safeguards, Washington, DC, 1981.

NRC, 1982 — *Final Environment Impact Statement on 10 CFR Part 61 "Licensing Requirements for Land Disposal of Radioactive Waste,"* NUREG-0945, U.S. Nuclear Regulatory Commission, Office of Nuclear Material Safety and Safeguards, Washington, DC, 1982.

NRC, 1989 — *BLT-MS (Breach, Leach, and Transport – Multiple Species) Data Input Guide: A Computer Model for Simulating Release of Contaminant from Low-Level Waste Disposal Facility*, NUREG/CR-6492, U.S. Nuclear Regulatory Commission, Washington, D.C., written by Brookhaven National Laboratory, 1989.

NRC, 1995 — *Revised Analyses of Decommissioning for the Reference Pressurized Water Reactor Power Station – Effects of Current Regulatory and Other Considerations on the Financial Assurance Requirements of the Decommissioning Rule and on Estimates of Occupational Radiation Exposure*, NUREG/CR-5884, G.J. Konzek, R.I. Smith, M.C. Bierschbach, and P.N. McDuffie, U.S. Nuclear Regulatory Commission, Washington, DC, 1995.

NRC, 1996a — *Low-Level Waste Shallow Land Disposal Source Term Model: Data Input Guides*, NUREG/CR-5387, U.S. Nuclear Regulatory Commission, Washington, D.C., written by Brookhaven National Laboratory, 1996.

NRC, 1996b — *Revised Analyses of Decommissioning for the Reference Boiling Water Reactor Power Station – Effects of Current Regulatory and Other Considerations on the Financial Assurance Requirements of the Decommissioning Rule and on Estimates of Occupational Radiation Exposure*, NUREG/CR-6174, R.I. Smith, M.C. Bierschbach, G.J. Konzek, and P.N. McDuffie, U.S. Nuclear Regulatory Commission, Washington, DC, 1996.

NRC, 1996 — Nuclear Regulatory Commission Papers SECY-96-103, http://www.nrc.gov/reading-rm/doc-collections/commission/secys/1996/secy1996-103/1996-103scy.html

NRC, 2000 — *A performance assessment methodology for low-level radioactive waste disposal facilities: recommendations of NRC's Performance Assessment Working Group*, NUREG-1573, U. S. Nuclear Regulatory Commission, Washington, DC, 2000.

SNL, 1998 — Wyss, G.D. and K.H. Jorgensen, *A User's Guide to LHS: Sandia's Latin Hypercube Sampling Software*, SAND98-0210, Sandia National Laboratories, Albuquerque, NM, 1998.

SNL, 2000	Helton, J.C. and F.J. Davis, *Sampling-Based Methods for Uncertainty and Sensitivity Analysis*, SAND99-2240, Sandia National Laboratories, Albuquerque, NM, 2000.
SNL, 2002	Ho, C.K., B.W. Arnold, J.R. Cochran, and R.Y. Taira, *Development of a Risk-Based Probabilistic Performance-Assessment Method for Long-Term Cover Systems -2nd Edition*, SAND2002-3131, Sandia National Laboratories, Albuquerque, NM, October 2002.
SNL, 2005	Cochran, J. and J. Schelling, *Recommended Quantitative Performance Objectives for the Safety Assessment of the Disposal of LLW in Taiwan*, SAND2005-6336P, Sandia National Laboratories, Albuquerque, NM, November 2, 2005.
Vicente et al., 2004	Vicente, R., G.-M. Sordi, and G. Hiromoto, *Management of Spent Sealed Radiation Sources*, Health Physics Society Journal, Vol. 86(5), pp. 497-504, 2004.
Zyvoloski et al., 1997	Zyvoloski, G.A.; B.A. Robinson; Z.V. Dash; L.L. Trease, *Summary of the Models and Methods for the FEHM Application-A Finite-Element Heat-and-Mass-Transfer Code*, LA-13307-MS, Los Alamos National Laboratory, Los Alamos, New Mexico, 1997.

Distribution

External Distribution

30 Institute of Nuclear Energy Research
No. 1000, Wenhua Rd. Chiaan Village
Lungtan Taoyuan. 325
TAIWAN. R.O.C.
Attn: Ching-Tsuen Huang
Wen-Shou Chuang (13)
Ching-Fang Shih
Li-Min Chi
Shin-Jon Ju
Ben-Li Pen
Fu-Lin Chang
Neng-Chuan Tien
Ming-Chuan Kuo
Chen-Chang Lee
Chih-Ming Ma
Ching-Chang Chang
Chih-Lung Chen
Chung-Ding Lu
Ching-Ping Wang
Ren-Jie Lai
Cong-Zhang Tong
Lee-Hao Wu

Lockheed Martin Corporation
1 Mr. Joe Ostuni
Deputy Director, Radar Systems and Offsets
Lockheed Martin Maritime Systems and Sensors
P.O. Box 4840
EP5-201, MD 21
Syracuse, NY 13221-4840

1 Mr. Robert Kelly
Regional Manager, Industrial Participation
Lockheed Martin Missiles and Fire Control –Orlando
5600 Sand Lake Road, MP-48
Orlando, FL 32819-8907

2 Los Alamos National Laboratory
P.O. Box 1663
Los Alamos, New Mexico 87545
Attn: George A. Zyvoloski
Bruce A. Robinson

1 Dr. Terry Sullivan
Environmental Sciences Department, Mailstop 830
Brookhaven National Laboratory
Upton, NY 11973-5000

1 Mr. Ralph Cady
Office of Nuclear Regulatory Research
Mail Stop T-9C34
U.S. Nuclear Regulatory Commission
Washington, DC 20555

Sandia National Laboratories Internal Distribution

5	MS1363	Hong-Nian Jow	6725
5	MS0778	Bill W. Arnold	6781
5	MS0779	Frank J. Schelling	6772
5	MS0734	Robert G. Knowlton	6334
5	MS0776	Patrick D. Mattie	6784
5	MS0719	John R. Cochran	6766
1	MS0735	Clifford K. Ho	6313
1	MS0735	Sean A. McKenna	6313
1	MS1399	M. Kathryn Knowles	6781
1	MS0776	Stephanie P. Kuzio	6782
2	MS9018	Central Technical Files	8944
2	MS0899	Technical Library	4536